Functional analysis of
mammalian *m*-AAA proteases

Inaugural-Dissertation

zur

Erlangung des Doktorgrades

der Mathematisch-Naturwissenschaftlichen Fakultät

der Universität zu Köln

vorgelegt von

Sarah Marie Ehses

aus Bonn

Köln, 2008

Berichterstatter:

Professor Dr. Thomas Langer

Professor Dr. Jens C. Brüning

Tag der mündlichen Prüfung: 22. Oktober 2008

Abstract

The *m*-AAA protease, an ATP-dependent proteolytic complex in the inner mitochondrial membrane, controls mitochondrial protein quality and, acting as a processing enzyme, regulates mitochondrial protein synthesis in yeast. Mammalian *m*-AAA proteases assemble into several isoenzymes with variable subunit composition. In mice, the three different subunits paraplegin, Afg3l1 and Afg3l2, are expressed in a tissue-specific manner. Loss-of-function mutations in the *m*-AAA protease subunit paraplegin cause the neurodegenerative disease hereditary spastic paraplegia (HSP) which is mainly characterized by a cell-specific axonal degeneration. Similarly, *Afg3l2* mutant mice exhibit neuropathological features with a severe defect in axonal development. The molecular basis of these neuron-specific phenotypes as well as cellular functions of mammalian *m*-AAA proteases in general remain unclear and are studied within this thesis.

Using an HSP mouse model lacking paraplegin, a liver-specific mitochondrial translation defect was observed which is consistent with a functional conservation of the *m*-AAA protease-dependent control of mitochondrial protein synthesis in mammals. However, a significant impairment of mitochondrial protein synthesis and mitochondrial respiration in brain and spinal cord was not observed suggesting that axonal degeneration in HSP due to a loss of paraplegin occurs in the absence of a general respiratory dysfunction.

The analysis of *m*-AAA isoenzymes on a cellular level using RNA interference revealed redundant functions of the subunits Afg3l1 and Afg3l2 and identified paraplegin as a new substrate which is processed by Afg3l1 and Afg3l2. Depletion of the *m*-AAA protease in MEFs resulted in mitochondrial fragmentation accompanied by an impaired biogenesis of OPA1, an essential component of the mitochondrial fusion machinery. Long OPA1 isoforms were destabilized and cleaved in an accelerated manner. The overexpression of a non-cleavable long OPA1 isoform in *m*-AAA protease-depleted cells restored the tubular mitochondrial network identifying impaired OPA1 processing as the primary cause for the mitochondrial morphology defect. Furthermore, the *m*-AAA protease was found to be essential for inducing mitochondrial hyperfusion, a cellular stress response which results in a highly interconnected mitochondrial network.

The findings of this study indicate that the *m*-AAA protease has crucial functions in the regulation of mitochondrial morphology by controlling the biogenesis of OPA1 isoforms which may provide new insights into the molecular mechanisms of axonopathies caused by the loss of *m*-AAA protease subunits in mammals.

Table of Contents

1 Introduction

1.1 *The proteolytic system of mitochondria*

Mitochondria are essential organelles in eukaryotic cells which house biosynthetic pathways and generate ATP by oxidative phosphorylation. Besides providing cellular energy, mitochondria are involved in multiple cell signalling cascades and the regulation of cellular metabolism, development, calcium homeostasis and apoptosis (McBride *et al.*, 2006). Therefore, it is not surprising that mitochondrial dysfunctions are linked to ageing and a variety of human disorders such as cancer, diabetes and neurodegeneration (Wallace, 2005; Chan, 2006). Since mitochondria are the primary producers of reactive oxygen species, oxidative damage of mitochondrial proteins or DNA might contribute to mitochondrial dysfunctions (Lin and Beal, 2006). To ensure mitochondrial integrity and function, a number of control and defense systems have evolved (Tatsuta and Langer, 2008). The first line of defense is conducted by an evolutionary conserved proteolytic system which controls the quality of mitochondrial proteins and subsequently degrades excess and misfolded proteins (Koppen and Langer, 2007). Mitochondrial proteases do not only remove proteins but also perform essential housekeeping and regulatory roles during mitochondrial biogenesis by processing of proteins.

1.1.1 Processing of mitochondrial proteins

In human, only 13 polypeptides of in total ~1500 mitochondrial proteins are encoded by the mitochondrial genome (Anderson *et al.*, 1981; Lopez *et al.*, 2000). The vast majority is encoded by the nuclear genome and synthesized as precursors on cytosolic ribosomes. Precursor proteins containing distinct mitochondrial targeting signals are imported into mitochondria via different import routes (Bolender *et al.*, 2008). One major import route for proteins designated mainly to the matrix, but also to the inner membrane (IM) and the intermembrane space (IMS), includes often cleavage of signal sequences by specific processing peptidases (Gakh *et al.*, 2002). Many mitochondrial precursors are synthesized with a characteristic N-terminal presequence forming a positively charged amphipatic helix. The presequence is necessary to target cytosolic precursors to the mitochondria and further across both mitochondrial membranes to the matrix where it is cleaved off by the **mitochondrial processing peptidase MPP** (Fig. 1.1) (Hawlitschek *et al.*, 1988). MPP

belongs to the zinc-dependent metalloproteases and functions as a heterodimer consisting of the conserved subunits α-MPP and β-MPP (Böhni *et al.*, 1983; Yang *et al.*, 1988; Gakh *et al.*, 2002). A subset of precursor proteins undergoes a second cleavage step in the matrix which is mediated by the **mitochondrial intermediate peptidase MIP** (Fig. 1.1) (Kalousek *et al.*, 1988; Kalousek *et al.*, 1992). The cleavage by MPP converts precursors into intermediate proteins characterized by an N-terminal octapeptide (Isaya *et al.*, 1991; Isaya *et al.*, 1992). The mature protein is generated by the subsequent removal of the N-terminal octapeptide mediated by the monomeric metalloprotease MIP. The **inner membrane peptidase IMP** mediates the maturation of intermediate forms of several nuclearly encoded proteins generated by MPP, as well as mitochondrially encoded subunit 2 of cytochrome *c* oxidase (Fig. 1.1) (Daum *et al.*, 1982; Pratje *et al.*, 1983; Nunnari *et al.*, 1993; Burri *et al.*, 2005). In the yeast *Saccharomyces cerevisiae*, the IMP complex consists of Som1 and the two catalytic subunits Imp1 and Imp2 and faces the intermembrane space (Nunnari *et al.*, 1993; Jan *et al.*, 2000). The catalytic domains of Imp1 and Imp2 are characterized by conserved dyads of serine/lysine residues but interestingly display non-overlapping substrate specificities. Potential substrates in mammals include the protein Smac/Diablo which functions in apoptosis (Burri *et al.*, 2005).

Other mitochondrial proteases have also been implicated in the maturation of newly imported mitochondrial proteins. In *S. cerevisiae*, the presequence of the mitochondrially encoded subunit Atp6 of the F_1F_O-ATP synthase complex is cleaved off by the metallopeptidase **Atp23** in the IMS (Fig. 1.1) (Osman *et al.*, 2007; Zeng *et al.*, 2007). Independent of its proteolytic activity, Atp23 acts as a chaperone protein and promotes the assembly of Atp6 into the membrane-embedded F_O-moiety of the ATP synthase complex (Osman *et al.*, 2007; Zeng *et al.*, 2007). Cytochrome *c* peroxidase (Ccp1), a haeme-binding ROS scavenger in the IMS of yeast, is processed in two successive steps to its mature form during mitochondrial import (Esser *et al.*, 2002). This processing is performed by the subsequent action of two inner membrane proteases, the *m*-AAA protease (discussed later) and the rhomboid protease **Pcp1** (Esser *et al.*, 2002; Tatsuta *et al.*, 2007). Rhomboid proteases comprise a conserved family of intramembrane cleaving peptidases characterised by a catalytic serine dyad (Lemberg *et al.*, 2005). Besides Ccp1 maturation, Pcp1 is involved in the processing of the dynamin-related GTPase Mgm1, a protein of the mitochondrial fusion machinery (Herlan *et al.*, 2003; McQuibban *et al.*, 2003; Sesaki *et al.*, 2003). At steady state, Mgm1 exists in a long isoform produced by MPP cleavage, and a short isoform which is generated by Pcp1 cleavage. Since the presence of the short Mgm1 isoform is required for

mitochondrial fusion, Pcp1-mediated processing of Mgm1 affects mitochondrial morphology (Herlan *et al.*, 2003; Herlan *et al.*, 2004).
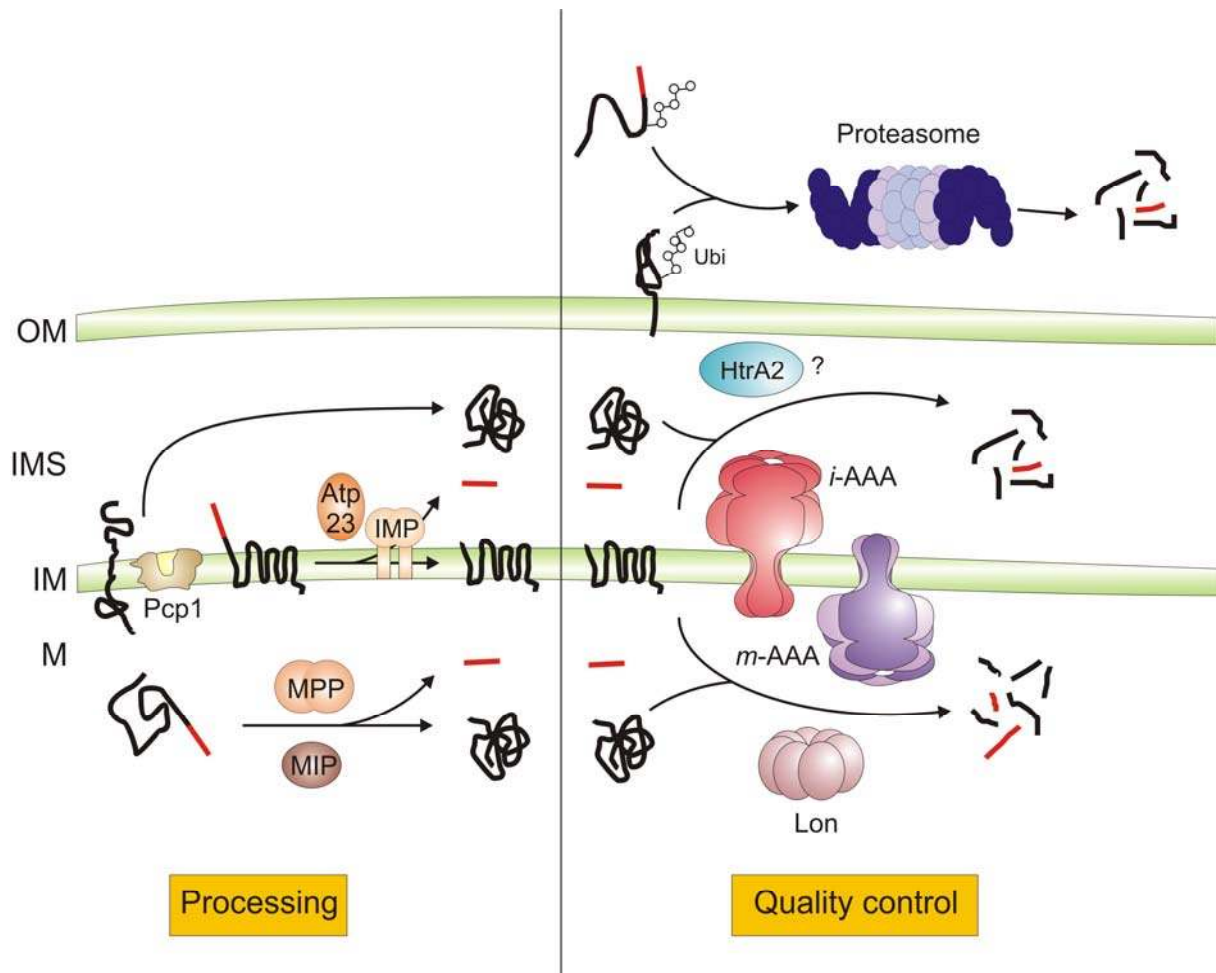
Figure 1.1 The proteolytic system of mitochondria.
Processing and protein quality control of proteins residing in the matrix (M), the inner membrane (IM) and the intermembrane space (IMS) are key functions of mitochondrial proteases. Proteases involved in protein quality control do not only degrade proteins to peptides but also can act as processing enzymes. Recent evidence links the cytosolic proteasome to mitochondrial quality control and the regulation of mitochondrial dynamics. Red lines represent mitochondrial targeting signals. See text for further details (Figure modified from Koppen and Langer, 2007).

The mammalian Pcp1 homologue **PARL** (presenilin-associated rhomboid like protease) can functionally substitute for Pcp1 (McQuibban *et al.*, 2003). Although PARL was found to physically interact with OPA1, the mammalian orthologue of Mgm1, the deletion of PARL in mouse has no obvious effect on mitochondrial morphology (Cipolat *et al.*, 2006).

Consistently, only a small fraction of OPA1 appears to be processed by PARL (Cipolat *et al.*, 2006; Duvezin-Caubet *et al.*, 2007). However, PARL was implicated in controlling apoptosis in an OPA1-dependent manner (Cipolat *et al.*, 2006). It should be noted that cleavage of OPA1 has also been linked to two AAA-proteases, the *i*- and the *m*-AAA protease, residing in the inner mitochondrial membrane (Ishihara *et al.*, 2006; Griparic *et al.*, 2007; Song *et al.*, 2007).

1.1.2 Quality control of mitochondrial proteins

Non-assembled and damaged proteins in mitochondria are recognized and degraded by a highly elaborate proteolytic system (Koppen and Langer, 2007; Tatsuta and Langer, 2008). Different ATP-dependent proteases with chaperone-like functions have been implicated in the quality control of mitochondrial proteins. They are characterized by a structurally conserved ATPase domain and assemble into multimeric protein complexes with a central proteolytic chamber (Sauer *et al.*, 2004; Hanson and Whiteheart, 2005). ATP-binding and -hydrolysis induce conformational changes which are required to unfold and deliver substrates into the proteolytic chamber (Baker and Sauer, 2006).

Two different ATP-dependent proteases have been identified in the mitochondrial matrix, the **Lon** (in yeast PIM1 protease) and the **ClpXP** protease (Suzuki *et al.*, 1994; Van Dyck *et al.*, 1994; Wang *et al.*, 1994; De Sagarra *et al.*, 1999). Besides the requirement of mitochondrial ClpXP in the unfolded protein response, not much is known about its role within mitochondria (Zhao *et al.*, 2002; Haynes *et al.*, 2007). Lon has been demonstrated to mediate the proteolysis of misfolded and unassembled matrix proteins (Fig. 1.1) (Bota and Davies, 2002; Major *et al.*, 2006). This serine protease forms soluble heptameric complexes in the mitochondrial matrix (Stahlberg *et al.*, 1999). Under oxidative stress, Lon is involved in the removal of damaged proteins including oxidized proteins, and thereby presumably prevents the extensive accumulation of protein aggregates (Bota and Davies, 2002; Bota *et al.*, 2005). Besides its role in protein quality control, deletion mutants in yeast indicate an essential function of Lon in mtDNA maintenance (Suzuki *et al.*, 1994; Van Dyck *et al.*, 1994). This is substantiated by the evolutionary conserved ability of Lon to bind DNA (Zehnbauer *et al.*, 1981; Fu and Markovitz, 1998; Lu *et al.*, 2003; Liu *et al.*, 2004). Furthermore, the human Lon protease was found to be associated with mtDNA under

physiological conditions, however, the exact molecular function of this protease in mtDNA quality control is not clear yet (Lu *et al.*, 2007).

Protein quality control in the inner membrane is of special importance. The inner membrane harbours the multimeric respiratory chain complexes, which are the main producer of reactive oxygen species (ROS) in the cell but also the prime target for oxidative damage. Two ATP-dependent proteases with overlapping substrate specificities, the **i-AAA** and the **m-AAA protease**, are responsible for degrading damaged and non-assembled proteins in the inner mitochondrial membrane (Fig. 1.1) (Langer, 2000; Koppen and Langer, 2007). Whereas the *i*-AAA protease exposes its catalytic side to the intermembrane space, the *m*-AAA protease is active on the matrix side. Their function and properties are discussed in detail below (Chapter 1.2).

In contrast to matrix and inner membrane protein degradation, little is known about turnover of proteins localised to the intermembrane space and the outer membrane of mitochondria. A putative candidate for the surveillance of protein quality in the IMS is **HtrA2/Omi**, a member of a conserved family of serine proteases (Fig. 1.1). Its *E. coli* homologue DegP is a key factor dealing with protein folding stress via its dual functions in protein refolding and degradation (Spiess *et al.*, 1999; Clausen *et al.*, 2002). In mammals, HtrA2/Omi is upregulated in response to several stress stimuli (Faccio *et al.*, 2000; Gray *et al.*, 2000). In contradiction to a potential protective role, several reports proposed HtrA2/Omi to promote cell death (Suzuki *et al.*, 2001; Hegde *et al.*, 2002; van Loo *et al.*, 2002; Verhagen *et al.*, 2002). Following apoptotic stimuli, HtrA2/Omi is released from mitochondria into the cytosol where it facilitates apoptosis by its protease activity. However, the discussed pro-apoptotic function of HtrA2/Omi is not supported by phenotypes of mice lacking HtrA2/Omi function (Jones *et al.*, 2003; Martins *et al.*, 2004). These mice exhibit a Parkinson-like neurodegenerative disorder which is caused by neuronal cell death indicating an essential and protective role of HtrA2/Omi *in vivo*. Moreover, loss-of-function mutations in the gene encoding HtrA2/Omi were recently identified in patients with Parkinson`s disease (Strauss *et al.*, 2005). It is still unclear how HtrA2/Omi protects mitochondria from stress, but it might prevent the accumulation of misfolded or damaged proteins in mitochondria in a manner similar to its *E. coli* counterpart DegP. Evidence for a processing activity was recently provided by the identification of β-amyloid precursor protein APP as a direct cleavage target of HtrA2/Omi in mitochondria (Park *et al.*, 2006).

Several reports indicate a function of the **ubiquitin-proteasome pathway** in the quality control of outer membrane proteins similar to the ER-associated degradation (ERAD). In

mammals, a specific ubiquitin ligase, MARCHV/MITOL, integrated into the outer mitochondrial membrane is implicated in the ubiquitination of two mitochondrial fission protein, Drp1 and Fis1 (Nakamura *et al.*, 2006; Yonashiro *et al.*, 2006; Karbowski *et al.*, 2007). However, it is currently not clear if this ubiquitination results in protein degradation or exerts a regulatory function. A further role of the 26S proteasome in the quality control has been proposed for mitochondrial precursor proteins in the cytosol prior to their import (Margineantu *et al.*, 2007; Radke *et al.*, 2008). Several proteomic studies have identified ubiquitin-modified proteins that finally reside in different mitochondrial subcompartments, suggesting that non-imported proteins are substrates of the ubiquitin-proteasome pathway (Peng *et al.*, 2003; Matsumoto *et al.*, 2005; Jeon *et al.*, 2007).

1.2   AAA proteases in the inner mitochondrial membrane

1.2.1 Domain structure and assembly of AAA proteases

AAA proteases form a conserved subclass of ATP-dependent proteases (AAA^+ proteases) (Langer *et al.*, 2001; Sauer *et al.*, 2004). They are membrane-embedded metallopeptidases which are ubiquitously present in eubacteria as well as in chloroplasts and mitochondria of eukaryotic cells (Juhola *et al.*, 2000). Two AAA protease complexes are integrated into the mitochondrial inner membrane exposing their catalytic sites to opposite membrane surfaces: the *i*-AAA protease exposing its catalytic side to the intermembrane space and the *m*-AAA protease which is active on the matrix side (Fig. 1.2 B) (Arlt *et al.*, 1996; Leonhard *et al.*, 1996; Weber *et al.*, 1996; Arlt *et al.*, 1998). They form large complexes which are composed of either closely related or identical subunits of 70-80 kDa (Atorino *et al.*, 2003; Urantowka *et al.*, 2005; Koppen *et al.*, 2007). Whereas the *i*-AAA protease is a homo-oligomeric complex consisting of identical subunits, *m*-AAA proteases also assemble into hetero-oligomeric complexes of highly homologous subunits.

Mitochondrial localisation of AAA protease subunits is ensured by mitochondrial targeting sequences. Subunits of the *i*-AAA protease are anchored to the mitochondrial inner membrane by one transmembrane segment, whereas *m*-AAA protease subunits contain two membrane-spanning domains at their N-terminal ends (Fig.1.2 A) (Arlt *et al.*, 1996; Weber *et al.*, 1996). A highly conserved AAA domain identifies them as members of the AAA^+ superfamily of P-loop ATPases (Sauer *et al.*, 2004; Hanson and Whiteheart, 2005). The AAA domain harbours the Walker A (or P-loop) and the Walker B motifs which are required for ATP binding and hydrolysis, respectively (Fig.1.2 A). A conserved region C-terminal to the Walker B motif, the second region of homology (SRH), defines the AAA proteases as members of the AAA-family. The second region of homology contains two conserved arginine residues which protrude into the catalytic sites of the neighbouring subunits (Hanson and Whiteheart, 2005). These residues are suggested to coordinate intermolecular conformational changes during ATPase cycles, thereby stimulating ATP hydrolysis. Consequently, oligomerization of AAA protein subunits is necessary for their ATPase activity (Akiyama and Ito, 2000; Akiyama and Ito, 2001). The proteolytic domain contains the metal binding sequence HEXGH (X represents a variable amino acid residue), a sequence motif which is conserved in the M41 family of metallopeptidases (Rawlings and Barrett, 1995). Whereas the two histidine residues coordinate a Zn^{2+}-metal ion, the glutamate

activates a water molecule for nucleophilic attack of the peptide bond (Hooper, 1994). Notably, mutation of the glutamate residue abolishes proteolytic activity whereas substrate binding still occurs (Guélin *et al.*, 1994; Arlt *et al.*, 1996; Leonhard *et al.*, 1996; Arlt *et al.*, 1998).
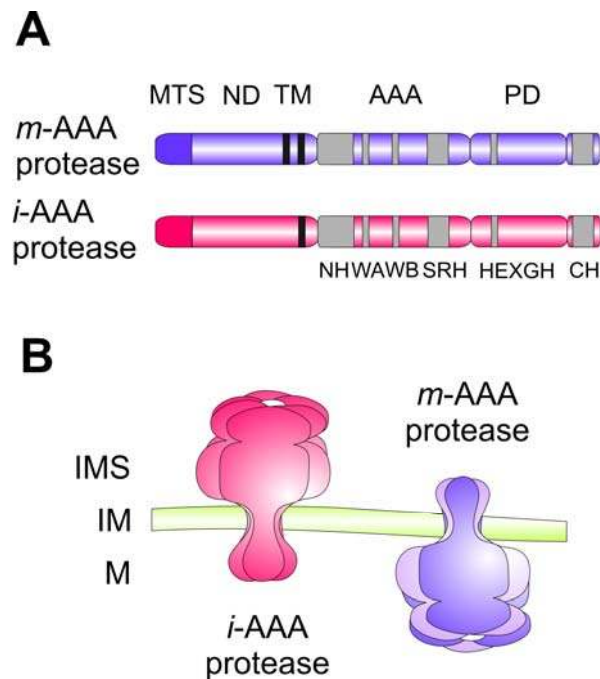
Figure 1.2 Mitochondrial AAA proteases.
(A) Domain structure of AAA proteases. The N-terminal mitochondrial targeting sequence (MTS) is cleaved off during import into mitochondria. AAA proteases are integrated into the inner membrane with one or two transmembrane segments (TM), respectively. Conserved sequence motifs are displayed in grey. ND, N-terminal domain; AAA, AAA domain; PD, proteolytic domain; NH, N-terminal helices; WA, Walker A-motif; WB, Walker B-motif; SRH, second region of homology, HEXGH, proteolytic center; CH, C-terminal helices.
(B) Topology of AAA proteases in the mitochondrial inner membrane (IM). Catalytic domains of the *i*-AAA and the *m*-AAA protease are located in the intermembrane space (IMS) and the matrix (M), respectively. AAA protease subunits share a common domain structure. The stoichiometry and arrangement of the subunits are speculative (Figure from Koppen and Langer, 2007).

Based on crystal structures of the homologous bacterial FtsH protease, a hexameric ring-like assembly of AAA proteases is proposed which consists of two structurally separated rings composed of the proteolytic and the AAA domains, respectively (Bieniossek *et al.*, 2006; Suno *et al.*, 2006). The AAA domains facing the membrane form a narrow central pore which allows substrates to enter the proteolytic chamber inside the complex. The mitochondrial AAA proteases recognize misfolded, solvent-exposed domains of substrates, loops of multi-

spanning membrane proteins or short terminal protein tails protruding from the membrane bilayer (Leonhard *et al.*, 1999). The involvement of the *i*-AAA or the *m*-AAA protease in the degradation of a protein appears to depend on its membrane topology. Further determinants for substrate specificity based on the chaperone-like properties of AAA proteases were recently identified in the *i*-AAA protease of yeast: the C-terminal helices-region (CH-region) within the proteolytic domain and the N-terminal helices-region (NH-region) which is part of the AAA domain (Graef *et al.*, 2007). They form helical structures and, according to the available crystal structure of FtsH from *Thermotoga maritima,* are located at the surface of the catalytic domain (Bieniossek *et al.*, 2006). This positions them ideally for an initial encounter with substrate proteins. Translocation of substrates into the proteolytic chamber was shown to depend on a conserved loop motif which is located in the AAA domain of other hexameric AAA^{+}-proteins and protrudes into the central chamber (Wang *et al.*, 2001; Graef and Langer, 2006).

1.2.2 Protein quality control by AAA proteases

The mitochondrial inner membrane harbours the respiratory chain complexes which are essential for cellular function. The assembly of the respiratory chain complexes depends on the coordinated expression and oligomerization of nuclear- and mitochondrial-encoded subunits. A quality control system is present to ensure that these complexes assemble properly and that unassembled subunits do not accumulate. To avoid defects caused by an accumulation of unassembled or misfolded proteins in the inner membrane, these proteins must be efficiently recognized, extracted from the membrane and degraded by the mitochondrial AAA proteases (Fig. 1.3 A) (Langer, 2000; Koppen and Langer, 2007).

The functions of AAA proteases in mitochondria are best characterized in the yeast *Saccharomyces cerevisiae.* Here, all observed defects associated with deletion of the *i*- or the *m*-AAA protease can be attributed to a loss of proteolytic activity as point mutations in the proteolytic sites result in the same phenotypes (Arlt *et al.*, 1996; Leonhard *et al.*, 1996; Weber *et al.*, 1996). In yeast, the homo-oligomeric *i*-AAA protease is composed of Yme1 subunits whereas the hetero-oligomeric *m*-AAA protease complex consists of the highly related subunits Yta10 (Afg3) and Yta12 (Rca1) (Arlt *et al.*, 1996; Leonhard *et al.*, 1996). The *m*-AAA protease was shown to degrade a number of non-assembeld mitochondrially encoded respiratory chain subunits of Complex II, IV and V and a peripheral membrane subunit of

Complex V, Atp7 (Arlt *et al.*, 1996; Korbel *et al.*, 2004). Deletion of the *m*-AAA protease in yeast results in respiratory deficiency due to the loss of assembled respiratory chain and F_1F_O-ATP synthase complexes (Arlt *et al.*, 1998; Galluhn and Langer, 2004). So far, only a few quality control substrates of the *i*-AAA protease have been identified. These include the non-assembled integral membrane proteins cytochrome *c* oxidase subunit 2 (Cox2), prohibitin 1 and prohibitin 2 as well as the soluble NADH dehydrogenase (Nde1) (Pearce and Sherman, 1995; Weber *et al.*, 1996; Kambacheld *et al.*, 2005).
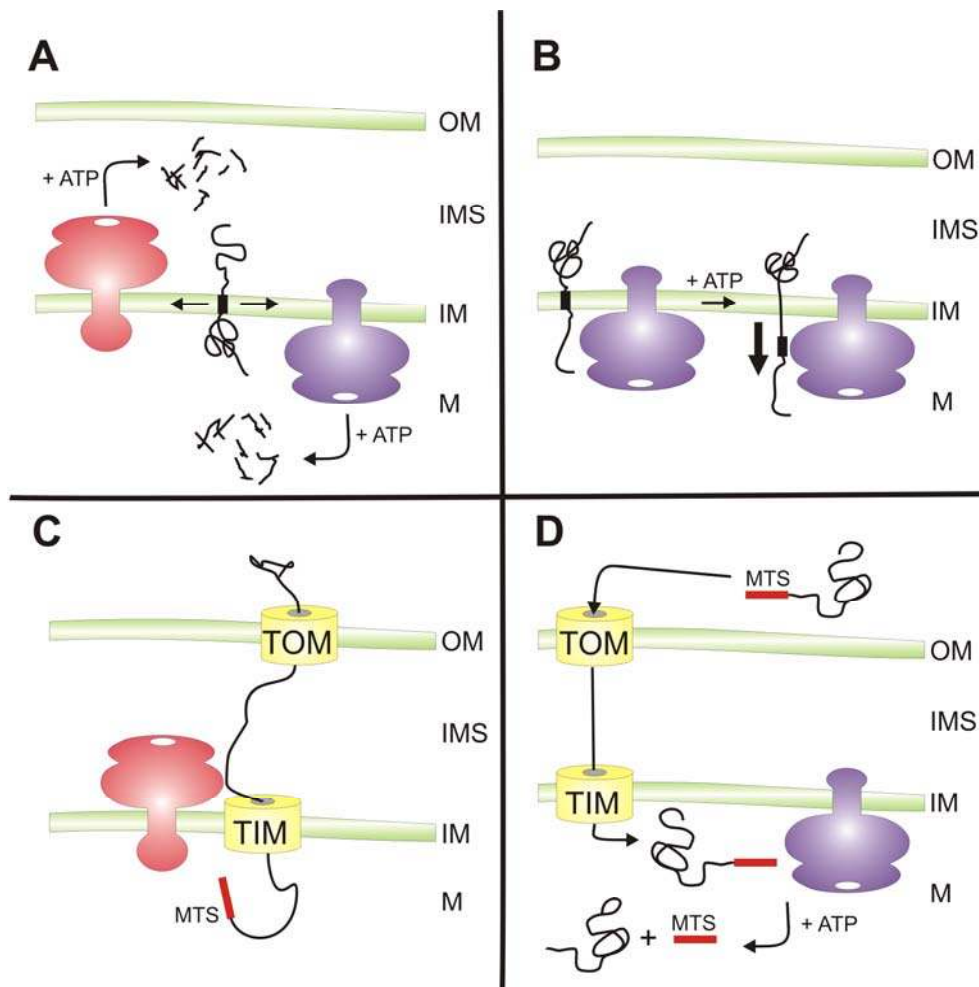
Figure 1.3 Functions of AAA proteases in mitochondria.
(A) Protein quality control of inner membrane proteins. AAA proteases degrade non-assembled and damaged proteins to peptides after their dislocation from the membrane. **(B)** ATP-dependent membrane dislocation of proteins. The *m*-AAA protease mediates the vectorial dislocation of Ccp1 precursor protein independent of its proteolytic function followed by Pcp1-mediated intramembrane cleavage. **(C)** Protein import into mitochondria. Import of mammalian PNPase into yeast mitochondria is dependent on the *i*-AAA protease. **(D)** Protein processing. The mitochondrial targeting sequence of yeast MrpL32 precursor is cleaved during import by the *m*-AAA protease to obtain mature MrpL32. OM, outer mitochondrial membrane; IMS, intermembrane space; IM, inner membrane; M, matrix; TOM, translocase of the outer membrane; TIM, translocase of the inner membrane; MTS, mitochondrial targeting sequence (Figure modified from Koppen and Langer, 2007).

Recently, non-proteolytic functions of AAA proteases have been identified in yeast. The maturation of cytochrome *c* peroxidase (Ccp1), a ROS-scavenger in the intermembrane space, is performed by two successive processing steps. During import, the bipartite targeting sequence of the Ccp1 precursor is removed by the dual actions of the *m*-AAA protease and the rhomboid protease Pcp1 (Esser *et al.*, 2002). Surprisingly, cleavage by Pcp1 is dependent solely on the ATP-dependent membrane dislocation of Ccp1 by the *m*-AAA protease but not on its proteolytic activity (Fig. 3.1 B) (Tatsuta *et al.*, 2007). Thus, the *m*-AAA protease is suggested to ensure the correct positioning of Ccp1 in the membrane allowing intramembrane cleavage by Pcp1. Notably, a mammalian homologue of the ROS-scavenger Ccp1 does not exist.

A similar non-proteolytic role has been suggested for the *i*-AAA protease during import of polynucleotide phosphorylase (PNPase) (Rainey *et al.*, 2006). PNPase contains an N-terminal targeting signal that is cleaved off by MPP in the matrix followed by translocation of mature PNPase into the IMS. Import of mammalian PNPase into yeast mitochondria was shown to depend on the presence of the *i*-AAA protease subunit Yme1 (Fig. 3.1 C). However, PNPase is neither processed nor degraded by the *i*-AAA protease suggesting a non-proteolytic function of Yme1 in the translocation of PNPase across the inner membrane.

1.2.3 Processing functions of AAA proteases

ATP-dependent proteases do not only function in cellular protein quality control by degrading misfolded proteins to peptides (Sauer *et al.*, 2004; Ciechanover, 2005; Hanson and Whiteheart, 2005). Moreover, they were shown to activate regulatory proteins with crucial cellular functions by proteolytic processing (Rape and Jentsch, 2004). This is exemplified by the cytosolic protein degradation machinery, the 26S proteasome, which partially degrades several transcription factors and thereby regulates gene expression (Palombella *et al.*, 1994; Sasaki *et al.*, 1999; Hoppe *et al.*, 2000). The mechanism how the complete proteolysis of proteins is prevented is currently not fully understood. Increasing evidence suggest that the folding state determines the fate of substrates bound by energy-dependent proteases (Piwko and Jentsch, 2006). To be degraded completely, the substrate must be unfolded in an ATP-dependent manner before entering the proteolytic cavity (Sauer *et al.*, 2004). Simple sequence stretches which precede a tightly folded domain may limit the unfolding capacity and result in

the dissociation of a processed substrate from the protease (Kenniston *et al.*, 2005; Tian *et al.*, 2005; Hoyt *et al.*, 2006).

Recently, usage of a proteolytic-inactive variant of the *m*-AAA protease as a substrate trap in yeast led to the identification of MrpL32, a subunit of the large ribosome particle in mitochondria (Grohmann *et al.*, 1991; Nolden *et al.*, 2005). The *m*-AAA protease mediates the proteolytic maturation of nuclear-encoded MrpL32 upon import into mitochondria (Fig. 1.3 D) (Nolden *et al.*, 2005). Processing of MrpL32 is necessary for its assembly into ribosomes (Fig. 1.4). Mitochondrial ribosomes lacking MrpL32 are functionally inactive and therefore mitochondrial translation is drastically impaired in the absence of the *m*-AAA protease. As essential subunits of the respiratory chain complexes are encoded in the mitochondrial genome, the lack of respiratory chain complexes in *m*-AAA protease-deficient yeast cells can solely be attributed to an impaired processing of MrpL32.
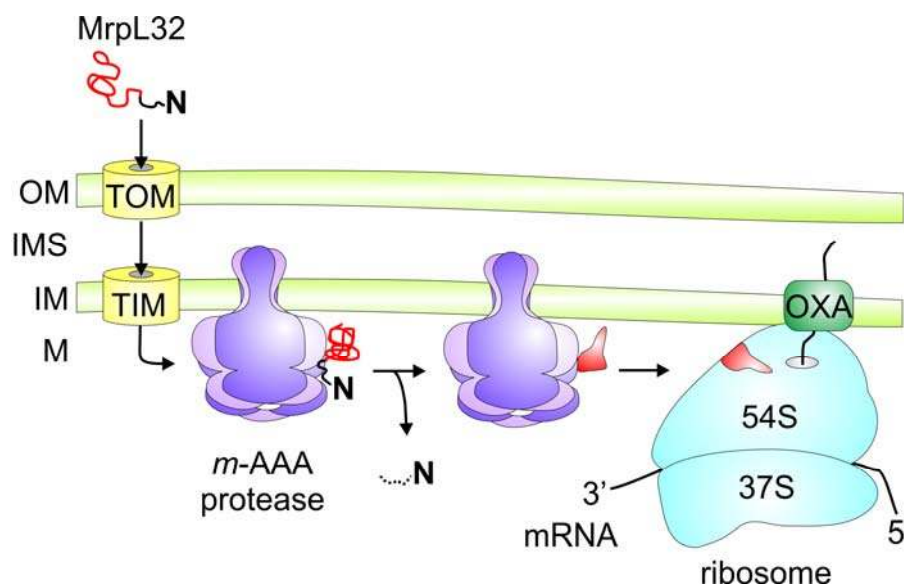
Figure 1.4 Processing of MrpL32 by the *m*-AAA protease.
The *m*-AAA protease cleaves off the N-terminal mitochondrial targeting sequence of MrpL32 precursor in the mitochondrial matrix. Processing of MrpL32 is most likely accompanied by a conformational change which allows the assembly of MrpL32 with pre-assembled mitochondrial ribosomes in close proximity to the inner membrane. OM, outer membrane; IMS, intermembrane space; IM, inner membrane; M, matrix; TOM, translocase of the outer membrane; TIM translocase of the inner membrane; OXA1, membrane insertion machinery containing Oxa1 (Figure from Koppen and Langer, 2007).

Downregulation of the *i*-AAA protease in mammalian cells using RNA interference identified the mitochondrial fusion component OPA1 as a putative substrate whose processing is affected by the *i*-AAA protease (Griparic *et al.*, 2007; Song *et al.*, 2007). OPA1 is present in different isoforms which besides alternative splicing are produced by proteolytic processing at two different cleavage sites. Cleavage at one of the processing sites is dependent on the *i*-AAA protease. However, whether the *i*-AAA protease directly cleaves OPA1 in a site-specific manner is not clear yet.

1.3 Mammalian m-AAA proteases

AAA proteases are conserved from yeast to mammals and share a high sequence identity (Fig. 1.5). Functional conservation of the *i*-AAA and the *m*-AAA protease was demonstrated by complementation studies in yeast (Shah *et al.*, 2000; Atorino *et al.*, 2003; Nolden *et al.*, 2005). A functional homologue of the *i*-AAA protease subunit Yme1 was identified in humans and mice, named Yme1l1 (Yme1-like gene 1) (Coppola *et al.*, 2000; Shah *et al.*, 2000). Three potential subunits of the *m*-AAA protease were found in mice: the two homologues subunits Afg3l1 (AFG3-like gene 1) and Afg3l2 (AFG3-like gene 2) with a sequence identity of 70% and additionally the subunit paraplegin (Casari *et al.*, 1998; Shah *et al.*, 1998; Banfi *et al.*, 1999). Notably, AFG3L1 is not expressed in humans and exists only as a pseudogene so that the human *m*-AAA protease is composed of AFG3L2 and paraplegin subunits (Kremmidiotis *et al.*, 2001).
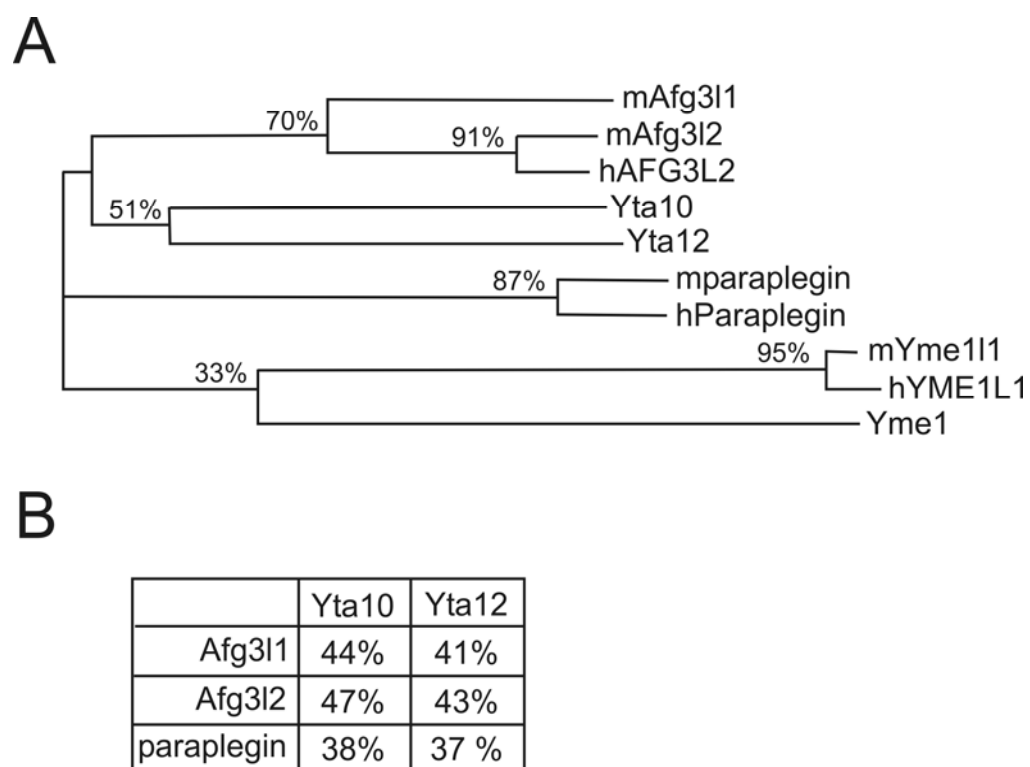
Figure 1.5 Phylogenetic relationships among mitochondrial AAA metalloproteases.
(A) Phylogenetic tree of the *i*-AAA and the *m*-AAA protease subunits. Multiple alignments of mitochondrial AAA protease subunits in yeast (Yta10, Yta12 and Yme1), mice (mAfg3l1, mAfg3l2, mparaplegin, mYme1l1) and human (hAFG3L2, hParaplegin, hYME1L1) were used to create a phylogenetic tree (www.ebi.ac.uk/Tools/clustalw2); Matrix: Gonnet 250. Sequence identities are indiciated in percent. (B) Pairwise identity comparison of yeast (Yta10, Yta12) and murine *m*-AAA protease subunits (Afg3l1, Afg3l2, paraplegin).

The *m*-AAA protease assembles with prohibitins into a large supercomplex in yeast and mammals (Steglich *et al.*, 1999; Metodiev, 2005). Prohibitins are multimeric complexes embedded in the mitochondrial inner membrane composed of the highly conserved subunits prohibitin 1 (Phb1) and prohibitin 2 (Phb2) (Steglich *et al.*, 1999; Nijtmans *et al.*, 2000; Artal-Sanz *et al.*, 2003). Deletion of prohibitins in yeast results in accelerated protein degradation by the *m*-AAA protease suggesting a regulatory function of prohibitins for the *m*-AAA protease (Steglich *et al.*, 1999; Metodiev, 2005). However, neither the molecular mechanism of this regulation is clear nor if this regulatory function of prohibitins is conserved in mammals.

1.3.1 Variable subunit composition of *m*-AAA protease complexes

Initial complementation studies identified the mammalian hetero-oligomeric complex of Afg3l2 and paraplegin as the functional orthologue of the yeast *m*-AAA protease (Atorino *et al.*, 2003; Nolden *et al.*, 2005). Interestingly, recent evidence indicates that, unlike their yeast counterparts, mammalian Afg3l2 as well as Afg3l1 are able to form homo-oligomeric complexes upon expression in yeast cells (Koppen *et al.*, 2007). Furthermore, these homo-oligomeric complexes exert proteolytic activity in yeast mitochondria and could substitute for the function of the yeast *m*-AAA protease (Koppen *et al.*, 2007). However, no evidence was obtained for the ability of paraplegin to homo-oligomerize (Koppen *et al.*, 2007). It was only found to assemble as part of hetero-oligomeric *m*-AAA protease complexes together with Afg3l1, Afg3l2 or both. The different homo- and hetero-oligomeric *m*-AAA protease complexes restored the respiratory growth in yeast cells lacking Yta10 and Yta12 because of their ability to process MrpL32 (Koppen *et al.*, 2007). This suggests that mammalian *m*-AAA protease complexes with variable subunit composition can exert housekeeping functions and functionally substitute for the yeast *m*-AAA protease. Co-immunprecipitation and immunodepletion studies in human and murine mitochondria provided evidence for the existence of different *m*-AAA protease complexes *in vivo* (Fig. 1.6) (Koppen *et al.*, 2007).
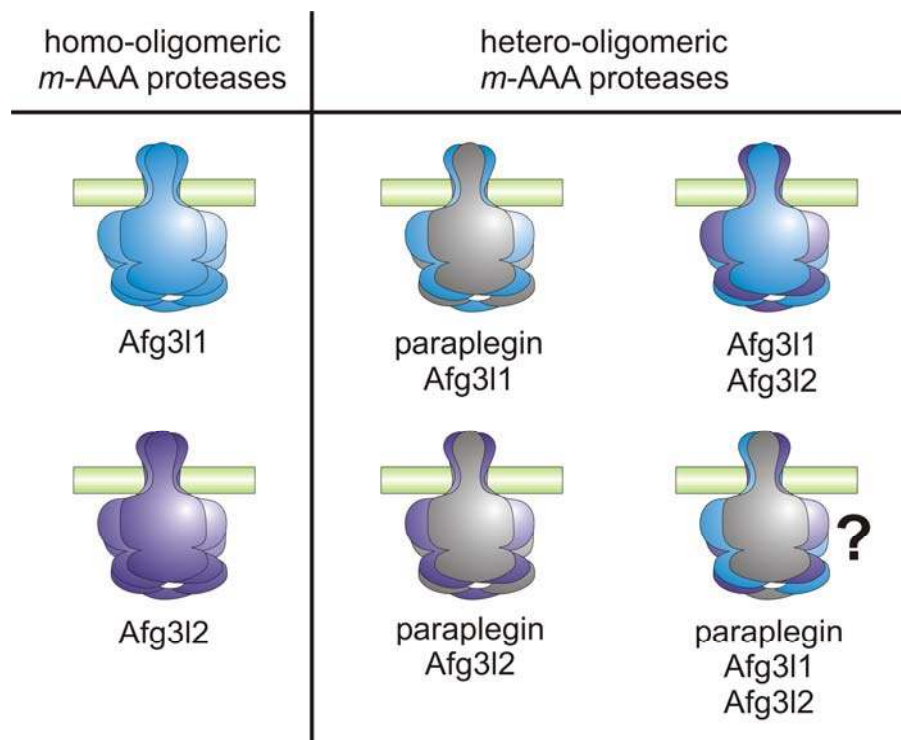
Figure 1.6 Mammalian *m*-AAA protease isoenzymes with variable subunit composition.
Immunodepletion and co-immunopreciptation experiments in mammalian mitochondria together with yeast complementation studies suggest the existence of at least five different *m*-AAA protease isoenzymes. The presence of a complex consisting of murine paraplegin, Afg3l1 and Afg3l2 is speculative. In human, only two AAA protease isoenzymes exist consisting of either paraplegin and AFG3L2 or AFG3L2 alone (Figure from Koppen and Langer, 2007).

1.3.2 The *m*-AAA protease paraplegin is involved in the neurodegenerative disease hereditary spastic paraplegia (HSP)

First insights into the role of mammalian *m*-AAA protease were obtained by the involvement of paraplegin gene (*SPG7*) mutations in the neurodegenerative disease hereditary spastic paraplegia (HSP) (Casari *et al.*, 1998). Neurodegenerative diseases are characterized by the progressive loss of a specific subset of neurons. Mitochondrial functions are particularly important in the nervous system and essential for versatile neuronal processes (Milakovic and Johnson, 2005; Lin and Beal, 2006; Manczak *et al.*, 2006). Many common neurodegenerative disorders such as Alzheimer`s, Parkinson`s and Huntington`s disease are linked to mitochondrial dysfunctions.

Hereditary spastic paraplegia (HSP) comprises a genetically heterogeneous group of neurodegenerative disorders (Fink, 2003; Soderblom and Blackstone, 2006; Depienne *et al.*, 2007). The major pathological feature is a progressive degeneration of the longest axons in the body, those of the corticospinal tracts and, to a lesser extent, the fasiculi gracilis. The axonal degeneration starts from the synaptic terminal and progresses towards the cells body. According to the patient`s symptoms, the disease is classified into "pure" and "complicated" forms. Besides progressive spasticity and weakness in the lower limbs, complicated forms are characterized by additional neurological symptoms including ataxia, mental retardation, optic atrophy, dementia and retinopathy (Harding, 1983).

So far, disease-associated mutations have been identified in 15 different genes (Depienne *et al.*, 2007). Based on known functions of the gene products, two major pathophysiological mechanisms have been implicated in autosomal forms of HSP (Fink, 2003; Soderblom and Blackstone, 2006). Intracellular trafficking and more particular axonal transport, appears to be impaired by mutations in gene products such as spastin (*SPG4*), atlastin (*SPG3A*) and kinesin heavy chain KIF5A (*SPG10*) (McDermott *et al.*, 2003; Xia *et al.*, 2003; Evans *et al.*, 2006; Sanderson *et al.*, 2006). Mutations in spastin are the most prevalent cause for autosomal forms of HSP (Hazan *et al.*, 1999). Spastin was shown to interact with microtubules and promote their disassembly (Errico *et al.*, 2002; Evans *et al.*, 2005). Mice lacking spastin display axonal swellings associated with accumulations of organelles and cytoskeletal compounds suggesting an impairment of axonal transport *in vivo* (Tarrade *et al.*, 2006).

Mitochondrial dysfunction is the second molecular mechanism implicated in the pathogenesis of HSP. Besides paraplegin, a mutation in the mitochondrial chaperone HSP60 (*SPG13*) has been identified in HSP (Casari *et al.*, 1998; Hansen *et al.*). Recently, two other disease-associated proteins, spartin (*SPG20*) and REEP1 (*SPG31*), have been localised to

mitochondria (Lu *et al.*, 2006; Züchner *et al.*, 2006). Whereas the function of REEP1 in mitochondria has not been elucidated yet, spartin was suggested to be involved in microtubule-mediated mitochondrial transport further underlining the roles of defective intracellular trafficking and mitochondrial integrity in the pathogenesis of HSP.

Several loss-of-function mutations in the paraplegin gene *SPG7* are associated with a autosomal-recessive form of HSP complicated by optic, cerebellar and cerebral atrophy (Casari *et al.*, 1998; McDermott *et al.*, 2001; Wilkinson *et al.*, 2004). Muscle biopsies from severely affected patients revealed defects in mitochondrial oxidative phosphorylation (Casari *et al.*, 1998; McDermott *et al.*, 2001). Reduced amounts of assembled complex I which result in a mild impairment of Complex I activity could by detected in muscles and fibroblasts derived from HSP patients (Wilkinson *et al.,* 2004; Atorino *et al.*, 2003). This might be consistent with a chaperone-like function of paraplegin in Complex I assembly (Atorino *et al.*, 2003).

1.3.3 Paraplegin-deficient mice as a model for HSP

To further analyze the molecular mechanisms underlying the axonal degeneration and the intriguing tissue specificity, a mouse model for HSP caused by loss-of-function mutations in the *SPG7* gene was generated by gene targeting (Ferreirinha *et al.*, 2004). Paraplegin-deficient mice display a progressive retrograde degeneration of long axons in the spinal cord, thus replicating central features of the human disease. At about 4 months of age, they start to develop a motor deficit together with the appearance of morphologically abnormal and enlarged mitochondria in distal regions of affected axons. Only three months later, first signs of axonal swelling were observed followed by axonal degeneration. The swelling of axons resulted from an accumulation of neurofilaments and organelles, often observed upon axonal transport disturbances. In line with this, retrograde axonal transport was slightly delayed in 17-month-old paraplegin-deficient mice (Ferreirinha *et al.*, 2004).

The occurrence of the mitochondrial phenotype together with the motor deficit several months prior to axonal degeneration suggests that mitochondrial dysfunction is the primary cause for the axonal defect. However, besides mitochondrial morphological abnormalities, key mitochondrial functions, such as respiratory chain activity and ATP synthesis are not significantly impaired in spinal cords of 17-month-old $Spg7^{-/-}$-mice (Ferreirinha *et al.*, 2004). Only in spinal cords of 23-month-old $Spg7^{-/-}$-mice a minor defect in ATP synthesis could be observed. Nevertheless, it should be emphasized that only a subset of mitochondria is affected

in specific neurons of the spinal cord and therefore represents only a minor fraction. Thus, only biochemical analysis of paraplegin-deficient mitochondria from affected axons and synapses might clarify a putative role of respiratory chain dysfunction in the pathogenesis of HSP.

So far, the primary defect in paraplegin-deficient mitochondria causative for the axonal degeneration is not clear. The yeast *m*-AAA protease degrades a number of non-assembled respiratory chain subunits (Arlt *et al.*, 1996; Korbel *et al.*, 2004). Thus, an accumulation of non-assembled inner membrane proteins might cause the pathology of HSP associated with mutations in paraplegin. A similar mechanism was proposed for HSP caused by mutations in the mitochondrial chaperonin Hsp60 (Hansen *et al.*, 2002). However, this hypothesis contradicts that protein aggregates have never been detected upon inactivation of *m*-AAA proteases.

New insights into potential molecular events that cause HSP might be provided by the recent identification of the *m*-AAA protease-dependent processing of the ribosomal subunit MrpL32 in yeast (Claypool and Koehler, 2005; Nolden *et al.*, 2005; Rugarli and Langer, 2006). A high sequence conservation of MrpL32 and *m*-AAA protease subunits as well as successful complementation studies in yeast indicate a conserved mechanism which regulates mitochondrial protein synthesis (Nolden *et al.*, 2005). Reconstitution of the mammalian *m*-AAA protease in yeast provided direct evidence for the ability to cleave murine Mrpl32 (Nolden *et al.*, 2005). It remains to be answered, if a mitochondrial translation defect caused by an impaired Mrpl32 maturation is the underlying mechanism for the axonal degeneration in *SPG7*-linked HSP. The neuron-specific phenotype of HSP seems to be difficult to reconcile with a mitochondrial translation defect, a housekeeping function in mitochondria. However, variable clinical phenotypes with mitochondrial dysfunction in different tissues have been observed in patients who carry mutations in mitochondrial DNA affecting mitochondrial protein synthesis (Jacobs, 2003; Jacobs and Turnbull, 2005; Taylor and Turnbull, 2005). Tissue-specific phenotypes might be rationalized by different sensitivities of various cells for mitochondrial dysfunction (Rossignol *et al.*, 2003). Tissues with a high energy demand like brain, muscle and heart are known to be vulnerable to an impairment of mitochondrial functions. Besides Mrpl32, the existence of additional tissue-specific substrates of *m*-AAA proteases can be envisioned which contribute to the axonal degeneration in HSP.

Recently, mice which carry deletions or homozygous mutations in the gene coding for the *m*-AAA protease subunit Afg3l2 have been described (Maltecca *et al.*, 2008). These mice die at postnatal day 16 and exhibit a severe defect in axonal development characterized by

delayed myelination and impairment of axonal radial growth in the central and peripheral nervous system (Maltecca *et al.*, 2008). Swollen and giant mitochondria with disrupted cristae membranes are detected in motor and sensory neurons (Maltecca *et al.*, 2008). Furthermore, the enzymatic activities of Complex I and III were found to be impaired in brain and spinal cord mitochondria isolated from *Afg3l2* mutant mice (Maltecca *et al.*, 2008). Thus, the neuron-specific phenotypes of paraplegin-deficient and *Afg3l2* mutant mice reveal crucial functions of the *m*-AAA protease in neuronal mitochondria.

1.4   Mitochondrial dynamics

Mitochondria are highly dynamic organelles in eukaryotic cells which move along cytoskeletal tracks and constantly change their shape by frequent fusion and fission events (Chan, 2006; Boldogh and Pon, 2007; Hoppins *et al.*, 2007). Maintenance of mitochondrial morphology in cells at steady-state is secured by a balance between fusion and fission events (Okamoto and Shaw, 2005). When mitochondrial fusion is reduced, mitochondria fragment due to ongoing fission (Fig. 1.7). Conversely, shifting the balance towards mitochondrial fusion results in elongated and highly interconnected mitochondria (Fig. 1.7). The control of mitochondrial shape is required for correct segregation and distribution of mitochondria. In addition, fission and fusion are also important for maintaining the bioenergetic function of mitochondria (Chan, 2006; Detmer and Chan, 2007). Therefore, mitochondrial dynamics have key roles in mammalian development, several neurodegenerative diseases and apoptosis.
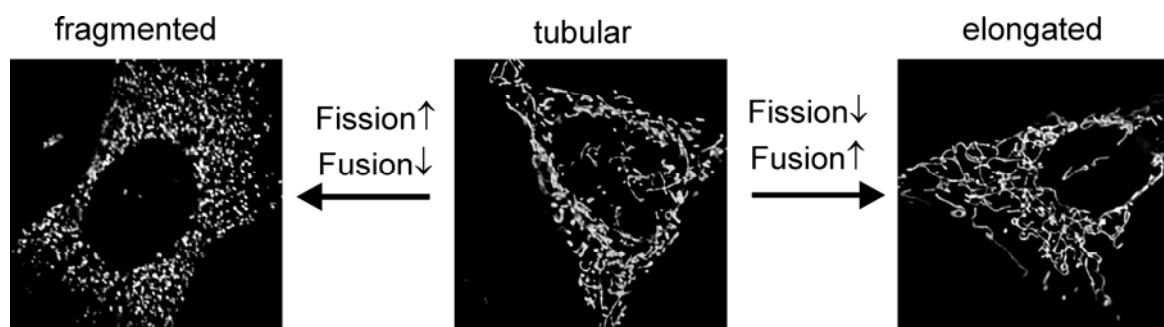
Figure 1.7 Mitochondrial dynamics.
Mitochondrial morphology is determined by the balance between fusion and fission events. In wt MEFs mitochondria form tubules of variable length (central panel). Shifting the balance towards fusion by either inhibition of fission and/or activation of fusion results in elongated and highly interconnected mitochondria (right panel). Conversely, when mitochondrial fission is induced and/or fusion is blocked, mitochondria fragment (left panel).

Mitochondrial fusion mainly plays a protective role by allowing the mixing of mitochondrial contents such as mtDNA molecules and presumably lipids, proteins and metabolites (Legros *et al.*, 2004; Detmer and Chan, 2007). Disruption of mitochondrial fusion in fibroblasts results in poor cell growth, a widespread heterogeneity of mitochondrial

membrane potential and decreased cellular respiration (Chen *et al.*, 2005). The dependency of mitochondrial respiration on fusion was shown to be caused by the loss of mtDNA nucleoids in the majority of fragmented mitochondria (Chen *et al.*, 2007). These nucleoid-deficient mitochondria lack essential respiratory subunits encoded by mtDNA and have no pathway for regaining either the requisite proteins or mtDNA. In fusion-competent cells defective mitochondria might retrieve essential components by fusion with functional mitochondria. This molecular exchange ensures that cells maintain a functional mitochondrial network with respiratory activity (Chen *et al.*, 2005; Chen *et al.*, 2007).

Disruption of mitochondrial fission in *C. elegans* results in embryonic lethality pointing also to an essential function of fission in cellular development (Labrousse *et al.*, 1999). In mammals, mitochondrial fission has been shown to be important for mitochondrial inheritance and distribution of mitochondria throughout the cell (Warren and Wickner, 1996; Hoppins *et al.*, 2007; Knott *et al.*, 2008). In addition, mitochondrial fission facilitates apoptosis (Suen *et al.*, 2008). A delay or reduction in apoptosis is observed when mitochondrial fragmentation is blocked (Suen *et al.*, 2008). Conversely, mitochondrial fragmentation in response to stress might also protect cells from apoptosis by sequestering damaged mitochondria from the intact mitochondrial network (Kim *et al.*, 2007; Tatsuta and Langer, 2008). Consequently, dysfunctional and fragmented mitochondria can be eliminated by autophagy before apoptosis is induced through the mitochondrial pathway.

The mitochondrial fusion and fission machineries have been best characterized in *S. cerevisae* (Hoppins *et al.*, 2007). In mammals, orthologues of most fusion and fission proteins exist indicating that the mechanisms of mitochondrial membrane fusion and fission are highly conserved (Chan, 2006). Several large dynamin-related GTPases which are essential for mitochondrial dynamics have been identified. Dynamin-1 (Dnm1) in yeast and its mammalian homologue dynamin-related protein (Drp1) are targeted to the mitochondrial outer membrane to promote mitochondrial fission (Otsuga *et al.*, 1998; Smirnova *et al.*, 2001). Mitochondrial fusion requires components of the outer and inner mitochondrial membrane (Hoppins *et al.*, 2007). Studies in yeast identified the proteins Fzo1 and Mgm1 as mediators of outer and inner membrane fusion, respectively (Hermann *et al.*, 1998; Sesaki *et al.*, 2003; Wong *et al.*, 2003; Meeusen *et al.*, 2006). The mammalian orthologues of Fzo1 are mitofusin 1 and 2 (Mfn1 and 2) (Fig. 1.8 A) (Santel and Fuller, 2001; Legros *et al.*, 2002). OPA1 (Optic atrophy 1) is the functional homologue of Mgm1 in mammals (Fig. 1.8 A) (Alexander *et al.*, 2000; Delettre *et al.*, 2000; Olichon *et al.*, 2003).

Intriguingly, inherited loss-of-function mutations of *MFN2* or *OPA1* cause progressive neuropathies in humans. *MFN2* mutations lead to Charcot-Marie-Tooth Type 2A (CMT2A), a peripheral neuropathy characterized by loss of motor and sensory neurons (Züchner and Vance, 2005). Mutations in *OPA1* result in autosomal dominant optic atrophy (ADOA) characterized by degeneration of retinal ganglion cells (Alexander *et al.*, 2000; Delettre *et al.*, 2000). Thus, a loss of mitochondrial fusion proteins and the consequent continuous fission appear to play a causal role in the initiation of neurodegeneration (Knott *et al.*, 2008).

1.4.1 Outer mitochondrial membrane fusion

Mfn1 and Mfn2 are anchored to the outer mitochondrial membrane by a bipartite transmembrane region (Fig. 1.8 A) (Rojo *et al.*, 2002). The N- and C-terminal regions protrude into the cytosol (Fig. 1.8 B). Besides a large GTPase domain, they harbour two characteristic hydrophobic heptad repeat regions which are predicted to form helical coiled-coil structures (Fig. 1.8 A). Through interactions of their coiled-coil structures the mitofusins are proposed to form hetero- and homo-oligomeric structures in *trans* and thereby tether outer membranes of adjacent mitochondria (Fig. 1.8 B) (Chen *et al.*, 2003; Ishihara *et al.*, 2004; Koshiba *et al.*, 2004). Cells lacking either Mfn1 or Mfn2 show greatly reduced mitochondrial fusion and consequently mitochondria are highly fragmented (Chen *et al.*, 2003; Eura *et al.*, 2003; Chen *et al.*, 2005). However, only in the absence of both mitofusins, mitochondrial fusion is completely abolished resulting in not only severely fragmented mitochondria but also reduced respiratory capacity (Chen *et al.*, 2005). Thus, Mfn1 and Mfn2 seem to have similar functions in mitochondrial fusion and can functionally replace each other when overexpressed (Detmer and Chan, 2007). Nevertheless, loss of either Mfn1 or Mfn2 leads to distinct phenotypes on the cellular level as well as in mouse models (Chen *et al.*, 2003; Eura *et al.*, 2003; Chen *et al.*, 2005; Chen *et al.*, 2007). These distinct phenotypes can be explained by tissue-specific differences in their expression levels (Detmer and Chan, 2007). Moreover, several observations point to different properties of Mfn1 and Mfn2. First, OPA1-mediated mitochondrial fusion is only dependent on Mfn1 but not on Mfn2 (Cipolat *et al.*, 2004). Second, an *in vitro* mitochondrial tethering assay revealed a higher tethering activity for Mfn1 than for Mfn2 (Ishihara *et al.*, 2004).
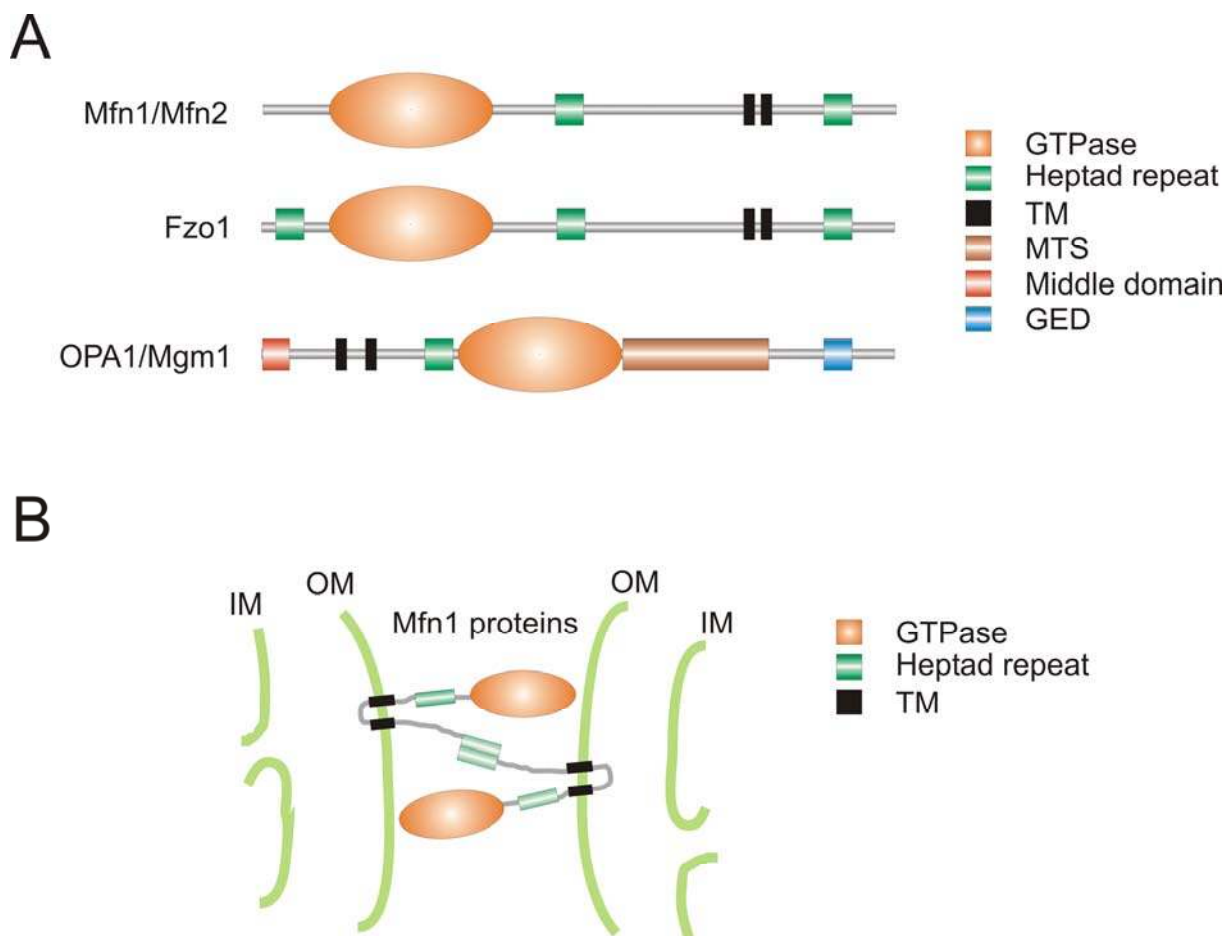
Figure 1.8 Mitochondrial fusion proteins.
(A) Schematic structure of mitochondrial GTPases involved in mitochondrial fusion in mammals and the yeast *S. cerevisiae*. These proteins contain a GTPase domain (GTPase) and hydrophobic heptad repeats. Mitofusins (Mfn1/Mfn2) and Fzo1 also contain a bipartite transmembrane domain (TM). OPA1/Mgm1 contains an N-terminal mitochondrial targeting sequence (MTS) followed by two putative transmembrane domains. The middle domain and the GTPase effector domain (GED) are characteristic for dynamin familiy members. **(B)** Mitochondrial tethering by Mfn1. Mfn1 is integrated into the outer membrane by its bipartite transmembrane region. Most of Mfn1 is exposed to the cytosol. Intermolecular interactions between Mfn1 proteins on opposing mitochondria are mediated by the C-terminal heptad repeat regions and result in tethering of mitochondrial outer membranes (OM). Inner membrane, IM. (modified from Chan *et al.*, 2006).

1.4.2 Inner mitochondrial membrane fusion

The dynamin-related protein OPA1, which is mainly localized at the inner mitochondrial membrane, is a further essential component of the mitochondrial fusion machinery in mammals (Olichon *et al.*, 2003; Chan, 2006; Duvezin-Caubet *et al.*, 2006; Ishihara *et al.*, 2006). OPA1 harbours an N-terminal mitochondrial targeting sequence (MTS) which is cleaved upon mitochondrial import by the mitochondrial processing peptidase (MPP) (Misaka

et al., 2002; Olichon *et al.*, 2002). The MTS is followed by short hydrophobic stretches and a coiled-coil domain located directly in front of the GTPase domain (Fig. 1.8 A). A middle domain and a further coiled-coil domain known as GTPase effector domain (GED) are present at the C-terminus of OPA1 (Fig. 1.8 A).

OPA1 is encoded by a single gene which gives rise to eight splice variants resulting from alternative splicing of the exons 4, 4b and 5b (Delettre *et al.*, 2001). The *OPA1* gene is ubiquitiously expressed with the highest levels in the retina, brain and muscle (Alexander *et al.*, 2000). Notably, differences in the relative abundance of each OPA1 splice variants in various tissues have been observed (Delettre *et al.*, 2001; Olichon *et al.*, 2006). Several long and short protein OPA1 isoforms are produced by a combination of alternative splicing and post-translational proteolytic processing (Duvezin-Caubet *et al.*, 2006; Ishihara *et al.*, 2006). Whereas long OPA1 isoforms are anchored to the inner membrane, short isoforms are only peripherally associated with it (Duvezin-Caubet *et al.*, 2006; Ishihara *et al.*, 2006). Fusion assays in mammalian cells have demonstrated the requirement of both, the short and long isoforms for mitochondrial fusion (Song *et al.*, 2007). *In vitro* studies of mitochondrial fusion in yeast revealed that the orthologue of OPA1, Mgm1, is required for inner membrane fusion, whereas strikingly outer membrane fusion can still occur in the absence of Mgm1 (Meeusen *et al.*, 2006). Similar to the mitofusins, Mgm1 seems to interact with itself in *trans* to tether inner mitochondrial membranes (Meeusen *et al.*, 2006).

Downregulation of OPA1 in MEFs does not only block mitochondrial fusion resulting in fragmentation of mitochondria (Olichon *et al.*, 2003; Cipolat *et al.*, 2004; Lee *et al.*, 2004). Furthermore, mitochondrial fragmentation is accompanied by defects in mitochondrial respiration, highly disorganized cristae in the inner membrane and an increased susceptibility to apoptosis (Olichon *et al.*, 2003; Griparic *et al.*, 2004; Lee *et al.*, 2004; Frezza *et al.*, 2006). Evidence exists that OPA1 has functions in mitochondria which might not be linked to mitochondrial fusion. Recent observations indicate that OPA1 might regulate cristae remodelling during apoptosis via oligomeric self-assembly independent of fusion (Frezza *et al.*, 2006). Moreover, large mtDNA deletions were detected in skeletal muscles of human patients with *OPA1*-linked dominant optic atrophy, thus, pointing to a function of OPA1 in mtDNA maintenance (Amati-Bonneau *et al.*, 2008; Hudson *et al.*, 2008).

1.4.3 Coordination of inner and outer membrane fusion

Analysis of mitochondrial fusion events *in vivo* by time-lapse fluorescence microscopy indicates that outer and inner membrane fusion events are temporarily linked. However, manipulations of mitochondrial fusion *in vitro* and *in vivo* have demonstrated that they can proceed separately and have different requirements (Meeusen *et al.*, 2004; Malka *et al.*, 2005). Dissipation of the mitochondrial membrane potential in mammalian cells selectively inhibits inner membrane fusion but not outer membrane fusion (Malka *et al.*, 2005). Interestingly, outer membrane fusion is directly followed by fission which results in the overall mitochondrial fragmentation observed upon dissipation of the membrane potential (Sesaki *et al.*, 2003; Malka *et al.*, 2005). This indicates that inner membrane fusion might be necessary for outer membrane fusion to occur *in vivo*. However, it is still unclear how these distinct and separate fusion machineries are coupled to each other to temporarily link inner and outer mitochondrial fusion events. In *S. cerevisiae,* a third protein, Ugo1, is part of the mitochondrial fusion machinery (Sesaki and Jensen, 2001). The outer membrane protein Ugo1 has been found to bind Mgm1 and Fzo1, thereby linking inner and outer membrane fusion proteins (Wong *et al.*, 2003; Sesaki and Jensen, 2004). Therefore, this two membrane-spanning complex formed by Ugo1 might play a role in coordinating inner and outer membrane fusion events in yeast. However, no mammalian homologues of Ugo1 have been identified so far.

1.4.4 Regulation of mitochondrial morphology by proteolytic processing of OPA1

Both OPA1 and its yeast orthologue Mgm1 undergo extensive proteolytic processing which controls mitochondrial fusion activity (Herlan *et al.*, 2003; McQuibban *et al.*, 2003; Duvezin-Caubet *et al.*, 2006; Ishihara *et al.*, 2006; Griparic *et al.*, 2007; Song *et al.*, 2007). In contrast to OPA1, processing of Mgm1 in yeast is well characterized and less complex. Mgm1 exists as a long and a short isoform, l-Mgm1 and s-Mgm1, respectively. L-Mgm1 is produced by MPP cleavage of the Mgm1 precursor and is integrated into the inner mitochondrial membrane by the first of its two hydrophobic segments (Fig. 1.9) (Herlan *et al.*, 2003). Alternatively, l-Mgm1 can be further pulled into the matrix until the second hydrophobic region is anchored to the inner membrane (Fig. 1.9). Subsequently, the

mitochondrial rhomboid protease Pcp1 cleaves Mgm1 at a second processing site to produce s-Mgm1 (Herlan *et al.*, 2003; McQuibban *et al.*, 2003). Formation of s-Mgm1 depends on the protein import motor machinery and on high ATP levels in the matrix (Herlan *et al.*, 2004). Both l-Mgm1 and s-Mgm1 are necessary for mitochondrial fusion (Herlan *et al.*, 2003). The deletion of Pcp1 results in the absence of s-Mgm1 and consequently, in loss of mitochondrial fusion activity.
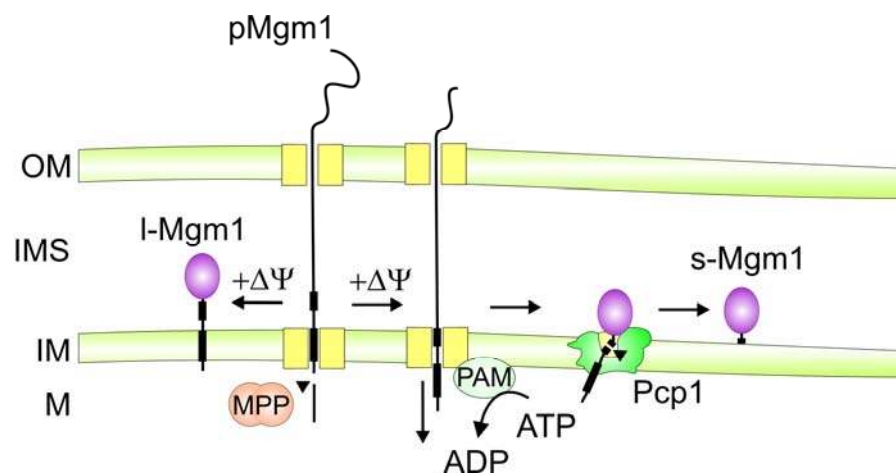
Figure 1.9 Processing of Mgm1 by the rhomboid protease Pcp1.
Newly synthesized Mgm1 precursor (pMgm1) is processed to the long form of Mgm1 (l-Mgm1) by the mitochondrial processing peptidase (MPP) during import into mitochondria and integrated into the inner membrane. Alternatively, l-Mgm1 is cleaved by Pcp1 to generate the short form of Mgm1 (s-Mgm1). Pcp1 cleavage depends on the mitochondrial membrane potential ($\Delta\Psi$), matrix ATP and a functional import motor (PAM). OM, outer membrane; IMS, intermembrane space; IM, inner membrane; M, matrix. (Figure from Koppen and Langer, 2007).

Similar to Mgm1, a balance of short and long OPA1 isoforms is required for mitochondrial fusion activity in mammals (Song *et al.*, 2007). At least five OPA1 isoforms can be detected in mammals resulting from alternative splicing and proteolytic processing (Delettre *et al.*, 2001; Duvezin-Caubet *et al.*, 2006; Ishihara *et al.*, 2006). They consist of two large OPA1-isoforms, L1 and L2, anchored to the inner membrane and three short isoforms, S3-S5, which are only loosely attached to the membrane (Duvezin-Caubet *et al.*, 2006). Long OPA1 forms can be processed constitutively at two different cleavage sites, S1 and S2, which are located N-terminal of the GTPase domain (Ishihara *et al.*, 2006; Duvezin-Caubet *et al.*,

2007). Recently, the *i*-AAA protease Yme1l1 was identified to be involved in cleavage at site S2 (Griparic *et al.*, 2007; Song *et al.*, 2007). However, the physiological consequences of this cleavage are still unclear. Cleavage at site S1 can be induced upon dissipation of the membrane potential (Duvezin-Caubet *et al.*, 2006; Ishihara *et al.*, 2006; Song *et al.*, 2007). This results in a fast conversion of long OPA1 into small OPA1 isoforms accompanied by simultaneous fragmentation of mitochondria. So far, the responsible protease regulating mitochondrial morphology by cleavage at site S1 has not been clearly identified. Nevertheless, besides Yme1l1 two additional proteases have been implicated in processing of OPA1.

The mammalian ortholgoue of Pcp1, PARL can functionally replace Pcp1 in yeast cells and mediate the processing of Mgm1 (McQuibban *et al.*, 2003). The physical interaction of PARL and OPA1, as demonstrated by co-immunopreciptitation studies support a role of PARL in processing of OPA1 (Cipolat *et al.*, 2006). Indeed, the generation of a soluble form of OPA1 was shown to be dependent on PARL (Cipolat *et al.*, 2006). However, this represents only a very minor fraction of OPA1 and the pattern of OPA1 isoforms is not significantly altered in PARL-deficient cells (Cipolat *et al.*, 2006; Duvezin-Caubet *et al.*, 2007). Consistently, PARL-deficient cells display a mitochondrial morphology similar to wt cells. Furthermore, PARL does not process OPA1 when they are co-expressed in yeast (Duvezin-Caubet *et al.*, 2007).

The *m*-AAA protease subunit paraplegin has also been implicated in processing of OPA1 at site S1 (Ishihara *et al.*, 2006). However, OPA1 processing is not affected in paraplegin-deficient cells (Duvezin-Caubet *et al.*, 2007). Since other mammalian *m*-AAA protease subunits form functional *m*-AAA protease complexes, they might substitute for paraplegin in regard to processing of OPA1 (Koppen *et al.*, 2007). Indeed, co-expression of OPA1 with *m*-AAA isoenzymes in yeast revealed that OPA1 can be cleaved by the mammalian *m*-AAA protease (Duvezin-Caubet *et al.*, 2007).

1.5   Aims of the thesis

Mammalian *m*-AAA proteases are composed of the subunits Afg3l1, Afg3l2 and paraplegin. Loss-of-function mutations in the subunit paraplegin are linked to the neurodegenerative disease hereditary spastic paraplegia (HSP). However, the molecular mechanisms which result in the tissue-specific axonal degeneration of HSP patients lacking paraplegin remain to be elucidated. The identification of the ribosomal subunit MrpL32 as a substrate for the *m*-AAA protease in yeast points to a link of HSP to defective mitochondrial protein synthesis. Thus, the first part of this thesis aimed at analyzing the conservation of the *m*-AAA protease-dependent processing of Mrpl32 in mammals. The usage of paraplegin-deficient mice which recapitulate major features of HSP allowed to further examine the role of this putative function in the pathogenesis of HSP.

In contrast to paraplegin which exists only in hetero-oligomeric *m*-AAA protease complexes, Afg3l1 and Afg3l2 have the ability to build up functional homo-oligomers. Therefore, in paraplegin-deficient mice functionally active *m*-AAA proteases consisting of Afg3l1 and Afg3l2 are still present and can compensate for the loss of paraplegin. To provide further insights into functions of mammalian *m*-AAA proteases on a cellular level, single subunits or combinations of subunits were transiently downregulated in MEFs using RNA interference. Reconstitution experiments in yeast revealed the ability of mammalian *m*-AAA protease complexes to directly cleave OPA1, a component of the mitochondrial fusion machinery. Notably, other mitochondrial proteases have also been implicated in the processing of OPA1. Thus, this approach might help to clarify the role of *m*-AAA isoenzymes in the processing of OPA1 *in vivo*.

2   Materials and Methods

2.1   *Molecular Biology Methods*

Standard methods in molecular biology were performed according to protocols published in (Sambrook and Russell, 2001). Enzymes used were purchased from NEB (New England Biolabs). Chemicals were purchased form Sigma or Merck unless stated otherwise.

2.1.1 Expression plasmids and cloning of pGEM4-Mrpl32

The cDNA of Mrpl32 was amplified by PCR from murine cDNA using the primers 5´CGGGGTACCATGGCTCCTTCGTTGCTGCTGCTTTC-3´ (TL2226) and 3´-GCTCTAG-ATTCAATTCTGGGTGAACCAAGATGGCCTC-5´ (TL2227). The purified PCR fragment was subcloned in pGEM-T easy (Promega) and finally cloned in the *Kpn*I-*Xba*I restriction sites of pGEM4 (Promega). The DNA sequence was verified with the ABI Big Dye Terminator Sequencing Kit (Applied Biosystem) and the ABI Prism 3730 DNA analyzer (Applied Biosystem).

Table 2.1 Expression plasmids

Plasmid	Reference
pGEM-T easy-Mrpl32	This study
pGEM4-Mrpl32	This study
pSV40	(Benoist and Chambon, 1981)
pDsRed2-mito	Clontech
p3xFlag-CMV14	(Ishihara *et al.*, 2006)
p3xFlag-CMV14-rat Opa1 splice variant 1	(Ishihara *et al.*, 2006)
p3xFlag-CMV14-rat OPA1 splice variant 1ΔS1	(Ishihara *et al.*, 2006)
p3xFlag-CMV14-rat OPA1 splice variant 7	(Ishihara *et al.*, 2006)
p3xFlag-CMV14-rat OPA1 splice variant 7ΔS1	(Ishihara *et al.*, 2006)
p3xFlag-CMV14-rat AIF(1-95)-OPA1 sp7 (230-997)	(Ishihara *et al.*, 2006)

2.1.2 RNA isolation

Total RNA from was extracted from mouse liver using the RNeasy Midi Kit (Qiagen) according to the manufacturer´s instructions. Briefly, 200 mg mouse liver were homogenized in 4 ml lysis buffer using a rotor-stator homogenizer. The RNA was eluted in 300 µl RNase-free water. Total RNA concentrations were determined spectrophotometrically at a wavelength of 260 nm. To increase the RNA concentration, RNA was precipitated and resuspended in RNase-free water to obtain a final concentration of 1 µg/µl.

2.1.3 Northern Blot and RNA hybridization

10 µg total RNA were size-fractionated on a 1.2% (w/v) agarose/1.5% (v/v) formaldehyde gel and transferred to positively charged nylon membranes (Hybond^{TM}-N+, Amersham Biosciences) by capillary transfer with 20x SSC (3 M NaCl, 0.3 M sodium citrate, pH 7.0). RNA was crosslinked to membranes using UV-light. 75 ng of each cDNA probe were radioactively labeled with [$^{\alpha 32}$P]-dCTP (Amersham) by random priming using the Ladderman^{TM} Labeling Kit (Takara). Non-incorporated radiolabeled nucleotides were removed with MicroSpin^{TM} S-200HR columns (Amersham). Before adding the probes to the hybridization solution, they were denatured for 5 min at 95 °C. Nylon membranes were prehybridized in hybridization solution (Express Hyb, Stratagene) supplemented with 100 µg/ml sonicated salmon sperm DNA for 2 hrs at 50°C. Hybridization of the probe was performed in hybridization solution (Express Hyb, Stratagene) at 50°C overnight. Hybridized blots were washed three times with 2x SSC/0.05% (w/v) SDS at RT followed by two washings for 15 min at 50°C with 0.1x SSC/0.1% (w/v) SDS. To detect radioactive signals, membranes were exposed to X-ray films (BioMAX MS, Eastman Kodak) at -80°C overnight or to a phosphoimager screen (Fuji) followed by detection (Molecular Imager, BioRad) and quantificitation (Quantity One; BioRad) of the phosphorence signals. To remove radioactive probes from membranes, they were incubated in 1% (w/v) SDS at 95°C for 10 min.

DNA probes for β-actin, mitochondrially encoded NADH dehydrogenase subunit 1 (mt-Nd1) and cytochrome *c* oxidase subunit 2 (mt-Cox2) were synthesized from C57BL/6 mouse genomic DNA using the primers listed in Table 2.2. To generate the probe for Mrpl32, the cDNA of Mrpl32 was excised with the restriction enzymes *Xba*I and *Kpn*I from pGEM-

Teasy-Mrpl32 and purified by agarose gel extraction (NucleoSpin® Extract II; Macherey-Nagel).

Table 2.2 Primers for DNA probe synthesis

Description	Sequence
5´-*β-actin* (TL1813)	5´-CAGAAGGAGATTACTGCTCTGGCT -3´
3´-*β-actin* (TL1814)	3´-AGGAGCCACCGATCCACACA-5´
5´-*Nd1* (TL2597)	5´-CGACCTGACAGAAGGAGAAT-3´
3´-*Nd1* (TL2598)	3´-GTAACGGAAGCGTGGATAAG-5
5´-*Cox2* (TL2593)	5´-GGCACCAATGATACTGAAGC-3´
3´-*Cox2* (TL2594)	3´-AGTGGAGGACGTCTTCAGAT-5´

2.2   Cell Biology Methods

2.2.1 Cell culture

Human HeLa cells (ATCC) were cultured in high-glucose Eagle´s Minimum Essential Medium (EMEM, PAA) supplemented with 10% (v/v) fetal bovine serum (FBS, Invitrogen). Cell lines derived from mouse embryonic fibroblasts (MEFs) were cultured in Dulbecco´s Minimum Essential Medium (DMEM, Invitrogen) supplemented with 10% (v/v) FBS. Additionally, 2 mM L-glutamine (PAA), 100 U/ml penicillin (PAA), 100 µg/ml streptomycin (PAA), 100 µM non-essential amino acids (PAA) and 1 mM sodium pyruvate (PAA) were added if necessary. Cells were cultured at 37°C/5% CO_2 and 90% humidity.

For cryofreezing of cells, they were harvested with 1x trypsin (PAA) and centrifuged at 800g for 5 min. The cell pellet was resupended in cold freezing medium consisting of 90% FBS (v/v)/10% (v/v) DMSO and slowly frozen to -80°C. For long-term storage, cells were placed in liquid nitrogen (-200°C) after a few days.

Primary mouse embryo fibroblasts were established from E14.5 embryos derived from intercrosses of time-mated $Spg7^{+/+}$ or $Spg7^{-/-}$-mice. Early passages of primary MEFs were immortalised by SV40 transformation (Todaro and Green, 1965).

Table 2.3 Cell lines used in this study

Cell line	Description	Reference
$Phb2^{fl/fl}$	SV40-immortalized MEF cell line	(Merkwirth *et al.*, 2008)
HeLa	Human cervix cancer cell line	ATCC® No. CCL-2
$Spg7^{+/+}$ and $Spg7^{-/-}$	SV40-immortalized MEF cell line	This study
$Parl^{+/+}$ and $Parl^{-/-}$	SV40-immortalized MEF cell line	(Cipolat *et al.*, 2006)
$Htra2^{+/+}$ and $Htra2^{-/-}$	SV40-immortalized MEF cell line	(Martins *et al.*, 2004)

2.2.2 Transfections

RNAi-mediated knockdown of genes was performed using specific Stealth™ RNAi (Invitrogen) listed in Table 2.4 and 2.5. The corresponding Stealth™ RNAi Negative Control (Invitrogen, 12935-100) served to exclude sequence-independent effects of RNAi delivery in cell lines. One day before transfection, 6-8x10^4 cells were plated in each well of a 6 well-plate in medium without antibiotics. 10-20 nM of each siRNA were transfected with

Lipofectamine™ RNAiMAX Transfection Reagent (Invitrogen) according to the manufacturer´s instructions. After 48-72 hrs of transfection, cells were harvested and further analyzed.

Transient transfection of cells with plasmid DNA was carried out using GeneJuice transfection reagent (Novagen) according to the manufacturer´s instructions.

Table 2.4 List of siRNAs directed against murine mRNA

Target mRNA	Accession nr.	siRNA Sequence
Paraplegin	NM_153176	5´-GCGCGUCAUUGCUGGUACUGCUAAA-3´
Afg3l2	NM_027130	5´-CCUGCCUCCGUACGCUCUAUCAAUA-3´
Afg3l1	NM_054070	5´-GCGAAACCAUGGUGGAGAAGCCAUA-3´
Yme1l1	NM_013771	5´-UUCAGUUCGACCCUUCACAUCUGGC-3´
Yme1l1	NM_013771	5´-AACAAUUUGAAUCUCUUUGGCAUCC-3´
Lon	NM_028782	5´-CCACACAAGGCAAGAUCCUCUGCUU-3´
Lon	NM_028782	5´-UGUGAUGAAAGAGAGUGCCCGCAUA-3´
Phb2	NM_007531	5´-AUUAACAAUGGACGGCAGCACUCGC-3´
OPA1	NM_133752	5´-CAAGAGCAGUGUGUUCACAACGAAA-3´

Table 2.5 List of siRNAs directed against human mRNA

Target mRNA	Accession nr.	Sequence
AFG3L2	NM_006796	5´-GGUAUUGGAGAAACCUUACAGUGAA-3´
Paraplegin	NM_003119	5´-GGAAGUCCGCGAGUUUGUGGAUUAU-3´

2.2.3 Fluorescence microscopy

To analyze mitochondrial morphology, MEFs were transfected with pDsRed2-mito (Clontech). At least one day before transfection, cells were seeded on cover slips in 6-well plates. 24-48 hrs after transfection, proteins were fixed with 3% (w/v) Paraformaldehyde in 1x PBS (PAA) for 15 min at 37°C and rinsed twice with 1x PBS. To visualize nuclear DNA, cells were incubated for 5 min at 37°C in 1 µg/µl DAPI (Roche) in 1x PBS. Afterwards, specimens were washed twice with 1x PBS and mounted in ProLong® Gold Antifade Reagent (Molecular Probes). Fluorescently labeled mitochondria were examined using the DeltaVision microscope system and the Softworx software (Applied precision). Images were deconvolved and further edited using CORELDRAW™ 11 Graphics Suite software (Corel Corporation).

2.2.4 Fluorescence-activated cell sorting (FACS)

2.2.4.1 Membrane potential measurement

Mitochondrial membrane potential of cells was measured 48 hrs after siRNA transfection using the lipophilic, cationic dye JC-1 (Molecular Probes) as recommended by the manufacturer. Briefly, $2x10^5$ were resuspended in 500 µl growth medium and incubated at 37°C with 2 µM JC-1 for 15 min. As a negative control, 20 µM CCCP was added to dissipate mitochondrial membrane potential. After incubation, cells were washed and resuspended in 1x PBS. Analysis of JC-1 fluorescence was examined with excitation at 488 nm and emission at 535 nm and 590 nm on a FACSCalibur equipped with CellQuest software (Becton Dickinson).

2.2.4.2 Measurement of reactive oxygen species

Three days after transfection with specific siRNAs, $2.5*10^5$ MEFs were harvested and resuspended in 500 µl growth medium without phenolred containing 1 µM carboxy-H_2DFCDA (Molecular Probes) and further incubated a 37°C for 15 min. Addition of 10 or 20 µM antimycin A induced reactive oxygen species (ROS) production. After incubation, cells were washed and resuspended in 1x PBS. Analysis of the oxidation-sensitive H_2DFCDA fluorescence was examined with excitation at 488 nm and emission at 535 nm. on a FACS Calibur equipped with CellQuest software (Becton Dickinson). Propidiumiodide (10 µg/ml) was added 1 min before flow cytometry

2.2.5 Oxygen consumption measurements in intact cells

Respiration of intact cells was measured at 37°C with a Clark-tape electrode oxygraph (Hansatech Inc.) in a water-jacketed chamber connected to a circulating water bath. The chamber volumes were set to 500 µl. $2.5x10^6$ cells were assayed in 250 mM saccharose, 20 mM HEPES pH7,4, 10 mM KH_2PO_4, 4 mM $MgCl_2$, 1 mM EDTA, 5 mM glucose, 2 mM pyruvate and 4 mM glutamate. The measurement started with recording the routine endogenous respiration. After observing steady state respiratory flux, ATP synthase was inhibited with 2 µM oligomycin for 5 min. This was followed by uncoupling of oxidative

phosphorylation using stepwise titration of CCCP with concentrations in the range of 250-750 nM. After 5 min recording, cellular respiration was inhibited with 2 mM KCN and was corrected to KCN-insensitive respiration. The respiratory control ratio was obtained dividing the rates of oxygen consumption achieved after and before the addition of CCCP.

2.2.6 Protease inhibitor studies

To inhibit specific classes of proteases, MEFs were incubated with different membrane-soluble protease inhibitors three days after co-transfection of plasmid DNA and siRNA. The following protease inhibitors were diluted in growth medium: 5 µM MG132 (Serva), 0.5 mM *o*-phenantroline (Sigma), 50 µM Pepstatin A (Serva), 0.5 mM Pefabloc SC (Roth) and 50 µM E-64 (Serva). To inhibit cytosolic protein synthesis, 100 µg/ml cycloheximide (CHX; Sigma) were added 30 min later. After 5 hrs of protease inhibition, MEFs were harvested, lysed in RIPA-buffer (Chapter 2.3.1) and further analyzed by SDS-PAGE and immunoblotting.

2.3   Biochemical methods

2.3.1 Preparation of protein extracts

Cells were trypsinized and washed once with 1x PBS (PAA). After incubation of the cells in RIPA buffer at 4°C for 1 hr, lysates were centrifuged for 20 min at 16.000g to remove unsolubilized cell membranes. The protein concentration was determined with a Bradford protein assay (BioRad) using IgG as standard and cell lysates were diluted with RIPA buffer to a final protein concentration of 10 µg/µl.

RIPA buffer
1 mM Tris-HCl, pH 7.4
150 mM NaCl
1% (v/v) Triton X-100
0.5% (w/v) Sodiumdeoxycholate
0.1% (w/v) SDS
1 mM EDTA
1 mM PMSF
Complete Mini Protease Inhibitor Cocktail Mix (Roche)

2.3.2 SDS-PAGE and immunoblotting

Proteins (50-150 µg) were size-fractionated with SDS-PAGE and transferred to nitrocellulose membranes (Immobilon-P; Millipore) according to established protocols (Laemmli, 1970; Towbin *et al.*, 1979). After transfer of proteins, membranes were incubated for at least 30 min at RT in blocking solution (5% (w/v) milkpowder in 1x TBS (10 mM Tris/HCl, pH 7.4; 150 mM NaCl). Immunodecoration with a specific antiserum diluted in blocking solution was carried out for at least 60 min at RT or overnight at 4°C. Nitrocellulose membranes were washed three times for 10 min with 1x TBS at RT. To detect bound antibodies, horseradish peroxidase-conjugated antibodies specific for immunoglobulin G of rabbit, mouse or rat were applied in a dilution of 1:5000-1:10000 in blocking solution for 60 min. After washing the membranes three times with 1x TBS, the chemiluminesence

reagents (Solution 1: 100 mM Tris-HCl, pH 8.5, 250 µM luminol, 400 µM p-coumaric acid; Solution 2: 100 mM Tris-HCl, pH 8.5 0.02% (v/v) H_2O_2) were added in a mixture of 1:1. Chemiluminesence was detected by exposing the membranes to light-sensitive X-ray films (Super RX, Fuji).

Table 2.6 Antibodies used in this study

Antibody	Antigen	Dilution	Reference
α-Paraplegin	Amino acids 121-139 of murine Paraplegin	1:200	(Koppen et al., 2007)
α-AFG3L2	Amino acids 413-828 of human Afg3l2	1:8000	F. Taroni, unpublished
α-Afg3l2	Amino acids 90-103 of murine Afg3l2	1:200	(Koppen et al., 2007)
α-Afg3l1	Amino acids 771-785 of murine Afg3l1	1:500	(Koppen et al., 2007)
α-YME1L1	Recombinant human YME1L1	1:500	ProteinTech Group, Inc.
α-Mrpl32	Amino acids 83-98 of murine Mrpl32	1:500	(Nolden et al., 2005)
α-TIM23	Amino acids 5-126 of rat TIM23	1:1000	BD Biosciences
α-CIII, subunit IIa	Purified Core IIa subunit of human Complex IIII	1:1000	Molecular Probes
α-OPA1	Amino acids 708-830 of human OPA1	1:1000	BD Biosciences
α-CII, 70 kDa subunit	Purified 70 kDa subunit of human Complex III	1:5000	Molecular Probes
α-Flag M2	Synthetic FLAG peptide DYKDDDDK	1:1000	Sigma
α-BAP37 (PHB2)	Recombinant C-terminus of human PHB2	1:500	BioLegend
α-Aconitase	Amino acids 767-780 of human Aconitase	1:1000	Ngo & Davies, unpublished
α-Porin	N-terminal peptide of human porin	1:1000	Calbiochem
α-Lon	Amino acids KKEFELSKLQQRLGREVEEK of human Lon	1:500	(Liu et al., 2003)
α-SLP2	Recombinant C-terminus of human SLP2	1:1000	Genway Biotech Inc.
α-HtrA2	Amino acids 134-458 of human HtrA2 with a C-terminal six histidine tag	1:2000	R&D Systems

2.3.3 Isolation of mitochondria from different murine organs

Liver, brain and spinal cord were dissected from mice, immediately minced and homogenized in isolation buffer with 6 strokes in a Teflon-glass pestle. The crude homogenate was centrifuged at $1000g$ for 10 min. To remove fatty acids, the supernatant of liver was strained through gauze. Mitochondria were pelleted by centrifugation at $8000g$ for 10 min and resuspended in isolation buffer without BSA. Protein concentration was determined using the Bradford protein assay (BioRad).

Isolation buffer:

220 mM D-mannitol

70 mM sucrose

20 mM HEPES, pH 7.2

2 mM EGTA

0.1% (w/v) BSA

Complete Mini Protease Inhibitor Cocktail Mix (Roche)

2.3.4 *In vitro* import of proteins into isolated mitochondria

SP6 promoter-driven *in vitro* transcription of Mrpl32 and subsequent translation in the presence of [^{35}S]-labeled methionine (MP Biomedicals) was performed using the TNT® Coupled Reticulocyte Lysate System (Promega) according to the manufacturer´s instructions.

For *in vitro* protein import studies, mitochondria were resuspended in import buffer to a final concentration of 1 mg/ml. After 3 min incubation at 30°C, [^{35}S]-labeled precursor proteins were added to a final concentration of 2% (v/v) and the samples were further incubated at 30°C for various times. The import of mitochondrial proteins was stopped by the addition of 0.2 µM valinomycin, 4 µM FCCP and 1 µM oligomycin. To remove non-imported precursor proteins, proteinase K (Roche) was added to a final concentration of 75 µg/ml and the samples were incubated for 10 min on ice. After addition of 1 mM PMSF to inhibit proteinase K activity, mitochondria were washed twice with SHKCl and finally resuspended in 1x SDS-sample buffer. The samples were analyzed by SDS-PAGE and autoradiography.

Importbuffer   SHKCl

250 mM sucrose   0.6 M sorbitol

20 mM HEPES, pH 7.4   50 mM HEPES, pH 7.4

5 mM magnesium acetate   60 mM KCl

80 mM potassium acetate

10 mM sodium succinate

2.5 mM ADP

1 mM DTT

2.3.5 Stability of newly imported, radioactively labeled proteins in isolated mitochondria (import-chase)

Import of radioactively labeled precursor proteins was performed at 30°C for 15 min as described above (Chapter 2.3.4). To stop the import reaction, samples were placed on ice and incubated with 100 µg/ml trypsin for 20 min at 4°C to remove non-imported proteins. Trypsin was inhibited with 1 µg/µl soy bean trypsin inhibitor (STI) for 5 min on ice. Afterwards, samples were incubated at 37°C for up to 30 min to induce degradation of newly-imported proteins. Aliquots were withdrawn at each time point and placed on ice. Mitochondria were isolated by centrifugation at 13.000g for 10 min at 4°C and washed twice with SHKCl. After the last washing step, the mitochondrial pellet was resupended in 15 µl 1x SDS-sample buffer and analyzed by SDS-PAGE and autoradiography.

2.3.6 *In organello* translation of mitochondrial proteins

To radioactively label mitochondrially encoded proteins, 1 mg/ml mitochondria were incubated at 30°C in translation buffer in the presence of 100 µg/ml cycloheximide. After 3 min preincubation, 200 µCi/ml [^{35}S]-methionine were added. The translation was stopped with 20 mM methionine and the mitochondrial pellet was washed twice with SHKCl before proteins were precipitated with 12.5% (w/v) ice-cold TCA. The protein pellet was washed twice with acetone (-20°C) and dissolved in 40 µl SDS-sample buffer. Samples were analyzed by SDS-PAGE and autoradiography. Incorporated radioactivity was determined by

scintillation counting after thourough vortexing of 1 ml scintillation solution (Ultima Gold) with 20 µl of each sample.

Translation buffer:

100 mM mannitol

80 mM sucrose

10 mM sodium succinate

80 mM KCl

5 mM $MgCl_2$

1 mM potassium phosphate

25 mM HEPES pH 7.2

300 µM of each of the aminoacids except methionine

5 mM ATP

20 µM GTP

6 mM creatine phosphate

60 µg/ml creatine kinase

2.3.7 Determination of respiratory chain activity in isolated mitochondria

Freshly isolated mitochondria were centrifuged at 8000g for 10 min and the resulting mitochondrial pellet was resuspended in respiration buffer (250 mM sucrose, 50 mM HEPES pH 7.4, 10 mM KH_2PO_4, 2 mM $MgCl_2$, 1 mM EDTA) to a concentration of 5 mg/ml. Polarographic measurements were performed at 30°C with a Clark-tape electrode oxygraph (Hansatech Inc.) in a water-jacketed chamber connected to a circulating water bath. State 2 respiration (basal respiration rate) was measured with 6 mM glutamate/malate or pyruvate/malate using 125 µg mitochondria. Measurement of state 3 respiration (maximal respiration rate) using 1 µM rotenone/12 mM succinate as substrates was initiated with 1 mM ADP and stopped with 2 mM KCN. Respiration rates were calculated as consumption of nmol O_2/min x mg protein.

2.4   Mouse analysis

2.4.1 Animal care

Care of all animals was within institutional animal care committee guidelines. All animal procedures were approved by local government authorities (Bezirksregierung Köln, Germany) and performed according to NIH guidelines. General handling and breeding of mice was conducted according to established protocols (Hogan B., 1987; Silver, 1995). Mice were housed in groups of three to five at 22-24 °C with a 12 hrs light/dark cycle.

2.4.2 Mice

$Spg7^{+/+}$-and $Spg7^{-/-}$-mice used in this study had a mixed C57BL/6-129Sv genetic background. $Spg7^{-/-}$-mice were generated by targeting of the first two exons of the $Spg7$ locus by homologous recombination (Ferreirinha *et al.*, 2004). The gene targeting vector contained the first two coding exons with the selectable neomycin resistance gene flanked by two loxP sites (Ferreirinha *et al.*, 2004).

3   Results

3.1   Analysis of mitochondrial dysfunctions in paraplegin-deficient mice

In humans, loss-of-function mutations in paraplegin cause an autosomal recessive form of hereditary spastic paraplegia (HSP), a neurodegenerative disorder mainly caused by axonal degeneration in central and peripheral nerves (Casari *et al.*, 1998). Recently, a paraplegin-deficient (*Spg7$^{-/-}$*) mouse model for HSP was generated which replicates important features of the human disease (Ferreirinha *et al.*, 2004). However, the primary molecular defects which result in this neurodegenerative disease remain to be elucidated. Studies of the *m*-AAA protease in yeast revealed new insights into the pathogenesis of HSP by identifying MrpL32, a nuclear-encoded protein of the mitochondrial ribosome, as a new substrate of the *m*-AAA protease. Moreover, the proteolytic maturation of MrpL32 by the *m*-AAA protease was shown to be essential for mitochondrial protein synthesis (Nolden *et al.*, 2005). Mrpl32 and *m*-AAA proteases are highly conserved in eukaryotes and functional complementation of the yeast *m*-AAA protease by its murine homologues could be demonstrated (Nolden *et al.*, 2005). However, it has not been analyzed yet whether the *m*-AAA protease-dependent maturation of murine Mrpl32 is conserved *in vivo* and whether this putative function of the *m*-AAA protease subunit paraplegin is causative for the axonal degeneration observed in HSP.

3.1.1 Reduced steady state levels of Mrpl32 in mitochondria lacking paraplegin

To investigate whether maturation of Mrpl32 by the *m*-AAA protease is conserved in mammals, protein steady state levels of mature Mrpl32 were analyzed in paraplegin-deficient mice. Thus, mitochondria were isolated from liver of *Spg7$^{+/+}$*- and *Spg7$^{-/-}$*-mice and subjected to SDS-PAGE. Immunoblotting with a polyclonal antiserum raised against Mrpl32 revealed a significantly reduced steady state level of mature Mrpl32 in liver mitochondria lacking paraplegin (Fig. 3.1 A). This result might give a first hint to a function of paraplegin in the maturation of Mrpl32.

To exclude that the reduced steady state level of mature Mrpl32 is caused by impaired transcription of the *Mrpl32* gene due to secondary effects of paraplegin deficiency, RNA was isolated from liver of wt and *Spg7*^{/-}-mice to perform Northern blot analysis using cDNA probes for Mrpl32, and for β-actin as a control. Radioactive signals were quantified and the expression level of Mrpl32 relative to β-actin in *Spg7*^{/-}-mice was compared to wt. No reduction in mRNA expression of *Mrpl32* in paraplegin-deficient mice compared to wt was observed, strongly indicating that the reduced protein steady state level of Mrpl32 is caused by posttranscriptional events (Fig. 3.1 B and C). Furthermore, this experiment revealed that the expression of the mitochondrial-encoded genes *Nd1* and *Cox2* in *Spg7*^{/-}-mice is not affected.
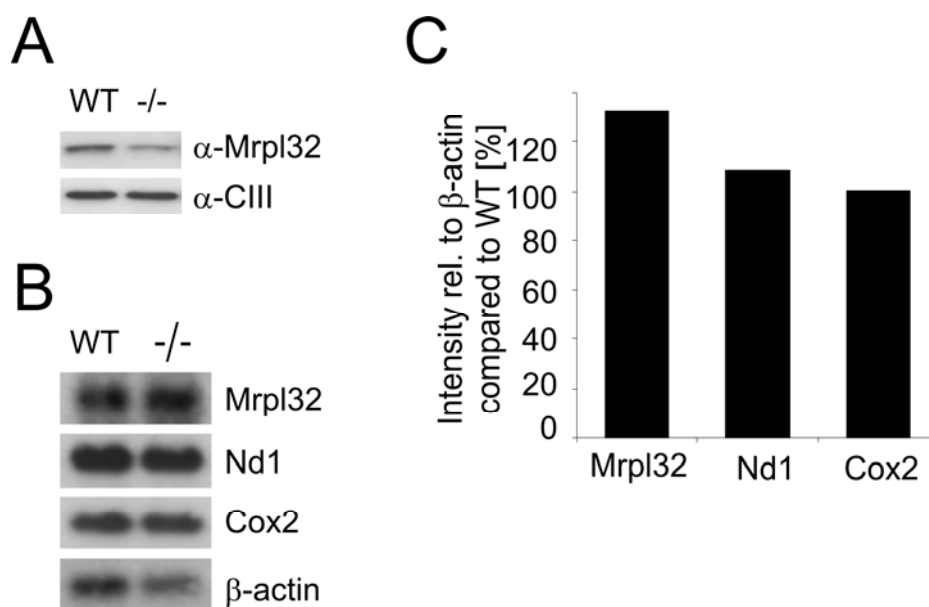
Figure 3.1 Reduced steady state level of Mrpl32 in paraplegin-deficient mitochondria.
(**A**) Steady state level of Mrpl32 in liver mitochondria lacking paraplegin. Immunoblotting of mitochondria isolated from *Spg7*^{+/+}-and *Spg7*^{/-}-mice was performed using a Mrpl32-specific antiserum. An antibody recognizing subunit 2 of Complex III (CIII) was used as a loading control. (**B**) Northern blot analysis of Mrpl32 mRNA expression in liver. Total RNA was isolated from liver of *Spg7*^{+/+}-and *Spg7*^{/-}-mice. Northern blot analysis was performed using probes recognizing mRNAs of Mrpl32, β-actin, Nd1 and Cox2 followed by autoradiography. (**C**) Quantification of Mrpl32 mRNA expression in liver isolated from paraplegin-deficient mice. Phosporescence signals of hybridized probes were quantified. Signals of Mrpl32, Nd1 and Cox2 were normalized to *β*-actin signals and the ratios in wt were set to 100 %.

Taken together, a decrease in the steady-state level of mature Mrpl32 was observed in paraplegin-deficient liver mitochondria compared to wt while the mRNA level of *Mrpl32* was not affected. Since reconstitution experiments in yeast provided direct evidence for the ability of mammalian *m*-AAA proteases to cleave murine Mrpl32, it is likely that posttranslational defects in the absence of the paraplegin are involved in the decrease of mature Mrpl32 (Nolden *et al.*, 2005).

3.1.2 Maturation of Mrpl32 proceeds normally in paraplegin-deficient mice

Considering the essential function of *m*-AAA protease-dependent proteolytic processing of MrpL32 in yeast (Nolden *et al.*, 2005), reduced protein levels of mature Mrpl32 in paraplegin-deficient murine liver mitochondria suggest a role of paraplegin in Mrpl32 maturation. To get insights into the involvement of paraplegin, the proteolytic maturation of Mrpl32 was investigated by *in vitro* import of precursor Mrpl32 into liver mitochondria derived from paraplegin-deficient and wt mice.

Radioactively labeled precursor protein of Mrpl32 was synthesized in a cell-free system and incubated with liver mitochondria isolated from $Spg7^{+/+}$- and $Spg7^{-/-}$-mice. Mrpl32 was imported into wt mitochondria in a membrane potential-dependent manner (Fig. 3.2 A). Upon import, the precursor of Mrpl32 was converted in the mature form by proteolytic processing and protected against protease treatment indicating successful import into mitochondria. However, an impairment in processing of Mrpl32 could not be observed in mitochondria lacking paraplegin (Fig. 3.2 B). Remarkably, immunodecoration with α-Mrpl32 antiserum revealed an increase in steady state levels of mature Mrpl32 upon import in paraplegin-deficient mitochondria (Fig. 3.2 B).

To further examine the function of paraplegin for the accumulation of mature Mrpl32, the stability of newly imported Mrpl32 in the absence of paraplegin was investigated. Mrpl32 precursor protein was imported into liver mitochondria and the degradation of radioactively labeled mature Mrpl32 was assessed at 37 °C. However, equal turnover rates of newly imported Mrpl32 were observed in wt and paraplegin-deficient mitochondria (Fig. 3.2 C). In summary, no defect in Mrpl32 maturation could be observed in paraplegin-deficient liver mitochondria *in vitro*.
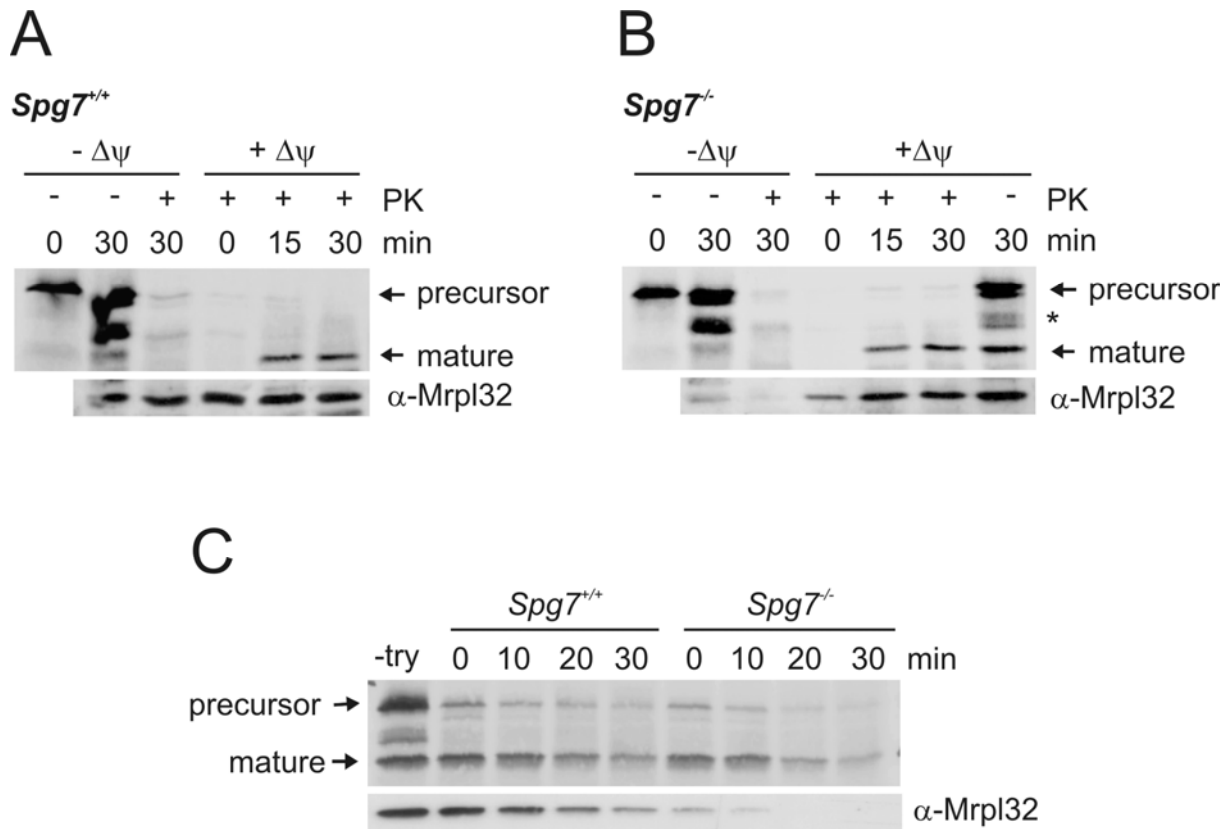
Figure 3.2 Proteolytic processing of Mrpl32 in paraplegin-deficient mitochondria.
(A) and **(B)** Processing of Mrpl32 upon import into mitochondria. Mrpl32 was synthesized in a cell-free system in the presence of [^{35}S]-methionine and imported into liver mitochondria isolated from $Spg7^{+/+}$- (A) and $Spg7^{-/-}$-mice (B) at 30 °C for up to 30 min. Membrane potential was dissipated by adding valinomycin, FCCP and oligomycin prior to import (-Δψ). Non-imported proteins were degraded by proteinase K (PK). Samples were analyzed by SDS-PAGE and autoradiography. Immunoblotting was performed using an antiserum directed against Mrpl32. **(C)** Stability of newly imported Mrpl32 in mitochondria. Radioactively labeled Mrpl32 was imported into liver mitochondria derived from $Spg7^{+/+}$- and $Spg7^{-/-}$-mice at 30 °C for 15 min. Non-imported proteins were removed by addition of trypsin. Samples were further incubated at 37°C for up to 30 min to allow protein degradation to occur. Analysis was conducted by SDS-PAGE and autoradiography. Membranes were immunodecorated with an antiserum raised against Mrpl32. try, trypsin.

3.1.3 Paraplegin is essential for optimal mitochondrial translation in liver

In yeast, *m*-AAA protease-dependent maturation of Mrpl32 is essential for mitochondrial translation (Nolden *et al.*, 2005). Defects in the mitochondrial translation machinery in human were shown to be the molecular cause for a number of inherited neurodegenerative diseases (Miller *et al.*, 2004; Sylvester *et al.*, 2004; Jacobs and Turnbull, 2005; Antonicka *et al.*, 2006). Although Mrpl32 processing proceeds normally in isolated liver mitochondria lacking paraplegin, it is a crucial point for the pathogenesis of HSP to determine the consequences of reduced Mrpl32 steady state levels on mitochondrial protein synthesis.

Figure 3.3 Impaired mitochondrial translation in murine liver mitochondria lacking paraplegin.
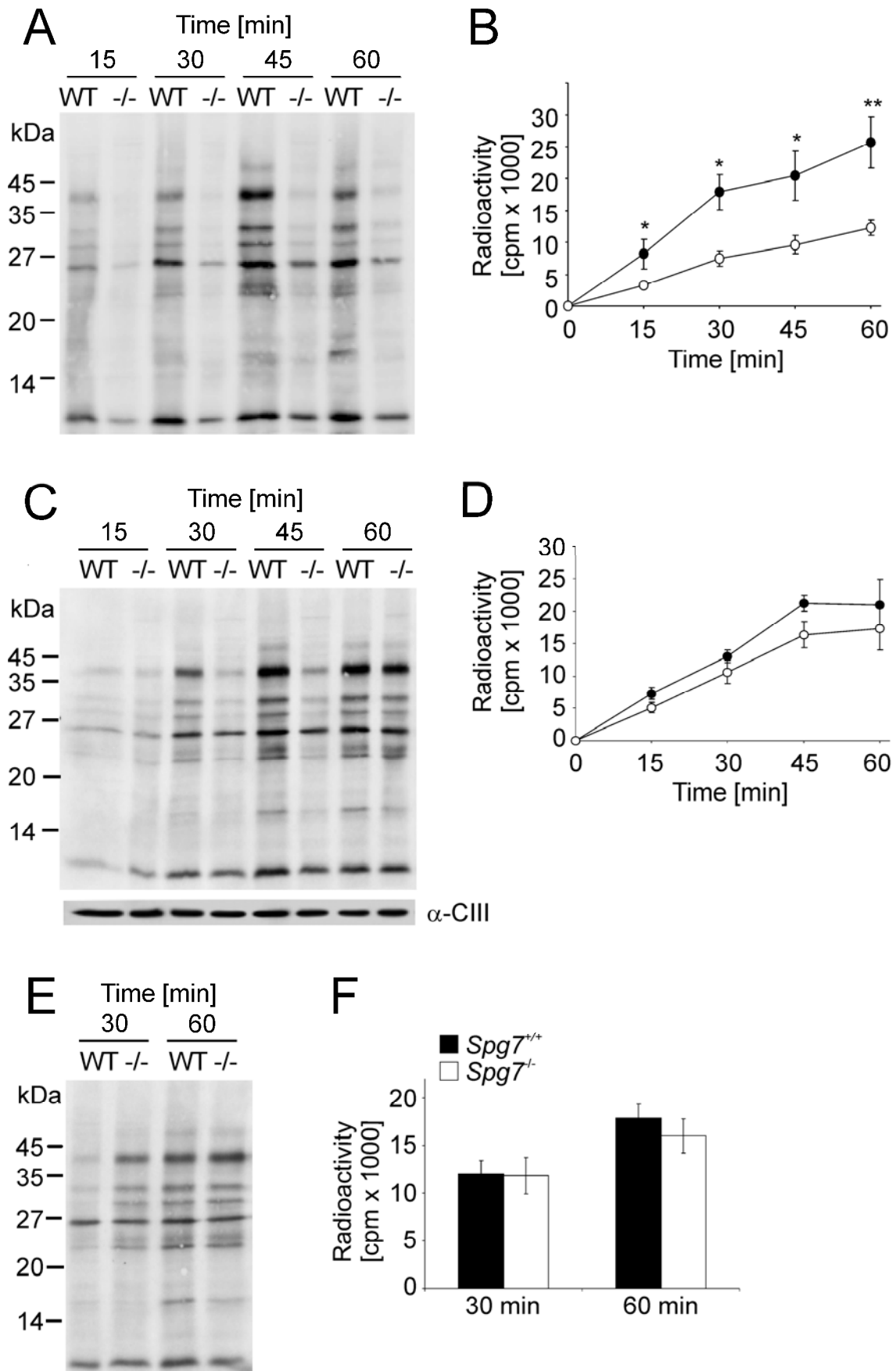Mitochondria from liver (**A and B**), brain (**C and D**) and spinal cord (**E and F**) were isolated from 11-month-old

To analyze mitochondrial protein synthesis, mitochondrial translation products were labeled in the presence of $[^{35}S]$-methionine in liver mitochondria isolated from 11-month old wt and paraplegin-deficient mice. The kinetics and efficiencies of mitochondrial protein synthesis were monitored via SDS-PAGE and autoradiography. Additionally, the incorporation of radioactivity into newly synthesized mitochondrial proteins was quantified by scintillation counting.

In the absence of paraplegin, mitochondrial translation was significantly impaired in liver mitochondria with a decrease of 50 % compared to wt (Fig. 3.3 A and B). These findings provide evidence that an impaired mitochondrial protein synthesis might be linked to axonal degeneration in HSP caused by loss of paraplegin. To substantiate these findings, the efficiency of mitochondrial translation was analyzed in brain and spinal cord, tissues which are mainly affected in $Spg7^{-/-}$-mice (Ferreirinha et $al.$, 2004). Remarkably, no statistically significant decrease in mitochondrial protein synthesis could be detected in brain and spinal cord of paraplegin-deficient mice (Fig 3.3 C, D and E, F).

In summary, these findings reveal an important function of paraplegin for mitochondrial protein synthesis in liver. However, this function of paraplegin seems to be tissue-specific since mitochondrial translation is largely unaffected in brain and spinal cord of paraplegin-deficient mice. Thus, a defective mitochondrial proteins synthesis seems not to be the underlying pathogenic mechanism in HSP.

wt (filled circles) and $Spg7^{-/-}$-mice (open circles). Mitochondrially encoded proteins were synthesized in the presence of $[^{35}S]$-methionine at 30°C for the indicated time points. **(A, C and E)** Mitochondrial protein synthesis was analyzed by SDS-PAGE and autoradiography. **(B, D and F)** Efficiency of mitochondrial translation was quantified by determining total incorporated radioactivity from seven independent experiments and the statistical significance was assessed by paired Student´s t-test. * $p<0.05$; ** $p<0.01$. Error bars represent ± standard deviation of the mean (SEM).

3.1.4 Mitochondrial respiratory function is not affected in paraplegin-deficient mice

The impaired mitochondrial translation detectable in liver prompted us to investigate the mitochondrial respiratory functions. Essential respiratory chain subunits are mitochondrially encoded. Hence, mitochondrial protein synthesis defects should result in impaired respiratory chain activity (Jacobs and Turnbull, 2005). To investigate this, oxygen consumption of freshly isolated liver mitochondria was measured in collaboration with A. Bernacchia (Istituto Nazionale Neurologico "C. Besta", Milan). The basal respiration rate (state 2) was quantified using glutamate/malate, substrates entering the electron transport chain at Complex I, whereas ADP-induced maximal respiration rate (state 3) was analyzed using succinate, which enters the electron transport chain at Complex II. Strikingly, in liver mitochondria lacking paraplegin neither state 2 respiration nor state 3 respiration was impaired (Fig. 3.4 A and B).
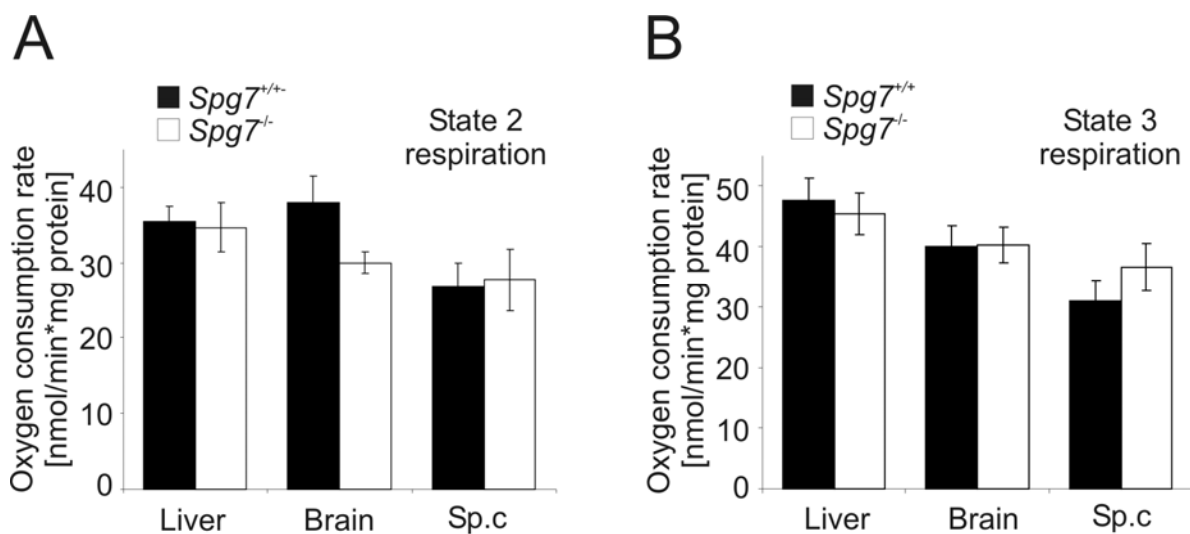
Figure 3.4 Maintenance of mitochondrial respiration rates in liver, brain and spinal cord of paraplegin-deficient mice.
Oxygen consumption rates in isolated mitochondria from liver, brain and spinal cord from 11-month-old $Spg7^{+/+}$- and $Spg7^{-/-}$-mice. **(A)** State 2 respiration was determined using glutamate/malate (liver) or pyruvate/malate (brain and spinal cord) as substrates. **(B)** Succinate was used to measure ADP-stimulated respiration (State 3). Error bars represent ± standard deviations (SD) of seven independent experiments. Sp.c, spinal cord.

In order to elucidate the role of mitochondrial dysfunction in the pathogenesis of HSP, oxygen consumption rates of isolated brain and spinal cord mitochondria were analyzed in parallel. Neither state 2 nor state 3 respiration rates were decreased in brain and spinal cord mitochondria of $Spg7^{-/-}$-mice (Fig. 3.4 A and B). This is consistent with the previous findings of a functional mitochondrial protein synthesis in brain and spinal cord (Fig. 3.3 C-F).

In summary, respiratory chain activity is generally not affected in mitochondria lacking paraplegin suggesting that a dysfunction in mitochondrial respiratory activity is not the molecular cause for HSP.

3.2   Functional analysis of m-AAA proteases in MEFs using RNA interference

In humans, *m*-AAA protease complexes are composed of the subunits Paraplegin and AFG3L2 (Atorino *et al.*, 2003). An additional subunit of the *m*-AAA protease, Afg3l1, is expressed in mice, which exists only as a pseudogene in human (Kremmidiotis *et al.*, 2001). Interestingly, *m*-AAA protease isoforms with variable subunit compositions have been identified recently (Koppen and Langer, 2007). Whereas paraplegin is only present in hetero-oligomeric complexes, Afg3l2 and Afg3l1 have additionally the ability to homo-oligomerize. Yeast complementation studies revealed proteolytic activity of different *m*-AAA protease assemblies. However, the function of *m*-AAA proteases has never been analyzed in mammalian systems besides paraplegin-deficient mice (*Spg7$^{-/-}$*). Since in *Spg7$^{-/-}$*-mice, functionally active *m*-AAA proteases consisting of Afg3l1 and Afg3l2 are still present, they can compensate for the loss of paraplegin (Koppen and Langer, 2007). Therefore, the aim was to investigate the function of *m*-AAA proteases and the role of the different subunits in mammals. Because knock-out mice for Afg3l1 and Afg3l2 were not available, different *m*-AAA protease subunits were transiently downregulated in mammalian cells using RNA interference.

3.2.1 Downregulation of *m*-AAA protease subunits in MEFs using RNA interference

3.2.1.1 Efficient depletion of single or combinations of m-AAA protease subunits

Transient knockdown of *m*-AAA protease subunits in MEFs was accomplished using Stealth™ RNAi (Invitrogen) directed against specific mRNA sequences. Stealth™ siRNAs are chemically modified double-stranded 25-mer RNA oligonucleotide sequences without a single-stranded overhang. Such modifications were reported to reduce non-specific off-target effects and to confer greater stability to siRNAs (Invitrogen). Specific siRNAs for efficient knockdown of different *m*-AAA proteases were designed using the Stealth™ RNAi design algorithm (Invitrogen). Stealth™ RNAi negative controls (Invitrogen) served as control for the RNAi response. At least three siRNAs directed against each *m*-AAA protease subunit

were tested for specificity and efficiency in downregulation and one was chosen for subsequent experiments.

Expression of paraplegin, Afg3l1 and Afg3l2 in MEFs was analyzed 48 hrs after double transfection with the respective siRNA. Afg3l1, Afg3l2 and paraplegin expression was more than 90% reduced on protein level (Fig. 3.5 A). Remarkably, similar knockdown efficiencies were achieved when two subunits or even all three *m*-AAA protease subunits were downregulated simultaneously. Additionally, SV40-immortalized MEF cell lines derived from *Spg7*$^{+/+}$-and *Spg7*$^{-/-}$-mice were established to benefit from the complete absence of paraplegin. After siRNA transfection, the expression of Afg3l1 and Afg3l2, either alone or together, was reduced more than 90% on protein level in *Spg7*$^{+/+}$- and *Spg7*$^{-/-}$-MEFs (Fig. 3.5 B). Notably, downregulation of Afg3l1 and Afg3l2 in MEFs resulted in the appearance of two bands which correspond to murine paraplegin. Otherwise, expression of Afg3l1, Afg3l2 and paraplegin was not affected upon knockdown of the respective other *m*-AAA subunits.

In summary, single or combinations of *m*-AAA protease subunits can be efficiently and specifically downregulated. Therefore, siRNA-mediated knockdown is a useful tool to study the function of different *m*-AAA protease complexes in mammalian cells.
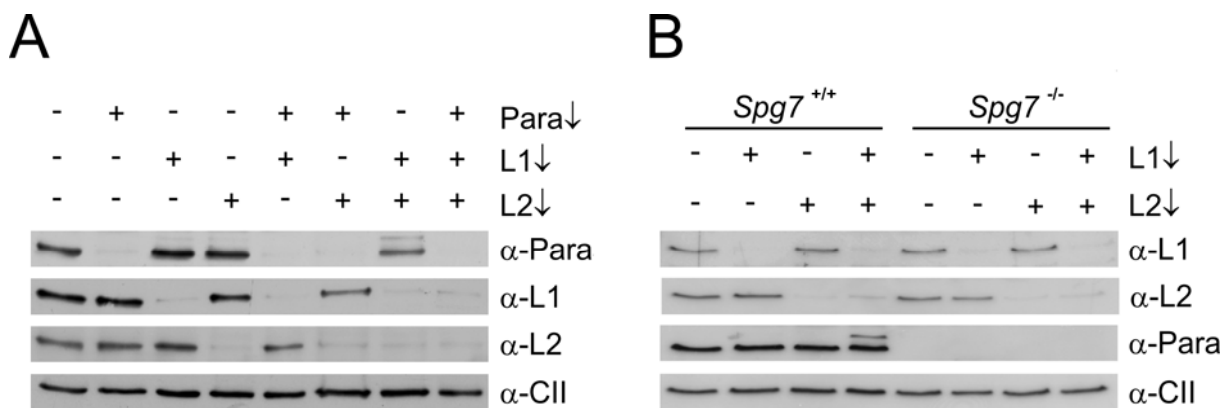
Figure 3.5 Downregulation of *m*-AAA protease subunits in MEFs.
Downregulation of Afg3l1, Afg3l2 and paraplegin in wt MEFs (**A**) and in *Spg7*$^{+/+}$ and *Spg7*$^{-/-}$-MEFs (**B**). Cells were transfected twice with Stealth siRNA directed against Afg3l1, Afg3l2 and paraplegin alone and in different combinations. Control cells were transfected twice with negative control siRNA. After 48 hrs, cells were lysed and analyzed by SDS-PAGE and immunblotting using specific antisera recognizing paraplegin, Afg3l1, Afg3l2 and, as a loading control 70 kDa subunit of Complex II (CII). Para, paraplegin; L1, Afg3l1; L2, Afg3l2.

3.2.1.2 Overlapping substrate specificities of the murine m-AAA protease subunits Afg3l1 and Afg3l2

The murine *m*-AAA protease subunits Afg3l1 and Afg3l2 share a high protein sequence identity of 70% pointing to similar activities of Afg3l1 and Afg3l2 in mice. The appearance of a larger band of paraplegin upon simultaneous knockdown of Afg3l1 and Afg3l2 indicates that these *m*-AAA protease subunits might be both involved in the maturation of paraplegin (Fig. 3.5 A and B). To verify the redundant functions of Afg3l1 and Afg3l2 in regard to paraplegin maturation, MEFs were transfected with siRNA specific for these *m*-AAA protease subunits. Cell lysates were analyzed by SDS-PAGE and immunoblotting with paraplegin-specific antiserum. Upon single knockdown of Afg3l1 or Afg3l2 only mature paraplegin was present. In contrast, concomitant knockdown of Afg3l1 and Afg3l2 resulted in the appearance of a larger band of paraplegin and in the reduction of the steady-state level of mature paraplegin (Fig. 3.6 A). These findings suggest that paraplegin is only partially processed to its mature form upon downregulation of Afg3l1 and Afg3l2.

Both, Afg3l1 and Afg3l2 were shown to substitute for the yeast *m*-AAA protease in the processing of yeast MrpL32 (Koppen and Langer, 2007). Therefore, the role of Afg3l1 and Afg3l2 in processing of murine Mrpl32 were investigated. Single *m*-AAA protease subunits or different combinations of subunits were downregulated and analyzed by immunoblotting using antiserum specific for murine Mrpl32. Upon knockdown of *m*-AAA proteases in MEFs, no significant reduction of mature Mrpl32 could be observed (Fig. 3.6 B). However, following depletion of Afg3l1 and Afg3l2 a larger band of Mrpl32 appeared that co-migrated with the precursor form of Mrpl32, indicating an impaired processing of Mrpl32. Notably, an additional downregulation of paraplegin did not result in an increased accumulation of the putative precursor of Mrpl32.

Remarkably, only AFG3L2 but not AFG3L1 is expressed in human (Kremmidiotis *et al.*, 2001). Therefore, it was analyzed whether human AFG3L2 exerts the overlapping functions of murine Afg3l1 and Afg3l2. Hence, HeLa cells were transfected with siRNA specific for human AFG3L2 and Paraplegin. Western blots of cell lysates, decorated with the antibodies α-AFG3L2 and α-Paraplegin, revealed efficient downregulation of both proteins in human HeLa cells (Fig. 3.6 C). Strikingly, no band specific for Paraplegin could be detected in AFG3L2-depleted cells suggesting an increased turnover of paraplegin. In agreement with observations in MEFs, knockdown of AFG3L2 resulted in the appearance of the precursor form of Mrpl32 without reduction in the steady state level of mature Mrpl32.

Taken together, these results identify Mrpl32 and paraplegin as putative substrates of the mammalian *m*-AAA protease. In MEFs, Afg3l1 and Afg3l2 seem both to be involved in the maturation of paraplegin and Mrpl32 indicating that they have at least partially overlapping substrate specificities.
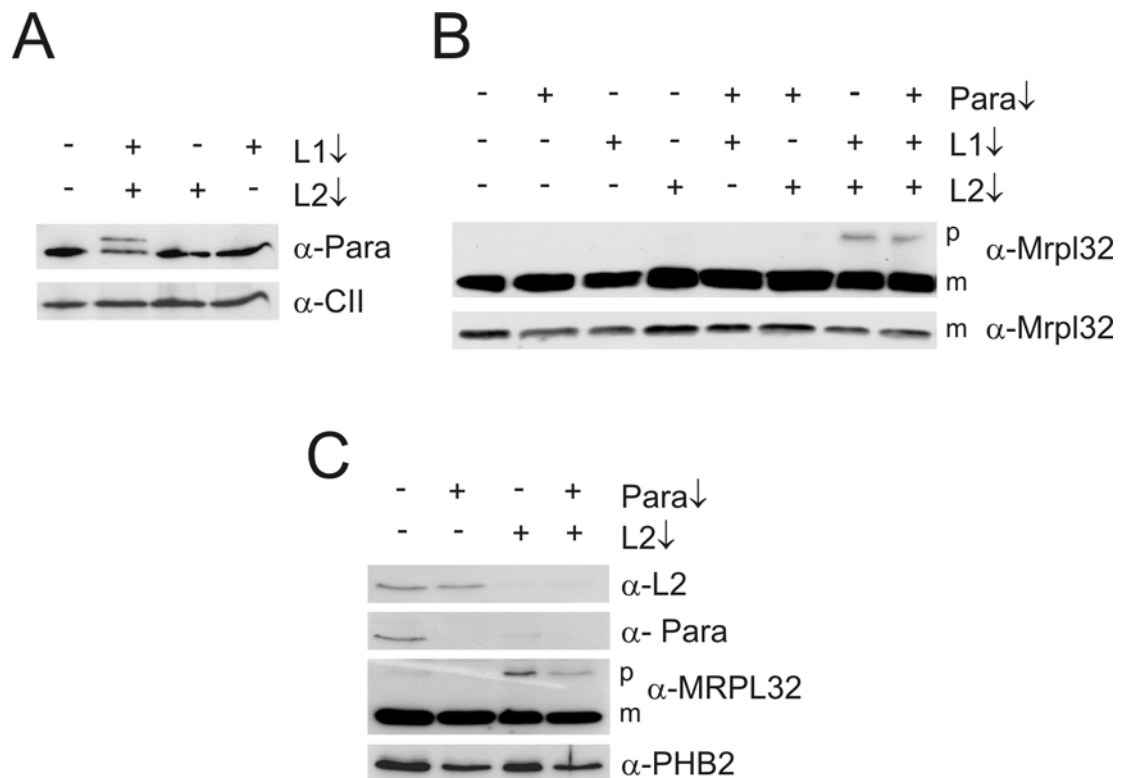
Figure 3.6 Overlapping substrate specificities of Afg3l1 and Afg3l2 in MEFs.
(A) and (B) Impaired processing of paraplegin and Mrpl32. Cells were transfected twice with respective siRNAs directed against murine *m*-AAA protease subunits and harvested after 48 hrs. Control cells were transfected with Stealth siRNA negative controls. 48 hrs after transfection, cells were lysed and subjected to SDS-PAGE and immunoblotting. (A) Immunoblot analysis of MEFs after knockdown of Afg3l1 and Afg3l2 with specific antibodies recognizing paraplegin and the 70 kDa subunit of Complex II (CII). (B) Immunoblot analysis of MEFs after knockdown of Afg3l1, Afg3l2 and paraplegin with Mrpl32-specific antiserum. Films developed with either a short or a long exposure time are shown (C) Immunoblot analysis of HeLa cells after siRNA-mediated downregulation of Paraplegin and AFG3L2. HeLa cells were analyzed as above after siRNA transfection with stealth siRNA specific for human AFG3L2 and Paraplegin. Immunoblotting was performed using antisera recognizing human paraplegin, AFG3L2, MRPL32 and, as a loading control PHB2. Para, paraplegin; L1, Afg3l1; L2, Afg3l2 or AFG3L2; p, precursor; m, mature form.

3.2.2 Loss of long OPA1 isoforms in *m*-AAA protease-depleted MEFs results in mitochondrial fragmentation

The dynamin-like GTPase OPA1 functions in mitochondrial fusion and inner membrane remodelling (Olichon *et al.*, 2003; Cipolat *et al.*, 2004; Griparic *et al.*, 2004). Mutations in the human *OPA1* gene cause autosomal dominant optic atrophy (ADOA), a prevalent hereditary neuropathy of the optic nerve (Alexander *et al.*, 2000; Delettre *et al.*, 2000). At least five apparent different OPA1 isoforms have been identified in different tissues and cell lines (Delettre *et al.*, 2001; Olichon *et al.*, 2003; Duvezin-Caubet *et al.*, 2006; Ishihara *et al.*, 2006). They were shown to result from at least eight different splice variants and proteolytic cleavage of large isoforms to small isoforms (Delettre *et al.*, 2001; Olichon *et al.*, 2002; Satoh *et al.*, 2003; Ishihara *et al.*, 2006; Duvezin-Caubet *et al.*, 2007). So far, the rhomboid protease PARL and the *m*-AAA protease subunit paraplegin were proposed to be involved in the processing of OPA1 (Cipolat *et al.*, 2006; Ishihara *et al.*, 2006). However, no drastic differences in the pattern of OPA1 isoforms were observed in cells lacking PARL or paraplegin compared to wt (Duvezin-Caubet *et al.*, 2007). Recently, the mitochondrial *m*-AAA subunits Afg3l1 and Afg3l2 were shown to be capable of cleaving OPA1 when reconstituted in yeast (Duvezin-Caubet *et al.*, 2007). Thus, the aim of the following experiments was to further clarify the role of mammalian *m*-AAA proteases in the processing of OPA1.

3.2.2.1 Loss of long OPA1 isoforms in the absence of the m-AAA proteases Afg3l1 and Afg3l2

To investigate the requirement of *m*-AAA-proteases in OPA1 processing, Afg3l1 and Afg3l2 were downregulated in $Spg7^{+/+}$- and $Spg7^{-/-}$-MEFs and analyzed by immunoblotting using α-OPA1 antibodies. As previously published, five OPA1 isoforms could be detected corresponding to two long isoforms, L1 and L2, which can be processed to three short isoforms, S3-S5 (Fig. 3.7 A) (Duvezin-Caubet *et al.*, 2007). Upon knockdown of either Afg3l1 or Afg3l2 in wt and paraplegin-deficient cells, no drastic alterations in the pattern of isoforms occurred compared to control cells (Fig. 3.7 A). Strikingly, simultaneous depletion of Afg3l1 and Afg3l2 resulted in the loss of the long OPA1 isoforms L1 and L2 whereas the short isoforms S5 and, to a lower extent, S3 accumulated (Fig. 3.7 A). The steady-state level

of the short isoform S4 was slightly reduced. In contrast to Afg3l1 and Afg3l2, the absence of paraplegin in *Spg7*$^{-/-}$-MEFs did not lead to any changes in the pattern of OPA1 isoforms (Fig. 3.7 A). Similar results were obtained in human HeLa cells in which downregulation of AFG3L2 (see Fig. 3.6 C) resulted as well in a decrease of L-OPA1 isoforms (Fig. 3.7 B).

Taken together, no stabilization of L-OPA1 isoforms in the absence of Afg3l1, Afg3l2 and paraplegin could be observed suggesting that the processing of OPA1 in mammals can occur independently of *m*-AAA proteases. Surprisingly, concomitant knockdown of Afg3l1 and Afg3l2 resulted in drastically reduced levels of L-OPA1 isoforms accompanied by an accumulation of S-OPA1 isoforms. These results point to an increased processing or turnover of L-OPA1 isoforms in Afg3l1/Afg3l2-depleted MEFs.
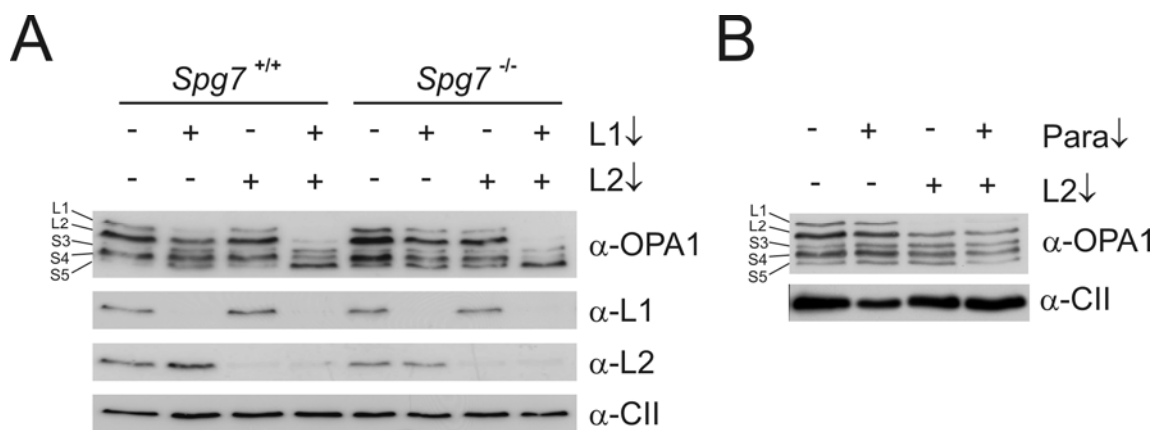
Figure 3.7 Loss of L-OPA1 isoforms in the absence of Afg3l1 and Afg3l2.
(**A**) Immunoblot analysis of OPA1 isoforms in MEFs. 48 hrs after transfection of *Spg7*$^{+/+}$ and *Spg7*$^{-/-}$-MEFs with siRNAs directed against Afg3l1 and Afg3l2, cells were lysed and subjected to SDS-PAGE followd by immunblot analysis. Specific anitsera recognizing OPA1, Afg3l1, Afg3l2 and 70 kDa subunit of Complex II (CII) were used. OPA1 isoforms are indicated and named L1, L2, S3, S4 and S5 according to Duvezin-Caubet *et al.*, 2006. Afg3l1, L1; Afg3l2, L2. (**B**) Immunoblot analysis of OPA1 isoforms in HeLa cells. HeLa cells were transfected with siRNA specific for human AFG3L2 and Paraplegin. Immunoblot analysis was performed with α-OPA1 and α-CII. OPA1 isoforms were labeled as described in (A). Protein levels of Paraplegin and AFG3L2 are shown in Fig. 3.6 C.

3.2.2.2 Downregulation of Afg3l1 and Afg3l2 results in mitochondrial fragmentation

The dynamin-related GTPase OPA1 is essential for mitochondrial fusion (Olichon *et al.*, 2003; Cipolat *et al.*, 2004; Chen and Butow). The presence of both, long and short OPA1 isoforms was shown to be required for mitochondrial fusion activity (Song *et al.*, 2007). Because knockdown of Afg3l1 and Afg3l2 resulted in loss of long OPA1 isoforms, it is conceivable that mitochondrial morphology is affected. Thus, mitochondria-targeted red fluorescent protein (mito-DsRed) was expressed in MEFs depleted of Afg3l1 and Afg3l2. Control cells displayed tubular mitochondrial morphology (Fig. 3.8 A). Furthermore, mitochondrial morphology was not drastically altered in Afg3l1- or Afg3l2-depleted MEFs when compared to control cells (Fig. 3.8 A and B). In contrast, more than 80% of the cells contained fragmented mitochondria after simultaneous knockdown of Afg3l1 and Afg3l2 (Fig. 3.8 B). Thus, mitochondrial fragmentation in Afg3l1- and Afg3l2-depleted cells correlated with the loss of long OPA1 isoforms.
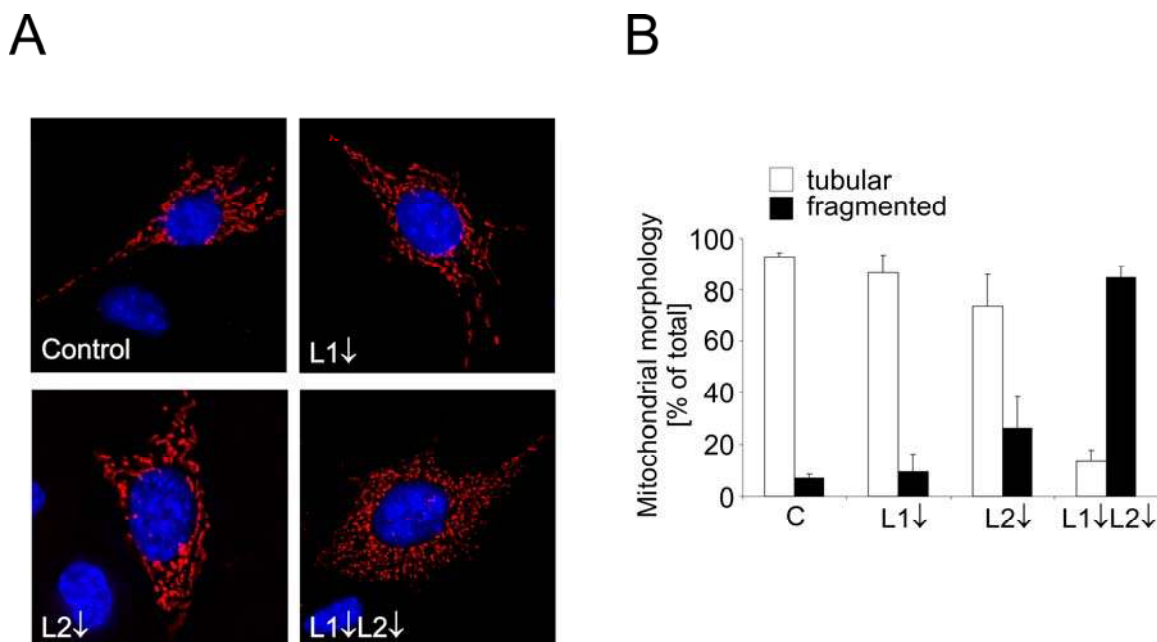
Figure 3.8 Concomitant knockdown of Afg3l1 and Afg3l2 results in mitochondrial fragmentation.
(A) Mitochondrial morphology after knockdown of Afg3l1 and Afg3l2. MEFs were transfected with siRNA against Afg3l1 and Afg3l2 followed by transfection with mito-DsRed. 48 hrs after transfection, cells were fixed with paraformaldehyde, nuclear DNA was stained with DAPI and mitochondrial morphology was analyzed by fluorescence microscopy. **(B)** Quantification of mitochondrial morphology. >150 cells were scored per experiment. Cells were classified into two classes containing either tubular or fragmented mitochondria. Bars represent means ± standard deviation (SD) of three independent experiments. C, control; L1, Afg3l1; L2, Afg3l2.

3.2.2.3 Expression of a non-cleavable long OPA1 isoform partially restores tubular morphology in Afg3l1/Afg3l2-depleted MEFs

The balanced expression of long and short OPA1 isoforms was shown to be important for mitochondrial fusion activity (Song *et al.*, 2007). This suggests that the mitochondrial fragmentation observed in Afg3l1/Afg3l2-depleted MEFs might be caused by the selective loss of long OPA1 isoforms. To substantiate this assumption, a Flag-tagged L-OPA1 isoform (OPA1-1ΔS1) lacking the processing site S1, was transiently transfected into MEFs followed by transfection of Afg3l1- and Afg3l2-siRNA (Fig. 3.9 A) (Ishihara *et al.*, 2006). In parallel, a Flag-tagged S-OPA1 construct composed of the short form of variant 7 (amino acid 230-970) fused to the mitochondrial targeting sequence of AIF (amino acids 1-95) was expressed (Fig. 3.9 A) (Ishihara *et al.*, 2006).

After 72 hrs, expression of the OPA1 constructs was monitored by immunoblot analysis. The expression of L-OPA1 variant 1ΔS1 was reduced after concomitant knockdown of Afg3l1 and Afg3l2 in MEFs (Fig. 3.9 B). Similarly, protein levels of S-OPA1 (AIF-variant 7) were decreased. To visualize mitochondria morphology in transfected cells by fluorescence microscopy, OPA1 constructs were co-transfected with mito-DsRed in a DNA ratio of 4:1. No significant changes in mitochondrial morphology of control cells occurred upon exogenous expression of the OPA1 constructs (Fig. 3.9 C). Despite reduced expression levels of L-OPA1 variant 1ΔS1 in MEFs depleted of Afg3l1 and Afg3l2, the tubular mitochondria network was restored in ~40% of the cells (Fig. 3.9 B and C). In contrast, expression of S-OPA1 did not significantly affect mitochondrial morphology (Fig. 3.9 C).

In summary, L-OPA1 variant 1ΔS1 was shown to partially suppress mitochondrial morphology defects in the absence of Afg3l1 and Afg3l2. This strongly indicates that mitochondrial fragmentation can be attributed to the loss of long OPA1 isoforms.
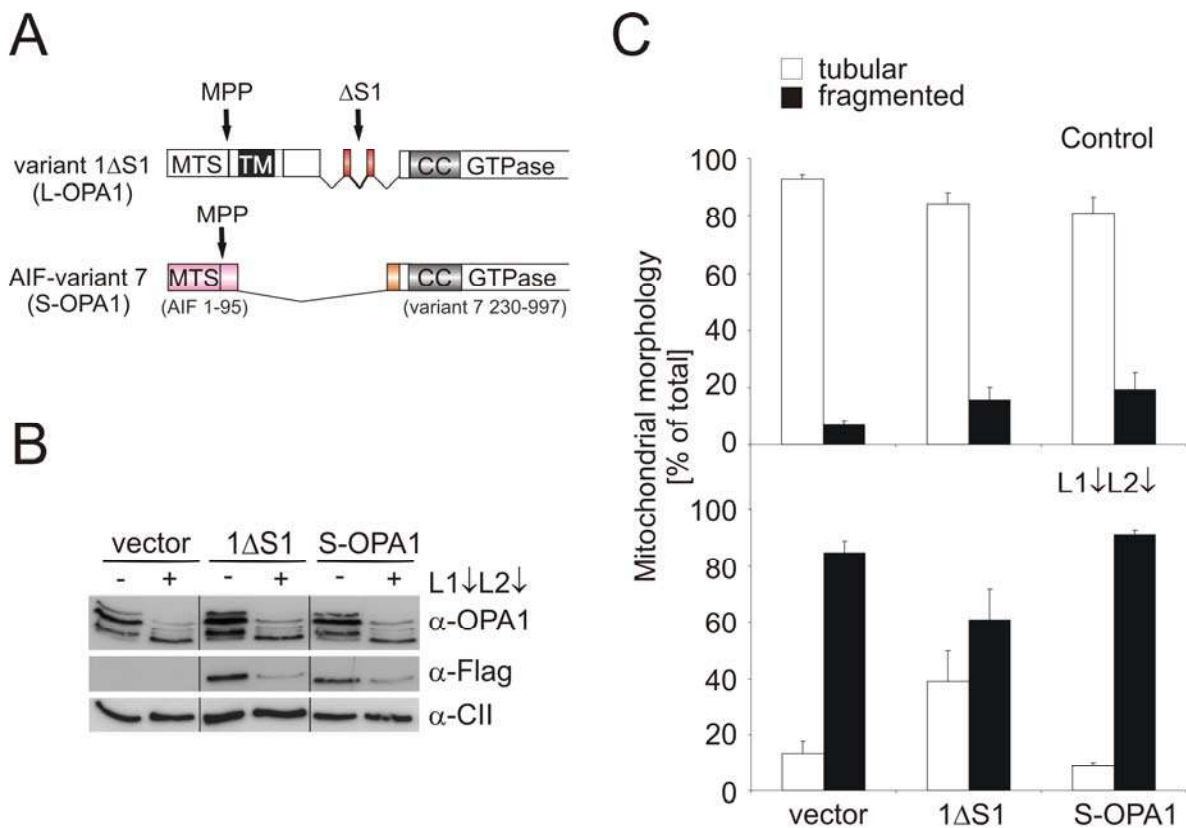
Figure 3.9 Expression of L-OPA1 variant 1ΔS1 partially restores mitochondrial morphology in MEFs depleted of the m-AAA protease subunits Afg3l1 and Afg3l2.
(A) Schematic representation of Flag-tagged OPA1 constructs. Variant 1ΔS1 (L-OPA1) represents rat splice variant 1 lacking processing site S1. AIF-variant 7 (S-OPA1) is composed of amino acids 230-997 of rat splice variant 7 fused to amino acids 1-95 of AIF (Ishihara *et al.*, 2006). Both variants are Flag-tagged at the C-terminus. MTS, mitochondrial targeting sequence; TM, transmembrane domain; CC, coiled coil domains; GTPase, GTPase domain. **(B)** Expression of OPA1 variants in MEFs. Immunoblot analysis of MEFs after transfection with OPA1-1ΔS1 and S-OPA1 (AIF-variant 7) and siRNA against Afg3l1 and Afg3l2. Endogenous OPA1 isoforms and transfected Flag-tagged OPA1 variants were detected with α-OPA1 and α-Flag antibodies, respectively. As a loading control, α-CII (70 kDa subunit of Complex II) antibody was used. **(C)** Quantification of mitochondrial morphology in Afg3l2/Afg3l1-depleted MEFs after transfection with OPA1 constructs. MEFs were transfected with mito-DsRed and the indicated OPA1 constructs followed by transfection with Afg3l1- and Afg3l2-siRNA. After 48 hrs, mitochondrial morphology was analyzed by fluorescence microscopy and >150 cells containing tubular or fragmented mitochondria were classified. Bars represent means ± SD of three independent experiments. L1, Afg3l1; L2, Afg3l2.

3.2.2.4 Mitochondrial respiration and membrane potential are maintained in m-AAA protease-depleted MEFs

Mitochondrial dysfunction and dissipation of the mitochondrial membrane potential can induce conversion of long into short OPA1 isoforms accompanied by mitochondrial fragmentation (Duvezin-Caubet *et al.*, 2006; Ishihara *et al.*, 2006). Thus, an impaired respiratory activity of mitochondria might cause the altered OPA1 isoform pattern in *m*-AAA protease-depleted cells. Further evidence gives the observation that human HSP fibroblasts lacking paraplegin showed an impaired assembly of Complex I pointing to a reduced mitochondrial respiration (Atorino *et al.*, 2003).

Therefore, mitochondrial respiration was analyzed in $Spg7^{+/+}$- and $Spg7^{-/-}$-MEFs after transfection with siRNA specific for Afg3l1 and Afg3l2. Endogenous respiration was not significantly affected under routine cell culture conditions (Fig. 3.10 A). However, when oligomycin-inhibited respiration was measured, a statistically significant increase of oxygen consumption upon downregulation of Afg3l1 and Afg3l2 was observed. This increase in respiration compared to wt cells indicates a proton leak across the inner membrane of Afg3l1/Afg3l2-depleted mitochondria. Furthermore, maximum respiratory capacity, mimicked by CCCP-induced uncoupled respiration, was decreased. The ratio of CCCP-induced respiration to oligomycin-inhibited respiration determines the respiratory control ratio (RCR), an indicator for the coupling efficiency between respiration and phosphorylation. Knockdown of Afg3l1 and Afg3l2 in $Spg7^{+/+}$- and $Spg7^{-/-}$-MEFs led a two-fold decrease in RCR. Respiratory defects due to differences in the mitochondrial content of the cells were excluded using citric synthase activity as a control (personal communication, A. Bernacchia). Taken together, concomitant depletion of the *m*-AAA protease subunits Afg3l1 and Afg3l2 resulted in a slight impairment of mitochondrial respiratory functions which most likely is caused by a partial uncoupling of oxidative phosphorylation. Nevertheless, under routine cell culture conditions, when ATP demand and turnover are low, endogenous respiration was not affected.

To analyze the mitochondria membrane potential in living cells, MEFs were stained with the lipohilic fluorescent dye JC-1 and analyzed by FACS. JC-1 is a cationic dye that visualizes mitochondrial polarization by shifting its fluorescence emission form from green (~525 nm) to red (~590 nm) due to a $\Delta\psi$-dependent uptake of red-fluorescent J-aggregates into mitochondria (Smiley *et al.*, 1991; Reers *et al.*, 1995). The mean of three independent

experiments revealed no significant differences in the intensity of red JC-1 fluorescence upon downregulation of any *m*-AAA protease subunit (Fig 3.10 B).
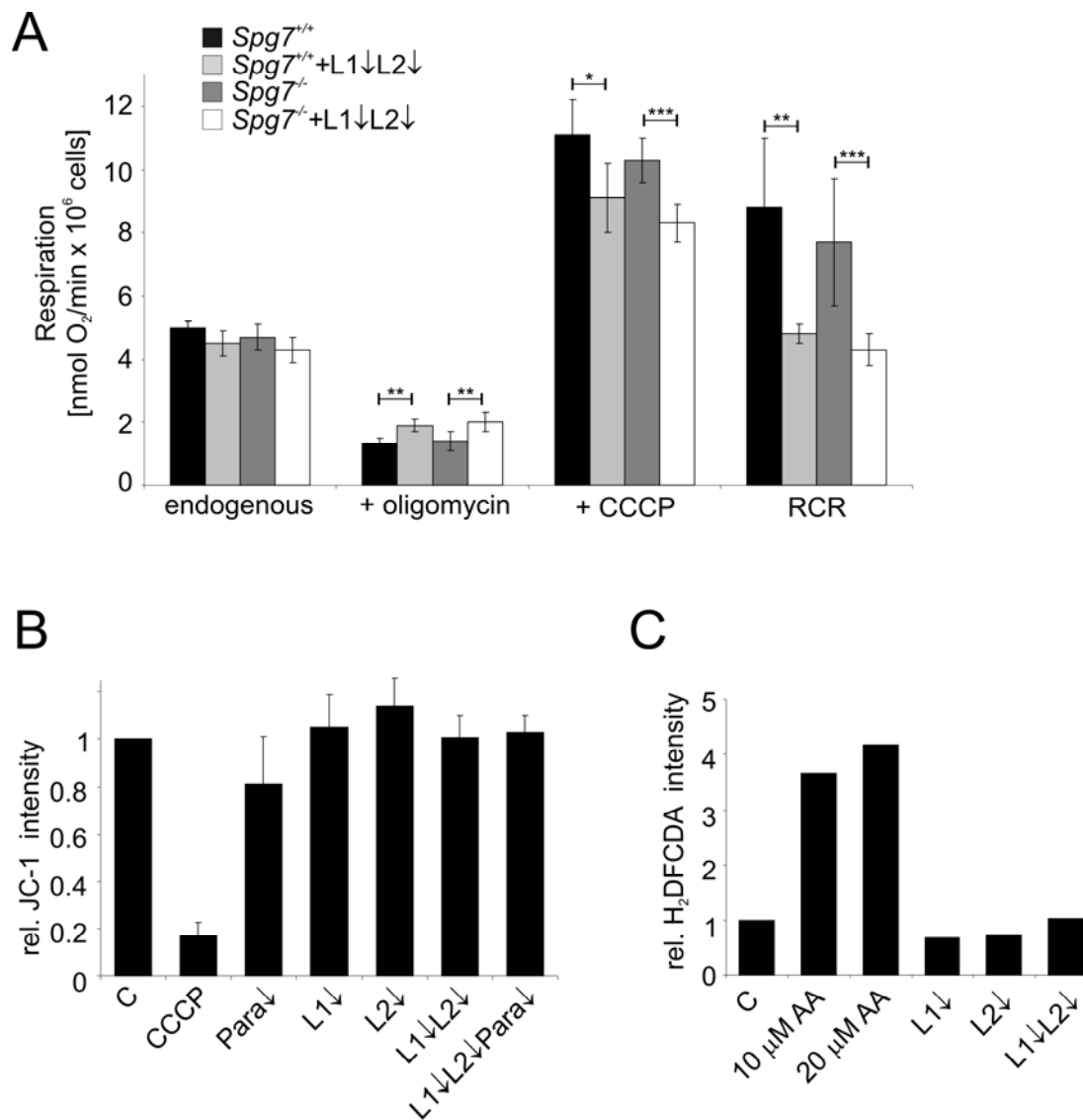
Figure 3.10 Analysis of mitochondrial respiratory functions in MEFs upon knockdown of *m*-AAA protease subunits.
(A) Measurement of oxygen consumption in intact cells. $Spg7^{+/+}$- $Spg7^{-/-}$-MEFs were transfected with siRNA against Afg3l1 and Afg3l2. Respiration was measured under routine conditions, after the addition of 2 μM oligomycin and during titrations with 250-750 nM of CCCP. Respiratory control ratio (RCR) was determined from the ratio of CCCP-induced to oligomycin-inhibited respiration. Bars represent means ± standard deviation (SD) of three independent experiments. **, p<0.01; ***, p<0.001. (B) Maintenance of membrane potential upon downregulation of *m*-AAA protease subunits. MEFs transfected with the indicated siRNAs were stained with the fluorescent dye JC-1 and fluorescence at 590 nm was measured by FACS. The relative fluorescence intensity compared to wt is indicated. CCCP-treated cells were used as a negative control. Data represent mean ± SD of three independent experiments. C, control. (C) Analysis of ROS production. Two days after transfection with siRNAs against Afg3l1 and Afg3l2, ROS production in intact cells was measured using carboxy-H_2DFCDA followed by FACS analysis. To induce endogenous ROS production, control cells were pretreated with 10 μM or 20 μM antimycin A (AA). Para, paraplegin; L1, Afg3l1; L2, Afg3l2.

The mitochondrial respiratory chain has been shown to be one of the major cellular producers of reactive oxygen species (ROS) due to electron leakage (Loschen and Azzi, 1974; Boveris and Cadenas, 1975). To analyze whether knockdown of Afg3l1 and Afg3l2 and the observed mitochondrial fragmentation are linked to increased ROS production, ROS levels in MEFs were measured using the oxidation-sensitive fluorescence dye carboxy-H_2DFCDA. Pretreatment of cells with 10 μM or 20 μM antimycin A resulted in a drastic increase of H_2DFCDA fluorescence because of induced ROS production by inhibition of Complex III (Fig. 3.10 C). However, depletion of Afg3l1 an Afg3l2 did not enhance intracellular ROS production.

In conclusion, these results indicate that the loss of long OPA1 isoforms in the absence of the *m*-AAA protease is not caused by an impaired mitochondrial respiration or membrane potential. Furthermore, contrary to published results, no statistically significant respiratory deficiencies could be detected in paraplegin-deficient MEFs (Atorino *et al.*, 2003).

3.2.3 Analysis of OPA1 processing in the absence of Afg3l and Afg3l2

3.2.3.1 *Induced cleavage at processing site S1 and destabilization of long OPA1 isoforms in the absence of Afg3l1 and Afg3l2*

Human OPA1 is encoded by eight different splice variants resulting from alternative splicing of exons 4, 4b and 5b (Delettre *et al.*, 2001). All OPA1 mRNA splice forms encode a processing site S1 in exon 5 in addition to the MPP cleavage site (Fig. 3.11 A). A second processing site S2 is encoded by exon 5b which is only present in splice variants 4, 6, 7 and 8 (Ishihara *et al.*, 2006; Olichon *et al.*, 2006; Song *et al.*, 2007). To further dissect the regulatory functions of *m*-AAA proteases for the processing of OPA1, we analyzed the consequences of *m*-AAA protease downregulation on individual splice variants. Therefore, Flag-tagged variant 1 harbouring cleavage site 1 and variant 7, which contains both cleavage sites were transiently expressed in MEFs followed by knockdown of Afg3l1 and Afg3l2.

The first focus was on the role of *m*-AAA proteases in processing at site S1 using expression of Flag-tagged OPA1 variant 1. In control cells, variant 1 produced a single L-OPA1 isoform and a less abundant S-OPA1 isoform resulting from S1-cleavage (Fig. 3.11 B). They were shown to correspond to OPA1 isoforms L2 and S5 of endogenous OPA1 (Duvezin-Caubet *et al.*, 2007) (Fig.3.7 A). Strikingly, depletion of Afg3l1 and Afg3l2 caused the complete loss of L-OPA1 accompanied by an accumulation of S-OPA1 pointing to accelerated cleavage at processing site S1 (Fig. 3.11 B). To investigate whether L-OPA1 is not only processed more efficiently but also faster degraded, cells were transfected with an L-OPA1 variant in which processing site S1 was deleted (OPA1-1ΔS1) (Fig. 3.9 A) (Ishihara *et al.*, 2006). Expression of OPA1-1ΔS1 in control cells resulted exclusively in the formation of L-OPA1 (Fig. 3.11 B). Remarkably, 72 hrs after transfection L-OPA1 could not be detected anymore in cells depleted of Afg3l1 and Afg3l2 (Fig. 3.11 B). To distinguish between impaired synthesis and increased degradation of OPA1-1ΔS1, the cytosolic protein synthesis was inhibited for 6 hrs using cycloheximide. In contrast to control cells in which L-OPA1 level remained stable after inhibition of protein synthesis, the protein level was drastically reduced in MEFs transfected with Afg3l1 and Afg3l2 siRNA (Fig. 3.11 C). This indicates that in the absence of Afg3l1 and Afg3l2 not only S1-cleavage but also turnover of L-OPA1 isoforms is increased.
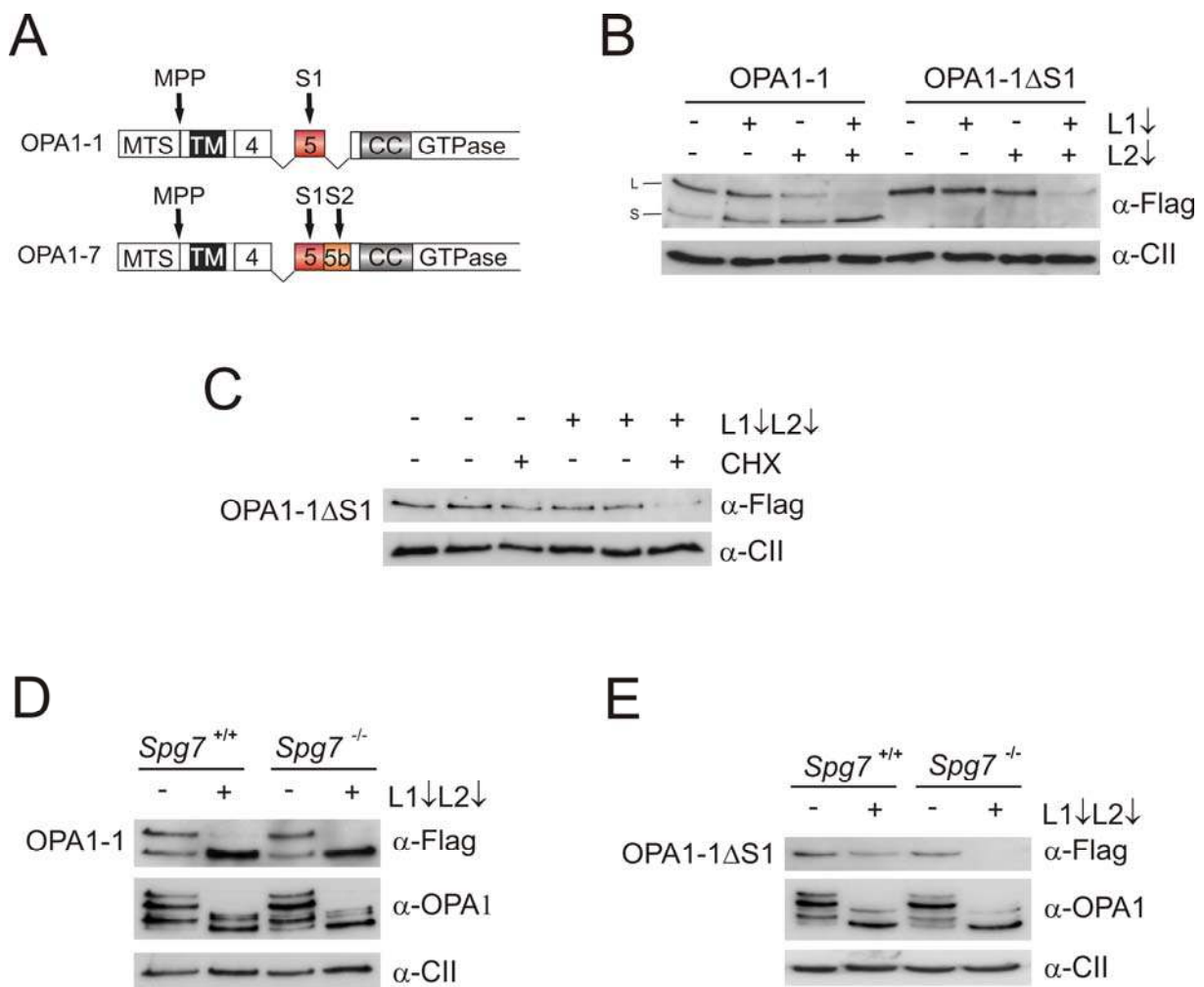
Figure 3.11 Depletion of Afg3l1 and Afg3l2 results in increased cleavage at processing site S1 and destabilization of L-OPA1 isoforms.
(A) Schematic representation of OPA1 splice variant 1 and splice variant 7. Splice variant 1 (OPA1-1) and splice variant 7 (OPA1-7) differ in the presence of exon 5b. Cleavage of the mitochondrial targeting signal (MTS) by the mitochondrial processing peptidase (MPP) produces the long isoforms. Additional cleavage at processing sites S1 or S2 leads to the short isoforms. TM, transmembrane domain; CC, coiled-coil region. **(B)** Effects of Afg3l1 and Afg3l2 siRNA on OPA1 splice variants 1 and 1ΔS1. MEFs were transfected with Flag-tagged OPA1 variants followed by siRNA transfection. 72 hrs after the first transfection cells were harvested. Cell lysates were analyzed by SDS-PAGE and immunoblotting with α-Flag and α-CII antibodies. Expression of variant 1 produces a long (L) and a short (S) OPA1 isoform. Upon deletion of processing site 1 (1ΔS1), only the L-OPA1 isoform is expressed. **(C)** Cycloheximide-chase of OPA1-1ΔS1 upon knockdown of Afg3l1 and Afg3l2. MEFs were transfected with OPA1 variant 1ΔS1 and siRNA directed against Afg3l1 and Afg3l2. Two days after transfection, cells were incubated for 6 hrs with 100 μg/ml cycloheximide (CHX) and analyzed as described in (B). **(D)** and **(E)** Expression of OPA1 splice variant 1 (D) and 1ΔS1 (E) in paraplegin-deficient MEFs. Spg7^{+/+}- and Spg7^{-/-}-MEFs were transfected with Flag-tagged OPA1 variants followed by transfection of Afg3l1 and Afg3l2 siRNA. Cell lysates were analyzed as described in (B) with antibodies recognizing the Flag-tag, OPA1 and CII (70 kDa subunit of Complex II). L1, Afg3l1; L2, Afg3l2.

Interestingly, the third subunit of the *m*-AAA protease, paraplegin, has been observed to stimulate cleavage at S1 when overexpressed (Ishihara *et al.*, 2006). This suggests that paraplegin might be involved in the accelerated processing caused by the absence of Afg3l1 and Afg3l2. Therefore, Afg3l1 and Afg3l2 were downregulated in *Spg7^{-/-}*-cells after transfection with OPA1 variant 1. The absence of paraplegin did not alter the balance of long and short isoforms compared to wt (Fig. 3.11 D). Furthermore, increased processing of variant 1 induced by knockdown of Afg3l1 and Afg3l2 could be observed to similar extents in *Spg7^{+/+}*-and *Spg7^{-/-}*-MEFs (Fig. 3.11 D). To assign whether the degradation of L-OPA1 is mediated by paraplegin, OPA1 variant-1ΔS1 was expressed in paraplegin-deficient cells. However, loss of L-OPA1 was also observed in the absence of paraplegin (Fig. 3.11 E).
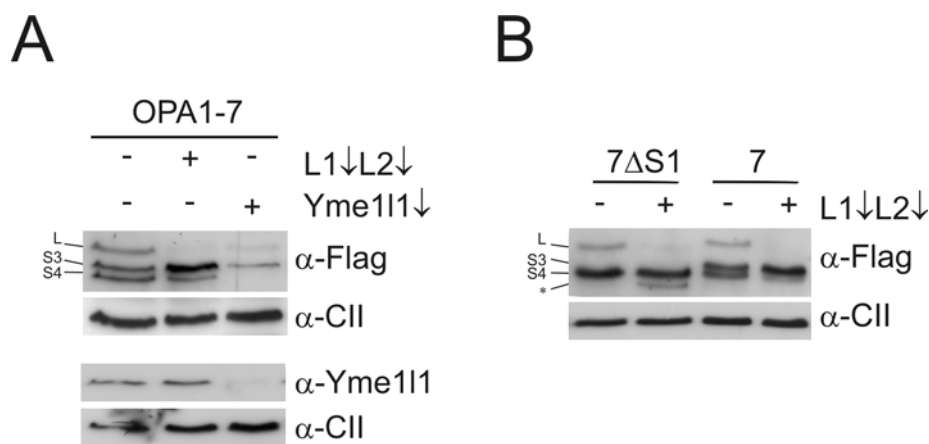
Figure 3.12 The *m*-AAA protease does not affect cleavage at processing site S2.
(A) Effect of Afg3l1 and Afg3l2 knockdown on S2-cleavage of OPA1 splice variant 7. MEFs were transfected with Flag-tagged rat OPA1 variant 7 (OPA1-7) followed by siRNA transfection to downregulate either Afg3l1 and Afg3l2 or Yme1l1. Expression of OPA1 variant 7 was analyzed by immunoblotting using α-Flag antibodies. Downregulation of Yme1l1 was confirmed with α-Yme1l1 immunoblotting. **(B)** Effects of Afg3l1 and Afg3l2 knockdown on S2-cleavage of OPA1 splice variant 7ΔS1. Flag-tagged OPA1 variant 7 and variant 7ΔS1 were expressed in MEFs and expression was detected by immunoblotting with α-Flag antibody. The resulting OPA1 isoforms are labeled according to Fig. 3.7 A. OPA1 isoform S3 is produced by processing of L-OPA1 at cleavage site S1 whereas isoform S4 is the product of processing at cleavage site S2. The asterisk indicates a novel cleavage product for 7ΔS1. CII, 70 kDa subunit of Complex II. L1, Afg3l1; L2, Afg3l2.

Given the enhanced cleavage at site S1 in the absence of Afg3l1 and Afg3l2, possible effects on processing at site S2 were examined. Notably, the *i*-AAA protease Yme1l1 was found to be important for cleavage at processing site S2 (Song *et al.*, 2007). As result of cleavage at processing sites S1 and S2, expression of OPA1 variant 7 in MEFs produced two

short OPA1 isoforms, presumably S3 and S4 (Fig. 3.12 A). Knockdown of Afg3l1 and Afg3l2 led to the accumulation of isoform S3 whereas S4 seemed not to be affected. In agreement with previous findings, the knockdown of Yme1l1 abolished S2-cleavage resulting in drastically reduced levels of isoform 4 (Fig. 3.12 A) (Song *et al.*, 2007). To substantiate that S2-cleavage occurs independently of Afg3l1 and Afg3l2, OPA1 variant 7ΔS1, lacking the processing site S1 was expressed (Ishihara *et al.*, 2006). Consistently, downregulation of Afg3l1 and Afg3l2 led to the loss of L-OPA1 without any impact on the short isoform S4 produced by S2-cleavage (Fig. 3.12 B). In addition, there is a slight accumulation of a novel cleavage product (Fig. 3.12 B).

In summary, these results indicate that downregulation of the *m*-AAA protease subunits Afg3l1 and Afg3l2 enhances OPA1 processing at cleavage site S1 but not at S2. Furthermore, the degradation of long OPA1 isoforms is accelerated which indicates a decreased stability in the absence of functional *m*-AAA protease complexes.

3.2.3.2 Functions of other mitochondrial proteases in OPA1 processing

Since mammalian *m*-AAA proteases seem to be dispensable for OPA1 processing, the involvement of other mitochondrial proteases was investigated. Of special interest was the identification of proteases responsible for the accelerated processing of L-OPA1 isoforms at processing site S1 in the absence of Afg3l1 and Afg3l2.

The *i*-AAA protease Yme1l1 has already been implicated in the proteolytic processing at site 2 (Song *et al.*, 2007). Therefore, MEFs were transfected with two different siRNAs against Yme1l1 which resulted in the efficient reduction of Yme1l1 protein level (Fig. 3.13 A). In agreement with published observations, immunoblot analysis using α-OPA1 antibody revealed a reduced protein level of OPA1 isoform S4, the cleavage product of processing at site S2 (Fig. 3.13 A) (Song *et al.*, 2007). However, induced processing of OPA1 after downregulation of Afg3l1 and Afg3l2 occured also in the absence of Yme1l1 (Fig. 3.13 A).

The mitochondrial protease Lon resides in the matrix and has been implicated in the quality control of proteins (Suzuki *et al.*, 1994; Van Dyck *et al.*, 1994; Bota and Davies, 2002). Therefore, the requirement of Lon for the degradation of L-OPA1 isoforms was examined. Although efficient downregulation of Lon was achieved, L-OPA1 isoforms were not stabilized in Afg3l1/Afg3l2-depleted MEFs (Fig. 3.13 B). Other likely candidates for

OPA1 processing are PARL (presenilin-associated, rhomboid like protease) residing in the inner mitochondrial membrane and the oligomeric serine protease HtrA2/Omi which is localized to the inter membrane space (Pellegrini *et al.*, 2001; Suzuki *et al.*, 2001; Hegde *et al.*, 2002). However, MEFs derived from *Parl$^{-/-}$*- and *HtrA2$^{-/-}$* mice did not show an effect on the OPA1 isoform pattern or on the induced proteolysis of long isoforms upon knockdown of Afg3l1 and Afg3l2 (Fig. 3.13 C and D) (Martins *et al.*, 2004; Cipolat *et al.*, 2006).

Figure 3.13 The mitochondrial proteases Yme1l1, Lon, Parl and HtrA2 are dispensable for the induced proteolysis of L-OPA1.
(A) MEFs were transfected with specific siRNAs against Yme1l1 or Lon alone or together with Afg3l1 and Afg3l2 siRNA. Downregulation of Yme1l1 and Lon was confirmed by immunoblotting using antibodies specific for Yme1l1 and Lon, respectively. (B) *Parl$^{-/-}$*-MEFs and *HtrA2$^{-/-}$*-MEFs and their corresponding wt controls were transfected with control siRNA or siRNA against Afg3l1 and Afg3l2. OPA1 isoform pattern was investigated by SDS-PAGE and immunoblotting with α-OPA1 and α-CII (70 kDa subunit of Complex II) antibodies. An unspecific crossreaction of α-Lon antibody is marked with an asterisk. L1, Afg3l1; L2, Afg3l2.

To further investigate the function of Parl, HtrA2 and Yme1l1 in the inducible processing of OPA1 at cleavage site S1, Flag-tagged OPA1 isoform 1 was expressed in MEFs transfected with Yme1l1 was well as in *Parl$^{-/-}$*- and *HtrA2$^{-/-}$*-MEFs (Fig. 3.14 A and B). Immunoblotting using an α-Flag antibody revealed that in the absence of these proteases,

downregulation of Afg3l1 and Afg3l2 still led to accelerated conversion of L-OPA1 to S-OPA1 isoforms (Fig. 3.14 A and B).

Taken together, these results revealed that the mitochondrial proteases Parl, HtrA2, Lon and Yme1l1 are dispensable for the induced proteolysis of L-OPA1 isoforms upon knockdown of Afg3l1 and Afg3l2. Furthermore, Yme1l1, HtrA2 and Parl are not required for constitutive cleavage of L-OPA1 isoforms whereas Yme1l1 is involved in the generation of isoform S4, as previously published (Griparic *et al.*, 2007; Song *et al.*, 2007).

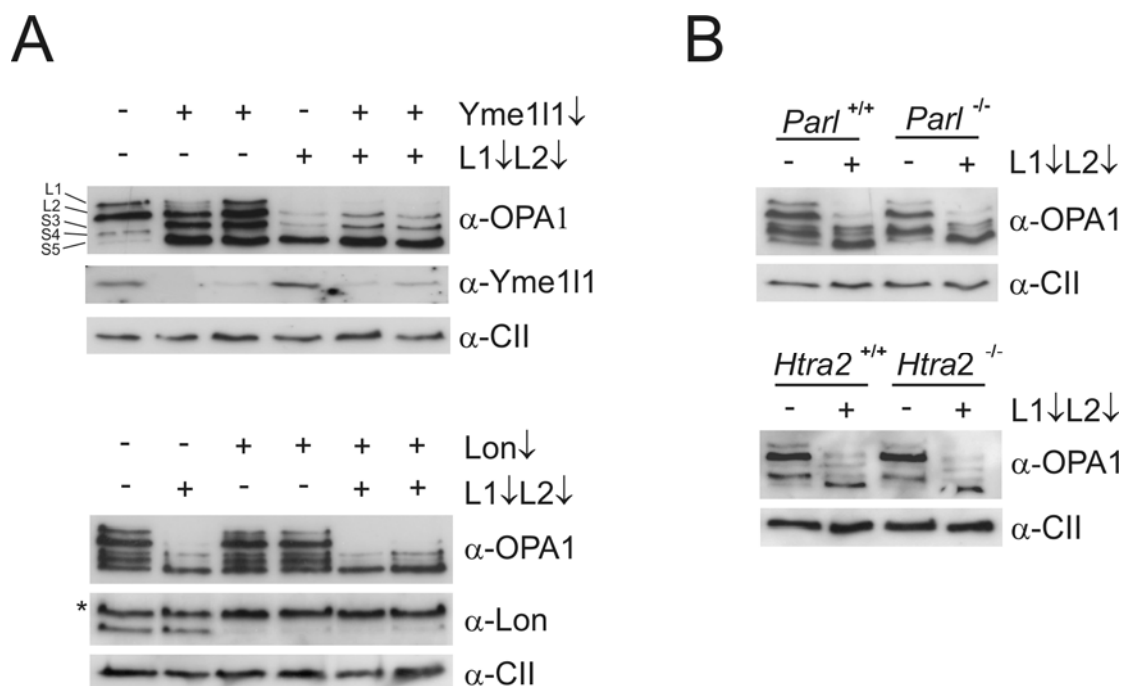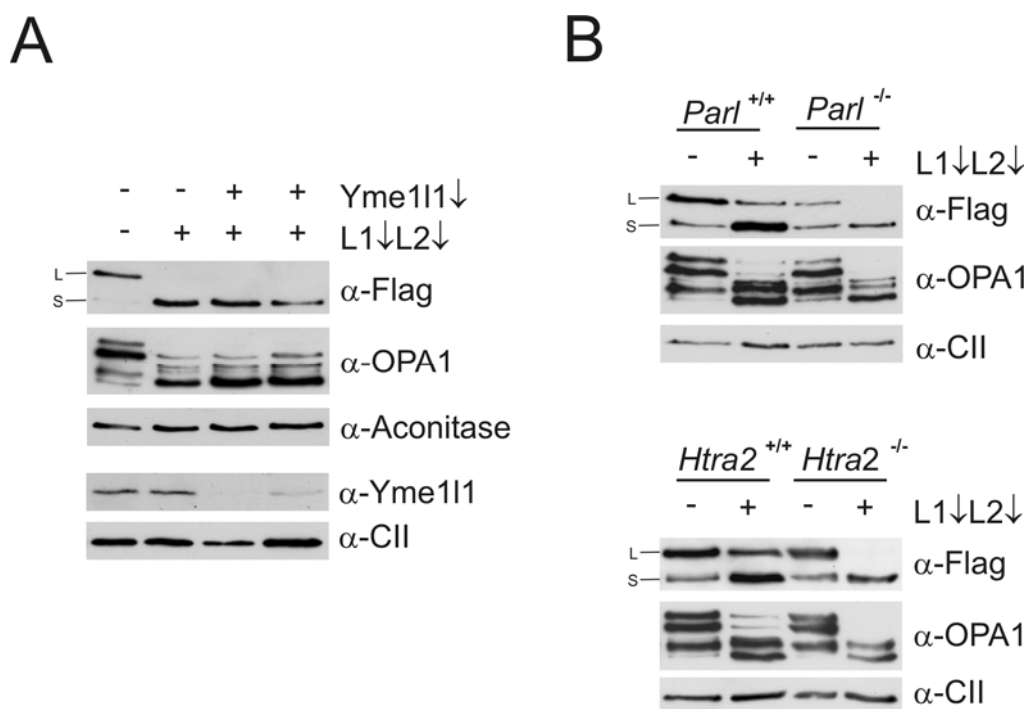**Figure 3.14 The mitochondrial proteases Yme1l1, Parl and HtrA2 are dispensable for induced processing at site S1.**
 (A) MEFs were transfected with Flag-tagged OPA1 variant 1 followed by transfection of specific siRNA against Yme1l1 alone and together with Afg3l1 and Afg3l2 siRNA. Downregulation of Yme1l1 was confirmed by immunoblotting using a-Yme1l1. **(B)** *Parl*^{-/-}-MEFs and *HtrA2*^{-/-}-MEFs and their corresponding wt controls were transfected with Flag-tagged OPA1 variant 1 and siRNAs against Afg3l1 and Afg3l2. Analysis was performed by SDS-PAGE and immunoblotting with α-OPA1 and α-Flag antibodies. As loading controls the antibodies α-CII (70 kDa subunit Complex II) and α-Aconitase (Aconitase 2) were used. L, L-OPA1 isoform; S, S-OPA1 isoform. L1, Afg3l1; L2, Afg3l2.

3.2.3.3 Analysis of OPA1 processing in the presence of different protease inhibitors

Similar to *m*-AAA protease depletion, loss of mitochondrial membrane potential by CCCP has been shown to enhance the cleavage of OPA1 (Duvezin-Caubet *et al.*, 2006; Ishihara *et al.*, 2006; Song *et al.*, 2007). Furthermore, CCCP-induced OPA1 processing was delayed in the presence of *o*-phenantroline, a membrane-permeable bivalent metal chelator known to inhibit metalloproteases (Duvezin-Caubet *et al.*, 2006; Ishihara *et al.*, 2006; Guillery *et al.*, 2008). Therefore, OPA1 processing was investigated after knockdown of Afg3l1 and Afg3l2 in the presence of *o*-phenantroline and other membrane-permeable protease inhibitors. Flag-tagged variant 1 was expressed in MEFs followed by transfection with Afg3l1 and Afg3l2 siRNA. To inhibit the four major groups of proteases, serineproteases, cysteineproteases, aspartylproteases and metalloproteases, cells were incubated with the respective inhibitors Pefabloc, E-64, Pepstatin A and *o*-phenantroline. Since recent reports suggest a role of the proteasome in mitochondrial protein quality control, the proteasome inhibitor MG132 was included in this study (Margineantu *et al.*, 2007; Radke *et al.*, 2008). As previously observed, downregulation of Afg3l1 and Afg3l2 resulted in the accumulation of the short isoform of variant 1 (Fig. 3.15 A). Incubation with any of the protease inhibitors did not impair the accelerated conversion of L-OPA1 to S-OPA1 (Fig. 3.15 A, left panel). However, positive controls for the inhibitory effect on proteases are missing. Strikingly, L-OPA1 and the putative precursor of OPA1 were stabilized in the presence of *o*-phenantroline and MG132 in Afg3l1/ Afg3l2-depleted MEFs (Fig 3.15 A, left panel). Similar accumulations of long OPA1 isoforms in the presence of these protease inhibitors were observed in control cells (Fig 3.15 A, right panel). From these experiments, it is unclear whether the accumulation of L-OPA1 and its putative precursor is due to an impaired processing of the L-OPA1 isoform or a stabilisation of newly synthesized OPA1 precursors.

A

B
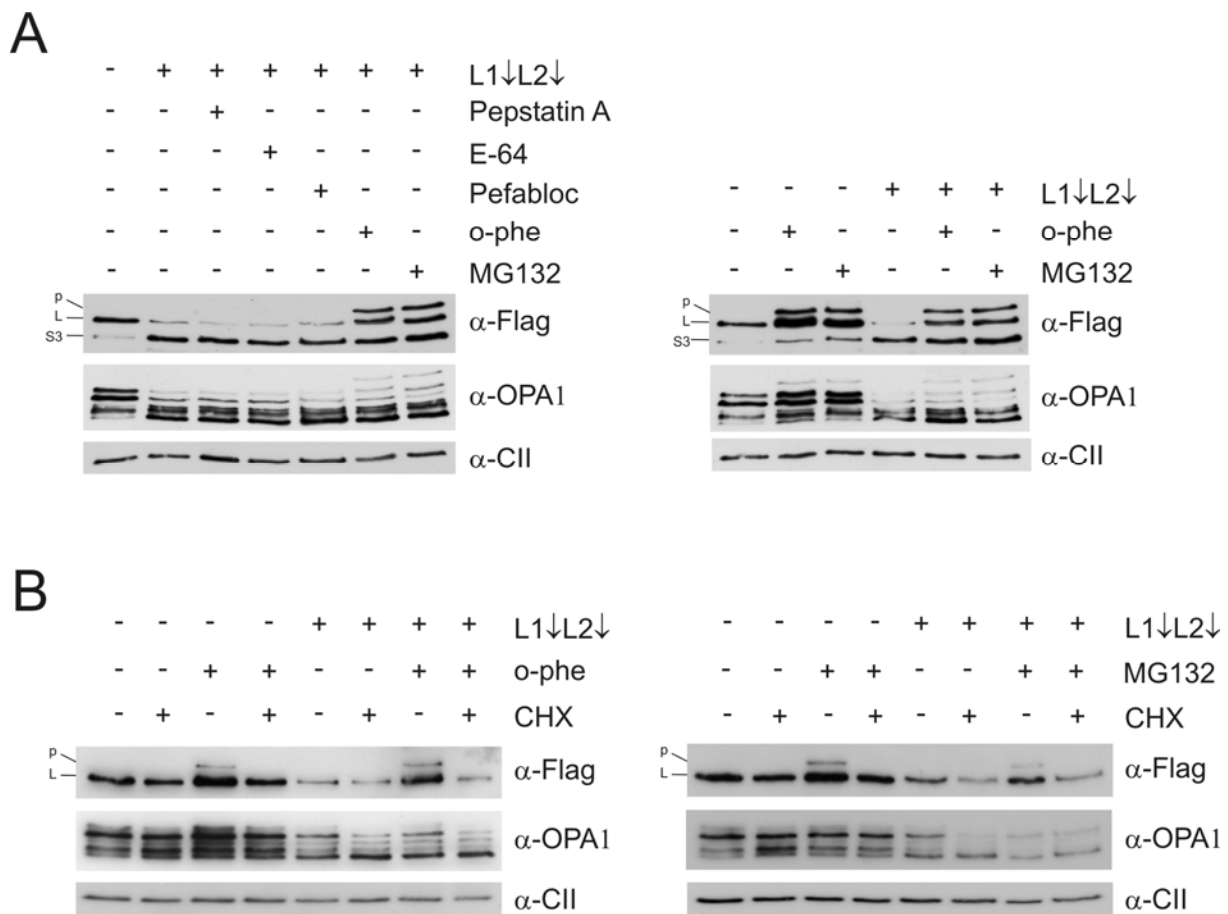
Figure 3.15 Stabilisation of newly synthesized OPA1 using the protease inhibitors MG132 and 1,10-phentantroline.
(A) Processing of OPA1 variant 1 in the presence of different protease inhibitors. MEFs were transfected with Flag-tagged OPA1 variant 1 together with Afg3l1 and Afg3l2 siRNA. After 48 hrs, MEFs were incubated for 5 hrs with 10 μM Pepstatin A, 50 μM E-64, 0.5 mM Pefabloc, 0.5 mM o-phenantroline (o-phe) or 5 μM MG132 and subsequently subjected to SDS-PAGE and immunoblotting. Expression of OPA1 variant 1 and endogenous OPA1 was analyzed using α-Flag and α-OPA1 antibodies, respectively, and as a control antibody against subunit 2 of Complex II (CII). **(B)** CHX-sensitive stabilization of OPA1 variant 1ΔS1 by o-phenantroline and MG132. MEFs were transfected with Flag-tagged OPA1 variant 1ΔS1 followed by siRNA transfection with Afg3l1 and Afg3l2. 72 hrs after transfection, 0.5 mM o-phenantroline and 5 μM MG132 were added and followed by addition of 100 μg/ml cyclohexmide after 30 min and further incubation for 4.5 hrs. MEFs were analyzed as described in (A). p, precursor; L, L-OPA1; S3, short OPA1 isoform 3. L1, Afg3l1; L2, Afg3l2.

To examine whether the inhibition of proteases with MG132 and o-phenantroline stabilizes only newly synthesized OPA1, cells were incubated in the presence of cycloheximide (CHX) to inhibit protein synthesis. Before, MEFs were transfected with Flag-tagged OPA1-1ΔS1 and siRNA against Afg3l1 and Afg3l2. As previously shown, an accelerated degradation of OPA1-1ΔS1 in the presence of CHX was observed in

Afg3l1/Afg3l2-depleted MEFs but not in control cells (Fig. 3.11 E and 3.15 B). After incubation with the inhibitors MG132 and *o*-phenantroline, L-OPA1 and its precursor were stabilized in MEFs (Fig. 3.15 B). However, if cytosolic protein synthesis was blocked 30 min after addition of the protease inhibitors, long OPA1 isoforms of endogenous OPA1 and transfected OPA1-1ΔS1 were degraded to similar extents as without protease inhibitors (Fig. 3.15 B). This indicates, that accumulation of long OPA1 isoforms after protease inhibition with MG132 and *o*-phenantroline results from stabilization of newly synthesized OPA1 precursor protein and not from an impaired processing of L-OPA1 isoforms. In line with previous publications, the proteasome inhibitor MG132 most likely stabilizes mitochondrial precursor protein in the cytosol resulting in increased mitochondrial import (Margineantu *et al.*, 2007; Radke *et al.*, 2008). The accumulation of OPA1 precursor by *o*-phenantroline might result from inhibition of the mitochondrial processing peptidase (MPP), a metalloprotease responsible for the removal of mitochondrial targeting sequences. However, it should be emphasized that from these results a metalloprotease-dependent cleavage at processing site S1 cannot be excluded. Consistently, accelerated cleavage of long OPA1 isoforms in isolated mitochondria can be inhibited in the presence of *o*-phenantroline (Ishihara *et al.*, 2006; Guillery *et al.*, 2008).

3.2.4 Mitochondrial hyperfusion in *m*-AAA protease- and prohibitin-depleted MEFs

3.2.4.1 *CHX-induced hyperfusion is dependent on the m-AAA protease but not on prohibitins*

Recently, it has been observed that mitochondria undergo extensive fusion events and form a highly interconnected network in MEFs exposed to low concentrations of diverse stress stimuli (D. Tondera and J.-C. Martinou, personal communication). Interestingly, this mitochondrial hyperfusion was shown to be dependent on a balanced expression of long and short OPA1 isoforms. Therefore, the dependence of mitochondrial hyperfusion on the *m*-AAA protease was investigated. Interestingly, depletion of prohibitin 2 has been recently demonstrated to affect the OPA1 isoform pattern and mitochondrial morphology in a manner similar to the *m*-AAA protease (Merkwirth *et al.*, 2008). The *m*-AAA protease and prohibitins, both residing in the inner mitochondrial membrane, were shown to interact and form a supercomplex (Metodiev, 2005). Thus, functional analysis of prohibitins in mitochondrial hyperfusion was included in addition to the analysis of *m*-AAA proteases.

Knockdown of either Afg3l1 and Afg3l2 or prohibitin 2 (Phb2) resulted in decreased levels of L-OPA1 isoforms and an accumulation of S-OPA1 isoforms (Fig. 3.16 A). This was accompanied by mitochondrial fragmentation (Fig. 3.16 B). To induce mitochondrial tubulation, MEFs were incubated in the presence of cycloheximide (CHX). Already after 3 hrs, tubular mitochondria were converted into a highly interconnected network in ~90% of control cells (Fig. 3.16 B and C). Strikingly, mitochondrial tubulation in the presence of CHX was completely abolished in Afg3l1- and Afg3l2-depleted MEFs and mitochondria stayed fragmented (Fig. 3.16 B and C). This is in contrast to fragmented mitochondria depleted of Phb2 which were observed to hyperfuse in ~80% of the cells (Fig. 3.16 B and C).

In conclusion, the absence of *m*-AAA proteases and prohibitins affects the loss of long OPA1 isoforms similarly whichr leads to mitochondrial fragmentation. In *m*-AAA protease-deficient MEFs mitochondrial hyperfusion was completely abolished. However, fragmented mitochondria formed highly interconnected networks in prohibitin-depleted MEFs indicating fusion activity despite an apparently impaired OPA1 function.
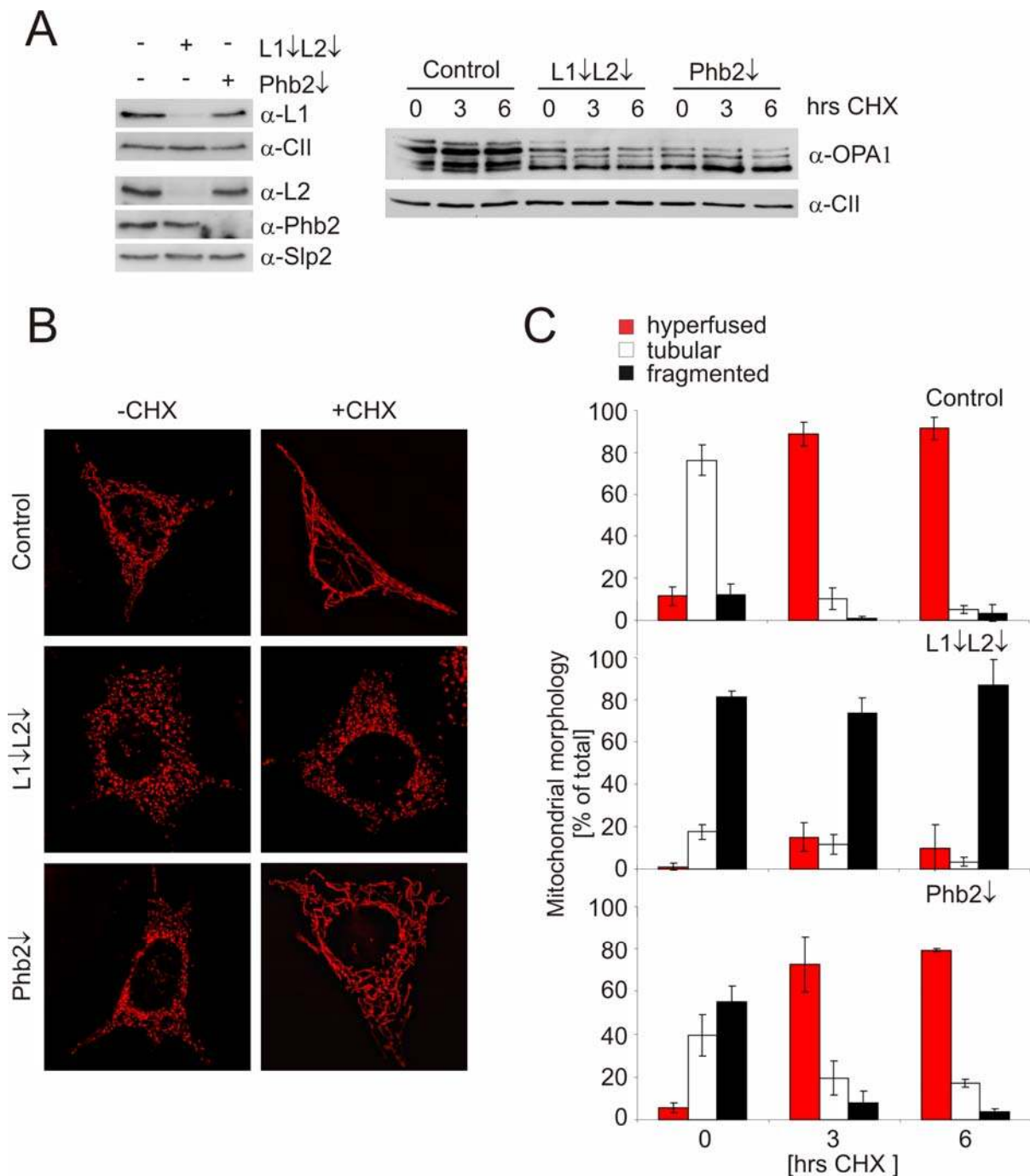
Figure 3.16 CHX-induced mitochondrial hyperfusion is dependent on the *m*-AAA protease but not on prohibitins.
(A) Immunoblot analysis of MEFs transfected with siRNA against Afg3l1 and Afg3l2 or Phb2. MEFs were transfected with siRNA against Afg3l1 and Afg3l2 or Phb2 followed by transfection with mito-DsRed. 48 hrs after transfection, cells were lysed and subjected to SDS-PAGE and immunoblotting. To assess the knockdown efficiency antisera recognizing Afg3l1, Afg3l2, Phb2, and as controls, Slp2 (stomatin-like protein 2) and CII (70 kDa subunit of Complex II) were used. In addition, the OPA1 isoform pattern was analyzed by immunodecoration with the antibodies α-OPA1 and, as a loading control, α-CII. **(B)** CHX-induced mitochondrial morphology. MEFs were transfected with siRNA against Afg3l1 and Afg3l2 or Phb2 followed by transfection with mito-DsRed. 48 hrs after transfection, the cells were incubated in the presence of cycloheximide (CHX) for 3 hrs and mitochondrial morphology was analyzed by fluorescence microscopy. **(C)** Quantification of mitochondrial morphology after CHX-induced hyperfusion. MEFs transfected with siRNA were incubated with CHX for 3 and 6 hrs. More than 150 cells were scored for each experiment. Cells were classified into three classes containing hyperfused, tubular or fragmented mitochondria. Bars represent means ± SD of three independent experiments. L1, Afg3l1; L2, Afg3l2.

3.2.4.2 Knockdown of Phb2 in OPA1- and m-AAA protease-depleted MEFs does not restore mitochondrial hyperfusion

In contrast to fragmented mitochondria in Afg3l1/Afg3l2-depleted MEFs, prohibitin-depleted fragmented mitochondria were shown to fuse in the presence of cycloheximide despite an altered OPA1 pattern. In both cases, mitochondrial fragmentation under steady state levels is ascribed to an imbalance of short and long OPA1-isoforms (Merkwirth *et al.*, 2008). Similarly to *m*-AAA protease depletion, it was shown that the loss of OPA1 results in mitochondrial fragmentation and a block in hyperfusion (D. Tondera and J.-C. Martinou, personal communication; Griparic *et al.,* 2004; Olichon *et al.,* 2003). Prohibitin-depleted mitochondria are fragmented under normal conditions due to an impaired function of OPA1 (Merkwirth *et al.*, 2008). Since OPA1 is implicated in the fusion of mitochondrial inner membranes, it is striking that prohibitin-depleted mitochondria are able to fuse under certain conditions unlike mitochondria depleted of OPA1 or the *m*-AAA protease. These observations led to the hypothesis, that the absence of prohibitins might suppress the dependence of mitochondrial fusion on OPA1 upon induction with CHX.

To investigate whether the knockdown of Phb2 restores the tubulation ability in fragmented mitochondria of *m*-AAA protease-depleted or OPA1-depleted MEFs, these proteins were simultaneously downregulated and mitochondrial morphology was analyzed. Efficient downregulation of either Phb2 or Afg3l1 and Afg3l2 resulted in the loss of L-OPA1 isoforms. Similar observations were made upon simultaneous knockdown of Afg3l1 and Afg3l2 together with Phb2 (Fig.3.17 A). Furthermore, OPA1 was efficiently depleted using siRNA-mediated downregulation (Fig.3.17 A). Under routine cell culture conditions, 80-90% MEFs depleted of either OPA1 or Afg3l1 and Afg3l2 contained fragmented mitochondria (Fig. 3.17 B). Similarly, fragmented mitochondria were observed in ~70 % of prohibitin-depleted cells. After incubation with CHX, mitochondria stayed fragmented in the absence of either OPA1 or Afg3l1 and Afg3l2 in contrast to prohibitin-depleted mitochondria which formed a highly elongated mitochondrial network in ~70% of the cells. However, the absence of Phb2 in either Afg3l1- and Afg3l2-depleted or OPA1-depleted MEFs did not restore the ability of fragmented mitochondria to tubulate under hyperfusion conditions. The requirement of active OPA1 in these cells for hyperfusion is not suppressed in the absence of prohibitins. Therefore, OPA1 and the *m*-AAA protease seem to be essential for mitochondrial hyperfusion.
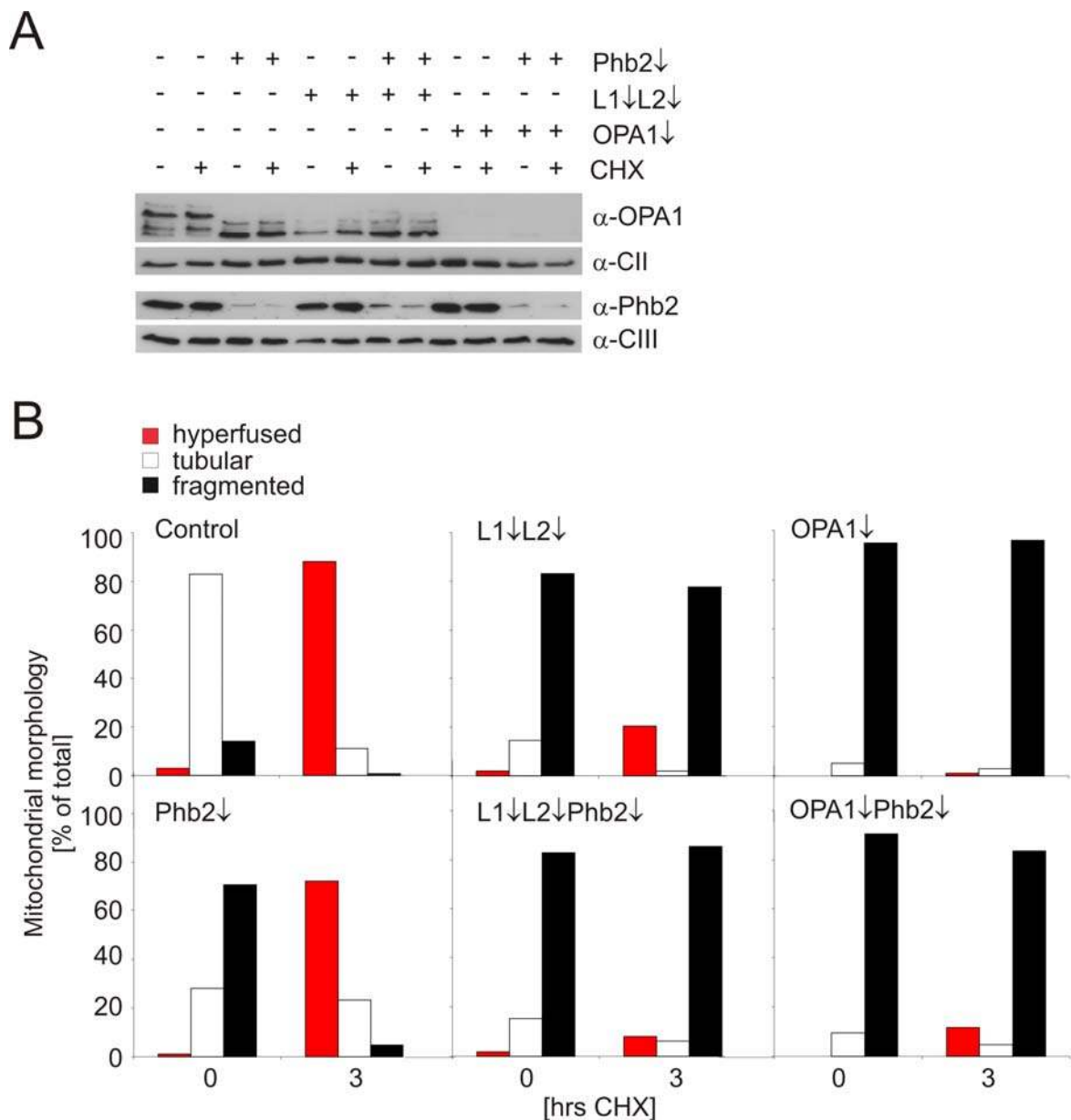
Figure 3.17 Knockdown of Phb2 does not restore CHX-induced mitochondrial hyperfusion in MEFs depleted of either OPA1 or Afg3l1 and Afg3l2
(**A**) Immunoblot analysis of MEFs transfected with siRNA against Afg3l1, Afg3l2, Phb2 and OPA1. MEFs were transfected with indicated siRNAs followed by transfection with mito-DsRed. Cells were lysed after incubation with cycloheximide (CHX) for 3 hrs and subjected to SDS-PAGE and immunoblotting. To assess consequences on OPA1 isoform pattern and knockdown efficency of Phb2, antisera recognizing OPA1 and Phb2 and, as loading controls, 70 kDa subunit of Complex II (CII) and subunit 2 of CIII (CIII) were used. (**B**) Quantification of mitochondrial morphology after CHX-induced hyperfusion in the absence of Phb2. MEFs transfected with indicated siRNAs and mito-DsRed were incubated with CHX for 3 hrs. More than 150 cells were scored for each experiment. Cells were classified into three classes containing hyperfused, tubular or fragmented mitochondria. L1, Afg3l1; L2, Afg3l2.

4   Discussion

4.1   Tissue-specific consequences of paraplegin deficiency on mitochondrial protein synthesis

Mutations in the mammalian *m*-AAA protease subunit paraplegin are associated with axonal degeneration in the neurodegenerative disease HSP. Studies in the yeast *S. cervisiae* revealed crucial functions of the *m*-AAA protease for mitochondrial biogenesis (Koppen and Langer, 2007; Tatsuta and Langer, 2008). In particular, the recent identification of the mitochondrial ribosomal subunit MrpL32 as substrate of the yeast *m*-AAA protease suggested an impaired mitochondrial translation as the molecular defect causative for the axonal degeneration upon loss of paraplegin (Nolden *et al.*, 2005; Rugarli and Langer, 2006). MrpL32 is cleaved by the *m*-AAA protease to its mature form which is essential for mitochondrial protein synthesis in yeast. The high sequence conservation of *m*-AAA proteases and MrpL32 from yeast to mammals and successful complementation studies suggest a functional conservation of the *m*-AAA protease-dependent proteolytic activation of MrpL32 (Atorino *et al.*, 2003; Nolden *et al.*, 2005). In this study, we used mitochondria isolated from paraplegin-deficient mice to further clarify the function of paraplegin in the regulation of Mrpl32 activity and its implication in the pathogenesis of HSP.

Reduced amounts of mature Mrpl32 were present in liver mitochondria lacking paraplegin consistent with an impaired proteolytic maturation. The mRNA level and protein stability of Mrpl32 were not affected in the absence of paraplegin suggesting that they are not the cause for reduced levels of mature Mrpl32. Import of Mrpl32 precursor protein into mitochondria lacking paraplegin revealed no defect in the maturation of Mrpl32. Since these import experiments were done with isolated mitochondria, in conditions far from *in vivo* ones, the presence of a slight impairment in the proteolytic maturation of Mrpl32 *in vivo* cannot be completely ruled out. Consistently, direct evidence for the ability of mammalian *m*-AAA proteases to process murine Mrpl32 were obtained by reconstitution experiments in yeast (Nolden *et al.*, 2005). Nevertheless, the analysis of paraplegin-deficient mice clearly demonstrate that Mrpl32 can be cleaved in the absence of paraplegin. Most likely as a consequence of a decreased Mrpl32 steady state level, protein synthesis rates were reduced to 50% in liver mitochondria lacking paraplegin compared to wt. Notably, mitochondrial

translation was not affected in brain and spinal cord isolated from paraplegin-deficient mice. Because essential components of the respiratory chain complexes are mitochondrially encoded, the reduced mitochondrial protein synthesis in liver should result in a respiratory deficiency. Conversely, no decrease in the respiration of paraplegin-deficient liver mitochondria was observed compared to wt. Since mitochondrial protein synthesis was not completely abolished, the residual translation activity may be sufficient to maintain respiratory activity. This implies that mitochondrially encoded respiratory chain subunits are synthesized in excess in wt liver mitochondria and can be used as a reserve to compensate for a respiratory deficit (Rossignol *et al.*, 2003).

The mild effects on Mrpl32 and mitochondrial translation in mitochondria lacking paraplegin point to proteases with redundant functions. Since additional *m*-AAA protease subunits are present in human and mice, they represent likely candidates to substitute for the loss of paraplegin. Indeed, evidence for the assembly of the murine *m*-AAA protease subunits Afg3l1 and Afg3l2 into proteolytically active homo- and hetero-oligomeric complexes in liver and brain mitochondria of paraplegin-deficient mice was obtained (Koppen *et al.*, 2007). Similarly, the ability of the human *m*-AAA protease subunit AFG3L2 to build up proteolytically active complexes in human HSP fibroblasts lacking paraplegin was proposed (Koppen *et al.*, 2007). Therefore, a lack of paraplegin does not result in a complete loss of *m*-AAA protease activity but might rather lead to a reduction of the amount of *m*-AAA protease complexes and differences in their subunit composition.

The liver-specific impairment of mitochondrial protein synthesis in the absence of paraplegin might be explained by a lower threshold level towards an impaired maturation of Mrpl32 in liver compared to brain and spinal cord (Rossignol *et al.*, 2003). Alternatively, the tissue-specific difference can be rationalized by a differential expression of the *m*-AAA protease subunits Afg3l1 and Afg3l2 in liver, brain and spinal cord. Indeed, Afg3l2 was found to be 10-fold more abundant in brain than in liver mitochondria compared to Afg3l1 (Koppen *et al.*, 2007). Remarkably, the relative abundance of Afg3l1 and Afg3l2 is not altered in the absence of paraplegin (Koppen *et al.*, 2007). Thus, *m*-AAA-protease complexes containing either Afg3l2 or also Afg3l1 might complement for the lack of paraplegin in brain to a higher extent than in liver. Conversely, the low abundance of Afg3l2 in liver might not be sufficient to substitute for the housekeeping functions of paraplegin-containing *m*-AAA proteases and results in reduced mitochondrial protein synthesis. A similar explanation has been proposed for tissue-specific defects due to mutations in the mitochondrial translation factor *EGF1* (Antonicka *et al.*, 2006). Here, a varying abundance of several mitochondrial translation

factors in different tissues was proposed to determine the variable effects on translation efficiency. Because brain and spinal cord are mostly affected in HSP, a defect in mitochondrial translation might not be the main molecular mechanism resulting in the neurodegeneration due to a loss of paraplegin. Nevertheless, it should be noted that only a subset of mitochondria was observed to be affected in neurons of paraplegin-deficient mice (Ferreirinha *et al.*, 2004). Thus, the possibility of a mitochondrial translation defect confined to this mitochondrial subpopulation cannot be ruled out.

In conclusion, paraplegin-deficient mice exhibit a liver-specific mitochondrial translation defect associated with reduced Mrpl32 levels which points to conserved functions of *m*-AAA proteases from yeast to mammals. While affected in liver, mitochondrial protein synthesis proceeds normally in brain and spinal cord mitochondria of paraplegin-deficient mice suggesting that an impaired mitochondrial protein synthesis does not seem to be the primary molecular defect causative for the axonal degeneration.

4.2   Axonal degeneration in paraplegin-deficient mice occurs in the absence of a general mitochondrial respiration defect

Many neurodegenerative diseases are caused by mutations in the mtDNA as well as in the nuclear genome and have been linked to defects in mitochondrial respiratory function (Lin and Beal, 2006). To investigate the involvement of a mitochondrial respiration defect in the pathogenesis of HSP, the respiration rate in isolated brain and spinal cord mitochondria lacking paraplegin was assessed. However, we failed to detect any statistically significant impairment in mitochondrial oxygen consumption in brain and spinal cord. Since axonal degeneration accompanied by mitochondrial abnormalities starts at the synaptic terminals and distal regions of affected axons, mitochondrial dysfunction might be confined to this subset of mitochondria (Ferreirinha *et al.*, 2004). Nevertheless, analysis of oxygen consumption and respiratory chain activities of brain synaptosomes revealed no defect in mitochondrial respiratory function (E. Rugarli and A. Bernacchia, personal communication). These observations suggest that neurodegeneration due to a lack of paraplegin is not caused by a general respiratory dysfunction. However, it cannot be excluded that a suboptimal purification of brain synaptosomes might mask a mitochondrial dysfunction. It should be noted that our

results contradict observations in fibroblast derived from human HSP patients in which a decreased complex I activity was measured (Atorino *et al.*, 2003). But given the tissue-specific phenotype of HSP, these cells might not be representative models for the affected tissues in this disease. Anyhow, a functional mitochondrial respiration does not necessarily exclude a defect in mitochondrial respiratory chain activity. The activity of individual respiratory complexes can be inhibited up to a tissue-dependent critical value without any effect on the rate of mitochondrial respiration or ATP synthesis under normal conditions (Rossignol *et al.*, 2000; Rossignol *et al.*, 2003). However, changes in the metabolic state of a certain tissues, e.g. energy demands or aging, might lower the threshold to tolerate a respiratory chain defect and consequently result in a decrease of respiratory rate (Ventura *et al.*, 2002). In fact, paraplegin-deficient mice show only at very old age a defect in ATP-synthesis in spinal cord mitochondria which further underlines that respiratory defects are not the primary molecular cause for the axonal degeneration (Ferreirinha *et al.*, 2004)

How can the neuron-specific phenotype of HSP be explained despite the ubiquitous expression of paraplegin? In most tissues, the presence of *m*-AAA protease complexes composed of only Afg3l1 and Afg3l2 seems to be sufficient to maintain housekeeping functions. Thus, neurons might be more susceptible to a reduced number of *m*-AAA protease complexes due to a lack of paraplegin than other tissues. In this respect, substrates of *m*-AAA proteases might be expressed in a tissue-specific manner or their proteolysis might be of special importance in specific cells such as neurons. Mice lacking functional Afg3l2 also exhibit a neuron-specific phenotype, however much more severe (Maltecca *et al.*, 2008). Afg3l2 mutant mice display a strong impairment in axonal development and finally die postnatally at day 16 (Maltecca *et al.*, 2008). Furthermore, swollen and giant mitochondria are observed primarily in neuronal cell bodies. The stronger phenotype of Afg3l2 mutant mice compared to paraplegin-deficient mice can be explained by the higher neuronal abundance of Afg3l2 (Koppen *et al.*, 2007). In addition, the inability of paraplegin to homo-oligomerize might further lower the presence of functional *m*-AAA protease complexes (Koppen *et al.*, 2007). Interestingly, a similar hypothesis was postulated for the neuron-specific phenotype of CMT2A caused by mutations in Mfn2 (Detmer and Chan, 2007). Mfn 2 and Mfn 1 are supposed to tether opposing mitochondria by forming homo- and hetero-oligomeric complexes (Chen *et al.*, 2003; Eura *et al.*, 2003; Koshiba *et al.*, 2004). Therefore, neuron-specific mitochondrial fusion defects in CMT2A were suggested to arise from low Mfn1 expression levels in peripheral nerves which results in a reduced number of functional mitofusin complexes (Detmer and Chan, 2007). Notably, the phenotypic differences of

paraplegin- and Afg3l2-deficient mice cannot only be explained by differences in their neuronal abundance but additionally might suggest the existence of specific substrates for *m*-AAA protease isoenzymes differing in their subunit composition, e.g paraplegin-containing complexes.

The putative absence of a detectable respiratory defect in HSP is reminiscent of the neurodegenerative disease CMT2A which is characterized by an axonal degeneration mainly affecting the longest axons of peripheral neurons (Züchner *et al.*, 2004). The transport of mitochondria in axons was significantly impaired in neurons expressing disease-mutated forms of Mfn2 due to an abnormal clustering of fragmented mitochondria (Baloh *et al.*, 2007). It is conceivable that long axons are preferentially dependent on the trafficking of organelles and proteins. Similar to CMT2A, long motor and sensory neurons in the spinal cord are mainly affected by a progressive and retrograde degeneration in HSP. The identification of HSP causing mutations in proteins implicated in intracellular trafficking indicates that deficits in the axonal transport of molecules and organelles play a role for the pathogenesis of HSP (Soderblom and Blackstone, 2006). In line with this, old paraplegin-deficient mice exhibit a delay in the retrograde axonal transport (Ferreirinha *et al.*, 2004; Rugarli and Langer, 2006). This might be caused by an accumulation of morphologically altered and giant mitochondria which can be observed already at early stages at synaptic terminals of motor axons in paraplegin-deficient mice (Ferreirinha *et al.*, 2004). Thus, an altered mitochondrial morphology in the absence of paraplegin might play a role in the pathogenesis of HSP. In this respect, it cannot be neglected that paraplegin has been linked to the proteolytic regulation of the mitochondrial fusion component OPA1, although the processing of OPA1 is not significantly affected in paraplegin-deficient MEFs (Ishihara *et al.*, 2006; Duvezin-Caubet *et al.*, 2007). However, it might be envisioned that a certain amount of *m*-AAA proteases complexes or the presence of paraplegin is crucial for OPA1 processing in special cell types and/or under certain physiological conditions.

In summary, an impaired mitochondrial respiration was not observed in brain and spinal cord mitochondria of paraplegin-deficient mice. Conclusively, axonal degeneration in HSP due to a loss of paraplegin might not arise from a general impairment in mitochondrial energy production. To unravel the neuron-specific molecular defects caused by a lack of paraplegin, it will be crucial to identify tissue-specific substrates of *m*-AAA protease isoenzymes. Moreover, it remains to be elucidated if paraplegin has special functions within *m*-AAA protease complexes.

4.3   Overlapping substrate specificities of Afg3l1 and Afg3l2 in mice and their role in the maturation of paraplegin

In addition to paraplegin, the *m*-AAA protease subunits Afg3l1 and Afg3l2 are present in mice. They both have the ability to form proteolytically active homo-oligomeric *m*-AAA protease complexes which can substitute for paraplegin-containing *m*-AAA protease complexes (Duvezin-Caubet *et al.*, 2007; Koppen *et al.*, 2007). To identify new substrates and functions of mammalian *m*-AAA proteases on a cellular level, single subunits or combinations were transiently downregulated in MEFs using RNA interference.

Mrpl32 is one of the few putative substrates known for mammalian *m*-AAA proteases. Indeed, the precursor of Mrpl32 accumulated upon simultaneous downregulation of Afg3l1 and Afg3l2 in MEFs pointing to an impaired proteolytic maturation. Nevertheless, processing of Mrpl32 still occurs which might be due to cleavage either by residual amounts of Afg3l1 and Afg3l2 or by another protease with redundant function. Remarkably, as long as either Afg3l1 or Afg3l2 are present, processing of Mrpl32 proceeds normally. Thus, homo-oligomeric complexes composed of Afg3l1 or Afg3l2 are both involved in the maturation of Mrpl32. This is substantiated by the ability of these homo-oligomeric *m*-AAA protease isoenzymes to mediate the proteolytic processing of yeast MrpL32 (Koppen *et al.*, 2007). Concomitant depletion of Afg3l1 and Afg3l2 also results in an impaired maturation of their assembly partner paraplegin. Conclusively, Afg3l1 and Afg3l2 might have at least partially overlapping substrate specificities which is underlined by their high sequence identity and the lack of AFG3L1 expression in humans (Kremmidiotis *et al.*, 2001).

The identification of paraplegin as a new substrate for Afg3l1 and Afg3l2 raises the questions if cleavage occurs before or after assembly into *m*-AAA protease complexes. It might be well envisioned that *m*-AAA proteases composed of Afg3l1 and Afg3l2 process paraplegin during import and prior to its assembly into hetero-oligomeric complexes. Alternatively, the presequence of paraplegin might be removed during or after assembly into hetero-oligomeric *m*-AAA protease complexes through either intra- or intermolecular cleavage. This is reminiscent of the assembly-dependent autocatalytic cleavage of preproteins of the mitochondrial protease PIM1 in yeast as well as the proteasome (Chen and Hochstrasser, 1996; Wagner *et al.*, 1997). PIM1 is processed in two successive steps. First, the matrix targeting signal is removed by the mitochondrial processing peptidase and second, a pro-region is cleaved off in an autocatalytic reaction (Wagner *et al.*, 1997). The pro-region

of PIM1 subunits was shown to be required for efficient sorting to mitochondria which might be envisioned for paraplegin as well (Wagner *et al.*, 1997). Alternatively, the presequence might inhibit the proteolytic activity of paraplegin-containing *m*-AAA protease complexes and thereby prevent premature proteolytic activity. The activation of proteolytic sites via autocatalytic cleavage is exemplified by cleavage of preproteins during proteasome assembly (Chen and Hochstrasser, 1996; Baumeister *et al.*, 1998). Furthermore, it is also conceivable that the presequence of paraplegin might play a role in the assembly of *m*-AAA proteases which could provide an explanation for the proposed inability of paraplegin to homo-oligomerize (Koppen *et al.*, 2007).

In conclusion, we provide evidence for overlapping substrate specificities of Afg3l1 and Afg3l2. The efficient processing of Mrpl32 and paraplegin is dependent on the presence of Afg3l1 or Afg3l2. Thus, Mrpl32 and paraplegin are identified as new substrates of the mammalian *m*-AAA protease *in vivo*.

4.4 The m-AAA protease is involved in the regulation of mitochondrial morphology

Processing of the mitochondrial fusion protein OPA1 is crucial for the regulation of mitochondrial morphology (Duvezin-Caubet *et al.*, 2006; Ishihara *et al.*, 2006). The presence of both, long and short OPA1 isoforms is required for mitochondrial fusion (Song *et al.*, 2007). Several lines of evidence indicate that the mammalian *m*-AAA protease is involved in the processing of OPA1. First, in the presence of a metalloprotease inhibitor, accelerated cleavage of long OPA1 isoforms in isolated mitochondria is inhibited pointing to processing by a mitochondrial metalloprotease (Ishihara *et al.*, 2006; Guillery *et al.*, 2008). Second, reconstitution experiments in yeast revealed that various mammalian *m*-AAA protease isoenzymes are able to cleave OPA1 (Duvezin-Caubet *et al.*, 2007).

Indeed, depletion of the murine *m*-AAA subunits Afg3l1 and Afg3l2 in MEFs led to an impaired processing of OPA1. Surprisingly, long OPA1 isoforms were not stabilized but drastically reduced accompanied by an accumulation of short OPA1 isoforms. Downregulation of human AFG3L2 affects the pattern of OPA1 isoforms in a similar manner. The conversion of long into short OPA1 isoforms is also induced upon dissipation of the

membrane potential which leads to reduced mitochondrial ATP levels (Duvezin-Caubet *et al.*, 2006; Baricault *et al.*, 2007; Song *et al.*, 2007; Guillery *et al.*, 2008). MEFs depleted of Afg3l1 and Afg3l2 show a partial uncoupling of oxidative phosphorylation. However, his partial uncoupling did affect neither mitochondrial membrane potential nor mitochondrial respiration which points to a direct function of the mammalian *m*-AAA protease in the biogenesis of OPA1 isoforms.

Mitochondrial fragmentation observed upon downregulation of Afg3l1 and Afg3l2 could be directly ascribed to impaired OPA1 functions since expression of a long OPA1 isoform rescues this phenotype at least partially. The requirement of long and short OPA isoforms for mitochondrial fusion is consistent with recent findings and implicates that mitochondrial fragmentation in Afg3l1/Afg3l2-depleted cells results from the inhibition of fusion rather than accelerated fragmentation (Song *et al.*, 2007).

The phenotypes of cells depleted of the *m*-AAA-protease subunits Afg3l1 and Afg3l2 are highly reminiscent of prohibitin-deficient cells (Merkwirth *et al.*, 2008). Deletion of prohibitins in MEFs induces the conversion of long into short OPA1 accompanied by mitochondrial fragmentation without any defects in respiratory chain activites (Merkwirth *et al.*, 2008). Interestingly, *m*-AAA proteases and prohibitins physically interact and assemble into large supercomplexes in the inner mitochondrial membrane (Steglich *et al.*, 1999; Metodiev, 2005). Because deletion of prohibitins in yeast results in accelerated proteolysis of *m*-AAA protease substrates, they are proposed to directly regulate the activity of the *m*-AAA protease or to modulate the accessibility of substrates to the *m*-AAA protease. A similar mechanism was proposed for the *E. coli* homologues of prohibitins, HflK and HflC, which are associated with and negatively modulate the AAA protease FtsH in the bacterial plasma membrane (Kihara *et al.*, 1996; Saikawa *et al.*, 2004). If *m*-AAA proteases are directly involved in OPA1 biogenesis, the negative regulation by prohibitins might explain the similar consequences on OPA1 isoform pattern upon depletion of these two proteins. Notably, concomitant downregulation of *m*-AAA proteases and prohibitins in MEFs also results in the loss of long OPA1 isoforms. Further experiments are needed to clarify the putative regulation of *m*-AAA protease activity by prohibitins in mammals. Since the supercomplex formed by *m*-AAA proteases and prohibitins is disrupted by the depletion of either prohibitins or *m*-AAA proteases, it might also be conceivable that this supercomplex mediates the regulation of OPA1 processing. In addition to mitochondrial fragmentation, cristae morphogenesis is highly disturbed in prohibitin-deficient cells caused by the selective loss of long OPA1 isoforms (Merkwirth *et al.*, 2008). The dependency of cristae morphogenesis on the presence of short

and long OPA1 isoforms suggests that cristae morphology is also altered in *m*-AAA protease-depleted cells. Likewise, depletion of OPA1 leads to a drastic disorganization of cristae membranes in fragmented mitochondria (Olichon *et al.*, 2003; Griparic *et al.*, 2004).

In conclusion, this study indicates an essential function of *m*-AAA proteases for mitochondrial morphology by regulating the processing of OPA1. Future experiments are needed to substantiate the direct link of OPA1 to the *m*-AAA protease in mammals. So far, the possibility that yet unknown functions of the mammalian *m*-AAA protease affect the OPA1 isoform pattern cannnot be excluded.

4.5   *The m-AAA protease is essential for stress-induced mitochondrial hyperfusion*

Mitochondria are highly dynamic organelles and they constantly adapt their morphology to varying physiological conditions by fusion and fission (Okamoto and Shaw, 2005). Upon exposure of cells to stress stimuli such as actinomycin D, UV irridation and cycloheximide, mitochondria were observed to hyperfuse and form a highly interconnected network (D. Tondera and J.-C. Martinou, personal communication). This stress-induced mitochondrial hyperfusion was shown to result mainly from increased fusion activity. However, the physiological function is not clear yet, although it might be envisioned that increased mitochondrial elongation serves as a stress response to protect cells from mitochondrial dysfunction.

The presence of short and long OPA1 isoforms as well as Mfn1, but not Mfn2, was shown to be required for mitochondrial hyperfusion activity (D. Tondera and J.-C. Martinou, personal communication). Like OPA1 and Mfn1, the *m*-AAA protease is essential for the maintenance of a tubular mitochondrial network. During stress conditions, also mitochondria in Afg3l1/Afg3l2-depleted cells do not form a highly interconnected network but remain fragmented. This indicates that *m*-AAA proteases are essential for fusion events under varying physiological conditions. Whether the inability to hyperfuse in Afg3l1/Afg3l2-depleted cells is linked to the loss of long OPA1 forms, like it has been shown for steady state fusion events, has to be further analyzed.

Depletion of prohibitins in MEFs results in mitochondrial fragmentation caused by the loss of long OPA1 isoforms (Merkwirth *et al.*, 2008). Remarkably, prohibitin-depleted cells which are exposed to stress stimuli contain a highly interconnected mitochondrial network pointing to the ability of fragmented mitochondria to hyperfuse in the absence of prohibitins. These findings indicate that the prohibitin-mediated control of OPA1 processing is dispensable for stress-induced mitochondrial hyperfusion. Conclusively, the supercomplex composed of prohibitins and *m*-AAA proteases controls mitochondrial morphology via OPA1 in non-stressed cells. However, it does not seem to be involved in the control of mitochondrial hyperfusion events pointing to crucial functions of *m*-AAA proteases in mitochondrial morphology independent of prohibitins.

Since long and short OPA1 isoforms are required for mitochondrial hyperfusion, it is quite remarkable that prohibitin-depleted mitochondria, despite the loss of long OPA1 isoforms, are able to hyperfuse (D. Tondera and J.-C. Martinou, personal communication). It might be envisioned that in the absence of prohibitins inner membrane fusion is inhibited via OPA1 whereas outer membrane fusion can be activated during mitochondrial hyperfusion. Although inner and outer membrane fusion events are coupled *in vivo*, they have different requirements and can proceed separately (Malka *et al.*, 2005). Therefore, a loss of long OPA1 isoforms most likely affects only inner membrane fusion in spite of an overall mitochondrial fragmentation which implies that inner and outer membrane fusion events can negatively regulate each other (Meeusen *et al.*, 2006). This raises the question if the loss of prohibitins might uncouple inner and outer membrane fusion events after stress treatment, thereby allowing outer membranes to fuse. Thus, additional loss of prohibitins in in *m*-AAA protease- and OPA1-depleted mitochondria would rescue the defect in mitochondrial hyperfusion. However, downregulation of prohibitins did not suppress the requirement of the *m*-AAA protease or OPA1 for mitochondrial hyperfusion. Conclusively, prohibitins are most likely not involved in the regulation of outer and inner membrane fusion. It remains unclear, how the distinct outer and inner membrane fusion machineries are linked to each other. In *S. cerevisiae*, the outer membrane protein Ugo1 physically interacts with the mitofusin homologue Fzo1 and the OPA1 homologue Mgm1 providing a link that might coordinate outer and inner membrane fusion (Wong *et al.*, 2003; Sesaki and Jensen, 2004). However, a mammalian homologue of Ugo1 has not been identified. Recently, OPA1 has been demonstrated to interact with both mitofusins by crosslinking experiments which points to transient interactions (Guillery *et al.*, 2008). Therefore, it is tempting to speculate that OPA1

isoforms do not only mediate inner membrane fusion but also regulate the coordination with the outer membrane fusion machinery by direct interactions.

The requirement of prohibitins for mitochondrial dynamics during steady state but not during stress conditions might also indicate that a protein homologous to prohibitins exists which acts in mitochondrial hyperfusion. The stomatin-like 2 protein (SLP-2), sharing the highly conserved SPFH-domain with prohibitins, was shown to be required for mitochondria to hyperfuse (Tavernarakis *et al.*, 1999; Browman *et al.*, 2007) (D. Tondera and J.-C. Martinou, personal communication). In contrast to prohibitins, depletion of SLP-2 has no effect on mitochondrial morphology in non-stressed cells (Hajek *et al.*, 2007). These findings indicate that different proteins and mechanisms for the regulation of mitochondrial fusion events exist. The fusion machinery which is needed for maintenance of a tubular mitochondrial network requires prohibitins, whereas for stress-induced mitochondrial hyperfusion SLP-2 might be essential. The homology of prohibitins and SLP-2 points to similar functions in these distinct fusion events**.** Indeed, reminiscent of the function of prohibitins in non-stressed cells, SLP-2 was proposed to regulate mitochondrial morphogenesis during stress by controlling the processing of OPA1 (D. Tondera and J.-C. Martinou, personal communication) (Merkwirth *et al.*, 2008). Thus, the different requirments of prohibitins and SLP-2 in the mitochondrial fusion events might point to the existence of a specific protein machinery executing stress-induced mitochondrial hyperfusion

In conclusion, crucial functions of the *m*-AAA protease in the regulation of mitochondrial morphology independent of prohibitins have been identified. Whether the *m*-AAA protease directly regulates mitochondrial hyperfusion via OPA1 remains to be established.

4.6   *The m-AAA protease controls the processing of OPA1*

So far, several mitochondrial proteases have been implicated in the proteolysis of OPA1. In addition to the *m*-AAA protease, the rhomboid protease PARL and the *i*-AAA protease were proposed to process long OPA1 isoforms. PARL was suggested to be responsible for the generation of a small amount of short OPA1 isoforms (Cipolat *et al.*, 2006). Nevertheless, the OPA1 isoform pattern is not drastically affected in PARL-deficient cells indicating that the majority of OPA1 isoforms can be generated in the absence of PARL (Duvezin-Caubet *et al.*,

2007; Griparic *et al.*, 2007). Downregulation of the *i*-AAA protease Yme1l1 clearly impairs the constitutive cleavage of long OPA1 isoforms at cleavage site S2, ALthough it remains to be demonstrated whether Yme1l1 directly cleaves OPA1 or affects another protease (Griparic *et al.*, 2007; Song *et al.*, 2007).

In this study, transfection of cells with different OPA1 isoforms revealed an increased cleavage of long OPA1 isoforms at cleavage site S1, but not S2, in the absence of the *m*-AAA protease subunits Afg3l1 and Afg3l2. Furthermore, long OPA1 isoforms were degraded in an accelerated manner which might indicate that these membrane-anchored OPA1 isoforms are stabilized by the *m*-AAA protease. In contrast, short OPA1 isoforms which are only peripherally attached to the membrane are not destabilized upon depletion of the *m*-AAA protease. Interestingly, dissipation of the mitochondrial membrane potential affects OPA1 processing in a similar manner and resulted in an accelerated cleavage at processing site S1 (Song *et al.*, 2007). It is tempting to speculate that reduced ATP synthesis upon the loss of membrane potential might compromise the function of the ATP-dependent *m*-AAA protease and induces cleavage by an ATP-independent protease.

Which mitochondrial protease(s) cleave(s) OPA1 at processing site S1? Constitutive and inducible OPA1 processing in cells devoid of the mitochondrial proteases PARL, HtrA2 or the murine *m*-AAA protease subunit paraplegin proceeds comparably to control cells. Also, downregulation of the mitochondrial matrix protease Lon or the *i*-AAA protease Yme1l1 did not strikingly affect cleavage at processing site S1 independent of Afg3l1 and Afg3l2. Therefore, all tested mitochondrial proteases are dispensable for processing at site S1. This might either reflect the presence of various proteases with redundant functions or the existence of a yet unidentified protease. Protease inhibitor studies in cells depleted of Afg3l1 and Afg3l2 revealed the stabilization of newly synthesized long OPA1 and its precursor in the presence of an inhibitor for metalloproteases as well as for the proteasome, which was recently implicated in the cytosolic degradation of mitochondrial precursor proteins (Margineantu *et al.*, 2007; Radke *et al.*, 2008). The accumulation of newly synthesized OPA1 and its precursor through inhibition of metalloproteases is most likely caused by blocking the Zn^{2+}-dependent mitochondrial processing peptidase MPP in the matrix (Luciano *et al.*, 1998). Therefore, no clear conclusion can be drawn about metal-dependent processing events affecting OPA1 downstream of MPP cleavage.

How does the *m*-AAA protease affect the biogenesis of OPA1? On the one hand, yeast reconstitution experiments provided direct evidence for the ability of mammalian *m*-AAA protease complexes to cleave OPA1 (Duvezin-Caubet *et al.*, 2007). On the other hand, in the

absence of the *m*-AAA protease in mammalian cells OPA1 processing not only occurs but is accelerated and accompanied by the destabilisation of long OPA1 isoforms. Combining these two observations in a model would first imply that the constitutive and the induced cleavage of long OPA1 isoforms are performed by different proteases. Whereas the protease(s) for the induced processing at site S1 remain(s) to be identified, the *m*-AAA protease might process OPA1 constitutively at cleavage site S1. In addition, it could be envisioned that the *m*-AAA protease has a non-proteolytic function in the biogenesis of long OPA1 isoforms which is needed for the subsequent *m*-AAA protease-dependent OPA1 processing. Since the putative cleavage product of Yme1l1, the OPA1 isoform S4, is also reduced in Afg3l1/Afg3l2-depleted cells, the non-proteolytic function of the *m*-AAA protease might also regulate OPA1 cleavage by the *i*-AAA protease (Griparic *et al.*, 2007; Song *et al.*, 2007). This hypothesis is supported by the identification of a non-proteolytic function of the *m*-AAA protease in yeast. The bipartite presequence of Ccp1 is removed by the consecutive actions of the *m*-AAA protease and the rhomboid protease Pcp1 (Esser *et al.*, 2002). Strikingly, the final cleavage of Ccp1 by the rhomboid protease depends only on the ATP-dependent membrane translocation of Ccp1 which is mediated by the *m*-AAA protease (Tatsuta *et al.*, 2007). Ccp1 processing in *m*-AAA protease-deficient yeast cells is restored upon expression of proteolytically active and inactive human AFG3L2 complexes, which strongly suggests that the ability for membrane dislocation is conserved in mammalian *m*-AAA proteases (Koppen, 2007). Interestingly, the *i*-AAA protease was also found to be required for the import of mammalian PNPase into the intermembrane space of yeast mitochondria consistent with a function for membrane translocation (Rainey *et al.*, 2006). Therefore, it might be conceivable that the *m*-AAA protease mediates the vectorial membrane translocation of OPA1 after MPP cleavage to allow subsequent processing by the *m*-AAA protease on the matrix side. In this context, *m*-AAA protease-dependent lateral sorting of long OPA1 isoforms and their stable integration into the inner membrane might be envisioned as well. Notably, cleavage of the OPA1 homologue Mgm1 in yeast depends also on ATP-dependent vectorial membrane translocation though exerted directly by the mitochondrial import motor Hsp70 (Herlan *et al.*, 2004).

In summary, these findings reveal that the *m*-AAA protease is involved in the regulation of OPA1 cleavage at processing S1 and is required for the stabilisation of long OPA1 isoforms. Further studies are clearly needed to substantiate the hypothesis that membrane translocation of OPA1 is mediated by the *m*-AAA protease and is required for constitutive processing of OPA1.

5   Zusammenfassung

Die *m*-AAA Protease, ein ATP-abhängiger proteolytischer Komplex in der inneren mitochondrialen Membran, kontrolliert in Hefe die mitochondriale Proteinqualität und reguliert durch ihre Funktion als Prozessierungsenzym die mitochondriale Proteinsynthese. Die *m*-AAA Proteasen in Säugern assemblieren in verschiedene Isoenzyme, die aus unterschiedlichen Untereinheiten bestehen. In der Maus werden die drei Untereinheiten Afg3l1, Afg3l2 und Paraplegin gewebespezifisch exprimiert. Mutationen in der *m*-AAA Proteaseuntereinheit Paraplegin führen zu hereditärer spastischer Paraplegie (HSP), einer neurodegenerativen Krankheit, die durch eine zellspezifische axonale Degeneration gekennzeichnet ist. Mäuse, die Mutationen in der Untereinheit Afg3l2 tragen, weisen ebenfalls neuropathologische Symptome auf und haben einen starken Defekt in der axonalen Entwicklung. Die molekulare Grundlage dieser neuronen-spezifischen Phänotypen sowie die Funktionen der *m*-AAA Proteasen in Säugern im Allgemeinen sind unklar und wurden in dieser Arbeit untersucht.

Die Analyse eines Mausmodels für HSP enthüllte einen leberspezifischen Defekt der mitochondrialen Proteinsynthese, der auf eine Konservierung der *m*-AAA Protease-vermittelten Kontrolle der mitochondrial Proteinsynthese in Säugern hindeutet. Eine signifikanter Beeinträchtigung der mitochondrialen Proteinsynthese wie auch der mitochondrialen Atmung konnte in Gehirn und Rückenmark jedoch nicht beobachtet werden. Dies lässt vermuten, dass die axonale Degeneration in HSP nicht durch einen generellen mitochondrialen Atmungsdefekt verursacht wird.

Die Analyse der *m*-AAA Isoenzyme auf zellulärer Ebene durch RNA Interferenz ergab redundante Funktionen der Untereinheiten Afg3l1 und Afg3l2 und identifizierte Paraplegin als ein neues Substrat, welches von Afg3l1 und Afg3l2 prozessiert wird. Der Verlust der *m*-AAA Protease in MEFs führte zu einer Fragmentierung der Mitochondrien, begleitet von einer gestörten Biogenese von Isoformen der mitochondrialen Fusionskomponente OPA1. Lange OPA1 Isoformen wurden destabilisiert und in einer beschleunigten Weise prozessiert. Die Überexpression einer langen OPA1 Isoform in Zellen, in denen die *m*-AAA Protease depletiert wurde, führte zu einer Wiederherstellung des tubulären mitochondrial Netzwerkes. Dies identifizierte die beeinträchtigte OPA1 Prozessierung als Hauptgrund für den Defekt der mitochondrialen Morphologie. Zudem konnte gezeigt werden, dass die *m*-AAA Protease essentiell für die Induzierung der mitochondrialen Hyperfusion ist, einer zellulären

Stressantwort, welche zu einem stark zusammenhängenden mitochondrialen Netzwerk in der Zelle führt.

Die Befunde dieser Arbeit lassen auf eine entscheidende Funktion der *m*-AAA Protease in der Regulation der mitochondrialen Morphologie schliessen, möglicherweise durch die Kontrolle der Biogenese von OPA1. Dies könnte dazu beitragen, neue Einsichten in die molekularen Mechanismen der Axonopathien zu erhalten, welche durch den Verlust von *m*-AAA Proteaseuntereinheiten in Säugern entstehen.

6   References

Akiyama, Y., and Ito, K. (2000). Roles of multimerization and membrane association in the proteolytic functions of FtsH (HflB). EMBO J. *19*, 3888-3895.

Akiyama, Y., and Ito, K. (2001). Roles of homooligomerization and membrane association in ATPase and proteolytic activities of FtsH in vitro. Biochemistry *40*, 7687-7693.

Alexander, C., Votruba, M., Pesch, U. E., Thiselton, D. L., Mayer, S., Moore, A., Rodriguez, M., Kellner, U., Leo-Kottler, B., Auburger, G*., et al.* (2000). *OPA1*, encoding a dynamin-related GTPase, is mutated in autosomal dominant optic atrophy linked to chromosome 3q28. Nat. Genet. *26*, 211-215.

Amati-Bonneau, P., Valentino, M. L., Reynier, P., Gallardo, M. E., Bornstein, B., Boissiere, A., Campos, Y., Rivera, H., de la Aleja, J. G., Carroccia, R*., et al.* (2008). OPA1 mutations induce mitochondrial DNA instability and optic atrophy 'plus' phenotypes. Brain *131*, 338-351.

Anderson, S., Bankier, A. T., Barrell, B. G., de Bruijn, M. H., Coulson, A. R., Drouin, J., Eperon, I. C., Nierlich, D. P., Roe, B. A., Sanger, F*., et al.* (1981). Sequence and organization of the human mitochondrial genome. Nature *290*, 457-465.

Antonicka, H., Sasarman, F., Kennaway, N. G., and Shoubridge, E. A. (2006). The molecular basis for tissue specificity of the oxidative phosphorylation deficiencies in patients with mutations in the mitochondrial translation factor EFG1. Hum. Mol. Gen. *15*, 1835-1846.

Arlt, H., Tauer, R., Feldmann, H., Neupert, W., and Langer, T. (1996). The YTA10-12-complex, an AAA protease with chaperone-like activity in the inner membrane of mitochondria. Cell *85*, 875-885.

Arlt, H., Steglich, G., Perryman, R., Guiard, B., Neupert, W., and Langer, T. (1998). The formation of respiratory chain complexes in mitochondria is under the proteolytic control of the *m*-AAA protease. EMBO J. *17*, 4837-4847.

Artal-Sanz, M., Tsang, W. Y., Willems, E. M., Grivell, L. A., Lemire, B. D., van der Spek, H., Nijtmans, L. G., and Sanz, M. A. (2003). The mitochondrial prohibitin complex is essential for embryonic viability and germline function in *Caenorhabditis elegans*. J. Biol. Chem. *278*, 32091-32099.

Atorino, L., Silvestri, L., Koppen, M., Cassina, L., Ballabio, A., Marconi, R., Langer, T., and Casari, G. (2003). Loss of *m*-AAA protease in mitochondria causes complex I deficiency and increased sensitivity to oxidative stress in hereditary spastic paraplegia. J. Cell. Biol. *163*, 777-787.

Baker, T. A., and Sauer, R. T. (2006). ATP-dependent proteases of bacteria: recognition logic and operating principles. Trends. Biochem. Sci. *31*, 647-653.

Baloh, R. H., Schmidt, R. E., Pestronk, A., and Milbrandt, J. (2007). Altered axonal mitochondrial transport in the pathogenesis of Charcot-Marie-Tooth disease from mitofusin 2 mutations. J Neurosci *27*, 422-430.

Banfi, S., Bassi, M. T., Andolfi, G., Marchitiello, A., Zanotta, S., Ballabio, A., Casari, G., and Franco, B. (1999). Identification and characterization of AFG3L2, a novel paraplegin-related gene. Genomics *59*, 51-58.

Baricault, L., Segui, B., Guegand, L., Olichon, A., Valette, A., Larminat, F., and Lenaers, G. (2007). OPA1 cleavage depends on decreased mitochondrial ATP level and bivalent metals. Exp Cell Res *313*, 3800-3808.

Baumeister, W., Walz, J., Zuhl, F., and Seemuller, E. (1998). The proteasome: paradigm of a self-compartmentalizing protease. Cell *92*, 367-380.

Benoist, C., and Chambon, P. (1981). In vivo sequence requirements of the SV40 early promotor region. Nature *290*, 304-310.

Bieniossek, C., Schalch, T., Bumann, M., Meister, M., Meier, R., and Baumann, U. (2006). The molecular architecture of the metalloprotease FtsH. Proc. Natl. Acad. Sci. U S A *103*, 3066-3071.

Böhni, P. C., Daum, G., and Schatz, G. (1983). Import of proteins into mitochondria. Partial purification of a matrix-located protease involved in cleavage of mitochondrial precursor polypeptides. J. Biol. Chem. *258*, 4937-4943. Order.

Boldogh, I. R., and Pon, L. A. (2007). Mitochondria on the move. Trends Cell Biol *17*, 502-510.

Bolender, N., Sickmann, A., Wagner, R., Meisinger, C., and Pfanner, N. (2008). Multiple pathways for sorting mitochondrial precursor proteins. EMBO Rep *9*, 42-49.

Bota, D. A., and Davies, K. J. (2002). Lon protease preferentially degrades oxidized mitochondrial aconitase by an ATP-stimulated mechanism. Nat. Cell. Biol. *4*, 674-680.

Bota, D. A., Ngo, J. K., and Davies, K. J. (2005). Downregulation of the human Lon protease impairs mitochondrial structure and function and causes cell death. Free Radic Biol Med *38*, 665-677.

Boveris, A., and Cadenas, E. (1975). Mitochondrial production of superoxide anions and its relationship to the antimycin insensitive respiration. FEBS Lett *54*, 311-314.

Browman, D. T., Hoegg, M. B., and Robbins, S. M. (2007). The SPFH domain-containing proteins: more than lipid raft markers. Trends Cell Biol *17*, 394-402.

Burri, L., Strahm, Y., Hawkins, C. J., Gentle, I. E., Puryer, M. A., Verhagen, A., Callus, B., Vaux, D., and Lithgow, T. (2005). Mature DIABLO/Smac is produced by the IMP protease complex on the mitochondrial inner membrane. Mol. Biol. Cell *16*, 2926-2933.

Casari, G., De-Fusco, M., Ciarmatori, S., Zeviani, M., Mora, M., Fernandez, P., DeMichele, G., Filla, A., Cocozza, S., Marconi, R., *et al.* (1998). Spastic paraplegia and OXPHOS impairment caused by mutations in paraplegin, a nuclear-encoded mitochondrial metalloprotease. Cell *93*, 973-983.

Chan, D. C. (2006). Mitochondria: dynamic organelles in disease, aging, and development. Cell *125*, 1241-1252.

Chan, D. C. (2006). Mitochondrial fusion and fission in mammals. Ann. Rev. Cell Dev. Biol. *22*, 79-99.

Chen, H., Detmer, S. A., Ewald, A. J., Griffin, E. E., Fraser, S. E., and Chan, D. C. (2003). Mitofusins Mfn1 and Mfn2 coordinately regulate mitochondrial fusion and are essential for embryonic development. J. Cell. Biol. *160*, 189-200.

Chen, H., Chomyn, A., and Chan, D. C. (2005). Disruption of fusion results in mitochondrial heterogeneity and dysfunction. J. Biol. Chem. *280*, 26185-26192.

Chen, H., McCaffery, J. M., and Chan, D. C. (2007). Mitochondrial fusion protects against neurodegeneration in the cerebellum. Cell *130*, 548-562.

Chen, P., and Hochstrasser, M. (1996). Autocatalytic subunit processing couples active site formation in the 20S proteasome to completion of assembly. Cell *86*, 961-972.

Chen, X. J., and Butow, R. A. (2005). The organization and inheritance of the mitochondrial genome. Nat. Rev. Genet. *6*, 815-825.

Ciechanover, A. (2005). Proteolysis: from the lysosome to ubiquitin and the proteasome. Nat. Rev. Mol. Cell Biol. *6*, 79-87.

Cipolat, S., Martins de Brito, O., Dal Zilio, B., and Scorrano, L. (2004). OPA1 requires mitofusin 1 to promote mitochondrial fusion. Proc. Natl. Acad. Sci. U S A *101*, 15927-15932.

Cipolat, S., Rudka, T., Hartmann, D., Costa, V., Serneels, L., Craessaerts, K., Metzger, K., Frezza, C., Annaert, W., D'Adamio, L., *et al.* (2006). Mitochondrial rhomboid PARL regulates cytochrome c release during apoptosis via OPA1-dependent cristae remodeling. Cell *126*, 163-175.

Clausen, T., Southan, C., and Ehrmann, M. (2002). The HtrA family of proteases: implications for protein composition and cell fate. Mol. Cell *10*, 443-455.

Claypool, S. M., and Koehler, C. M. (2005). Hereditary spastic paraplegia: respiratory choke or unactivated substrate? Cell *123*, 183-185.

Coppola, M., Pizzigoni, A., Banfi, S., Casari, G., Bassi, M. T., and Incerti, B. (2000). Identification and characterization of YME1L1, a novel paraplegin related gene. Genomics *66*, 48-54.

Daum, G., Bohni, P. C., and Schatz, G. (1982). Import of proteins into mitochondria. Cytochrome b2 and cytochrome c peroxidase are located in the intermembrane space of yeast mitochondria. J Biol Chem *257*, 13028-13033.

De Sagarra, M. R., Mayo, I., Marco, S., Rodriguez-Vilarino, S., Oliva, J., Carrascosa, J. L., and Castano, J. G. (1999). Mitochondrial localization and oligomeric structure of HClpP, the human homologue of *E. coli* ClpP. J Mol Biol *292*, 819-825.

Delettre, C., Lenaers, G., Griffoin, J. M., Gigarel, N., Lorenzo, C., Belenguer, P., Pelloquin, L., Grosgeorge, J., Turc-Carel, C., Perret, E.*, et al.* (2000). Nuclear gene *OPA1*, encoding a mitochondrial dynamin-related protein, is mutated in dominant optic atrophy. Nat. Genet. *26*, 207-210.

Delettre, C., Griffoin, J. M., Kaplan, J., Dollfus, H., Lorenz, B., Faivre, L., Lenaers, G., Belenguer, P., and Hamel, C. P. (2001). Mutation spectrum and splicing variants in the *OPA1* gene. Hum. Genet. *109*, 584-591.

Depienne, C., Stevanin, G., Brice, A., and Durr, A. (2007). Hereditary spastic paraplegias: an update. Curr Opin Neurol *20*, 674-680.

Detmer, S. A., and Chan, D. C. (2007). Functions and dysfunctions of mitochondrial dynamics. Nat Rev Mol Cell Biol *8*, 870-879.

Detmer, S. A., and Chan, D. C. (2007). Complementation between mouse Mfn1 and Mfn2 protects mitochondrial fusion defects caused by CMT2A disease mutations. J. Cell. Biol. *176*, 405-414.

Duvezin-Caubet, S., Jagasia, R., Wagener, J., Hofmann, S., Trifunovic, A., Hansson, A., Chomyn, A., Bauer, M. F., Attardi, G., Larsson, N. G.*, et al.* (2006). Proteolytic processing of OPA1 links mitochondrial dysfunction to alterations in mitochondrial morphology. J. Biol. Chem. *281*, 37972-37979.

Duvezin-Caubet, S., Koppen, M., Wagener, J., Zick, M., Israel, L., Bernacchia, A., Jagasia, R., Rugarli, E. I., Imhof, A., Neupert, W.*, et al.* (2007). OPA1 processing reconstituted in yeast depends on the subunit composition of the m-AAA protease in mitochondria. Mol Biol Cell *18*, 3582-3590.

Errico, A., Ballabio, A., and Rugarli, E. I. (2002). Spastin, the protein mutated in autosomal dominant hereditary spastic paraplegia, is involved in microtubule dynamics. Hum Mol Genet *11*, 153-163.

Esser, K., Tursun, B., Ingenhoven, M., Michaelis, G., and Pratje, E. (2002). A novel two-step mechanism for removal of a mitochondrial signal sequence involves the *m*-AAA complex and the putative rhomboid protease Pcp1. J. Mol. Biol. *323*, 835-843.

Eura, Y., Ishihara, N., Yokota, S., and Mihara, K. (2003). Two mitofusin proteins, mammalian homologues of FZO, with distinct functions are both required for mitochondrial fusion. J Biochem *134*, 333-344.

Evans, K., Keller, C., Pavur, K., Glasgow, K., Conn, B., and Lauring, B. (2006). Interaction of two hereditary spastic paraplegia gene products, spastin and atlastin, suggests a common pathway for axonal maintenance. Proc. Natl. Acad. Sci. U S A *103*, 10666-10671.

Evans, K. J., Gomes, E. R., Reisenweber, S. M., Gundersen, G. G., and Lauring, B. P. (2005). Linking axonal degeneration to microtubule remodeling by Spastin-mediated microtubule severing. J. Cell. Biol. *168*, 599-606.

Faccio, L., Fusco, C., Chen, A., Martinotti, S., Bonventre, J. V., and Zervos, A. S. (2000). Characterization of a novel human serine protease that has extensive homology to bacterial heat shock endoprotease HtrA and is regulated by kidney ischemia. J Biol Chem *275*, 2581-2588.

Ferreirinha, F., Quattrini, A., Priozzi, M., Valsecchi, V., Dina, G., Broccoli, V., Auricchio, A., Piemonte, F., Tozzi, G., Gaeta, L., *et al.* (2004). Axonal degeneration in paraplegin-deficient mice is associated with abnormal mitochondria and impairment of axonal transport. J. Clin. Invest. *113*, 231-242.

Fink, J. K. (2003). Advances in the hereditary spastic paraplegias. Exp Neurol *184 Suppl 1*, S106-110.

Frezza, C., Cipolat, S., Martins de Brito, O., Micaroni, M., Beznoussenko, G. V., Rudka, T., Bartoli, D., Polishuck, R. S., Danial, N. N., De Strooper, B., and Scorrano, L. (2006). OPA1 controls apoptotic cristae remodeling independently from mitochondrial fusion. Cell *126*, 177-189.

Fu, G. K., and Markovitz, D. M. (1998). The human Lon protease binds to mitochondrial promoters in a single-stranded, site-specific, strand-specific manner. Biochemistry *37*, 1905-1909.

Gakh, O., Cavadini, P., and Isaya, G. (2002). Mitochondrial processing peptidases. Biochim. Biophys. Acta *1592*, 63-77.

Galluhn, D., and Langer, T. (2004). Reversible assembly of the ATP-binding cassette transporter Mdl1 with the F_1F_O-ATP synthase in mitochondria. J. Biol. Chem. *279*, 38338-38345.

Graef, M., and Langer, T. (2006). Substrate specific consequences of central pore mutations in the *i*-AAA protease Yme1 on substrate engagement. J. Struct. Biol. *151*, 101-108.

Graef, M., Seewald, G., and Langer, T. (2007). Substrate recognition by AAA^+ ATPases: Distinct substrate binding modes in the ATP-dependent protease Yme1 of the mitochondrial intermembrane space. Mol. Cell. Biol. *in press*.

Gray, C. W., Ward, R. V., Karran, E., Turconi, S., Rowles, A., Viglienghi, D., Southan, C., Barton, A., Fantom, K. G., West, A., *et al.* (2000). Characterization of human HtrA2, a novel serine protease involved in the mammalian cellular stress response. Eur J Biochem *267*, 5699-5710.

Griparic, L., van der Wel, N. N., Orozco, I. J., Peters, P. J., and van der Bliek, A. M. (2004). Loss of the intermembrane space protein Mgm1/OPA1 induces swelling and localized constrictions along the lengths of mitochondria. J. Biol. Chem. *279*, 18792-18798.

Griparic, L., Kanazawa, T., and van der Bliek, A. M. (2007). Regulation of the mitochondrial dynamin-like protein Opa1 by proteolytic cleavage. J Cell Biol *178*, 757-764.

Grohmann, L., Graack, H. R., Kruft, V., Choli, T., Goldschmidt-Reisin, S., and Kitakawa, M. (1991). Extended N-terminal sequencing of proteins of the large ribosomal subunit from yeast mitochondria. FEBS Lett. *284*, 51-56.

Guélin, E., Rep, M., and Grivell, L. A. (1994). Sequence of the *AFG3* gene encoding a new member of the FtsH/Yme1/Tma subfamily of the AAA-protein family. Yeast *10*, 1389-1394.

Guillery, O., Malka, F., Landes, T., Guillou, E., Blackstone, C., Lombes, A., Belenguer, P., Arnoult, D., and Rojo, M. (2008). Metalloprotease-mediated OPA1 processing is modulated by the mitochondrial membrane potential. Biol Cell *100*, 315-325.

Hajek, P., Chomyn, A., and Attardi, G. (2007). Identification of a novel mitochondrial complex containing mitofusin 2 and stomatin-like protein 2. J Biol Chem *282*, 5670-5681.

Hansen, J. J., Dürr, A., I., C.-R., Georgopoulos, C., Ang, D., Nielson, M. N., Davoine, C. S., Brice, A., Fontaine, B., Gregersen, N., and Bross, P. (2002). Hereditary spastic paraplegia SPG13 is associated with a mutation in the gene encoding the mitochondrial chaperonin Hsp60. Am. J. Hum. Genet. *70*, 1328-1332.

Hanson, P. I., and Whiteheart, S. W. (2005). AAA+ proteins: have engine, will work. Nat. Rev. Mol. Cell Biol. *6*, 519-529.

Harding, A. E. (1983). Classification of the hereditary ataxias and paraplegias. Lancet Neurol. *1*, 1151-1155.

Hawlitschek, G., Schneider, H., Schmidt, B., Tropschug, M., Hartl, F. U., and Neupert, W. (1988). Mitochondrial protein import: identification of processing peptidase and of PEP, a processing enhancing protein. Cell *53*, 795-806.

Haynes, C. M., Petrova, K., Benedetti, C., Yang, Y., and Ron, D. (2007). ClpP mediates activation of a mitochondrial unfolded protein response in C. elegans. Dev Cell *13*, 467-480.

Hazan, J., Fonknechten, N., Mavel, D., Paternotte, C., Samson, D., Artiguenave, F., Davoine, C. S., Cruaud, C., Dürr, A., Wincker, P*., et al.* (1999). Spastin, a new AAA protein, is altered in the most frequent form of autosomal dominant spastic paraplegia. Nat. Genet. *23*, 296-303.

Hegde, R., Srinivasula, S. M., Zhang, Z., Wassell, R., Mukattash, R., Cilenti, L., DuBois, G., Lazebnik, Y., Zervos, A. S., Fernandes-Alnemri, T., and Alnemri, E. S. (2002). Identification of Omi/HtrA2 as a mitochondrial apoptotic serine protease that disrupts inhibitor of apoptosis protein-caspase interaction. J. Biol. Chem. *277*, 432-438.

Herlan, M., Vogel, F., Bornhövd, C., Neupert, W., and Reichert, A. S. (2003). Processing of Mgm1 by the rhomboid-type protease Pcp1 is required for maintenance of mitochondrial morphology and of mitochondrial DNA. J. Biol. Chem. *278*, 27781-27788.

Herlan, M., Bornhovd, C., Hell, K., Neupert, W., and Reichert, A. S. (2004). Alternative topogenesis of Mgm1 and mitochondrial morphology depend on ATP and a functional import motor. J. Cell Biol. *165*, 167-173.

Hermann, G. J., Thatcher, J. W., Mills, J. P., Hales, K. G., Fuller, M. T., Nunnari, J., and Shaw, J. M. (1998). Mitochondrial fusion in yeast requires the transmembrane GTPase Fzo1p. J. Cell Biol. *143*, 359-373.

Hogan B., C. F., Lacy, I. (1987). Manipulating the mouse embryo: Cold Spring Harbour Laboratory Press).

Hooper, N. M. (1994). Families of zinc metalloproteases. FEBS Lett. *354*, 1-6.

Hoppe, T., Matuschewski, K., Rape, M., Schlenker, S., Ulrich, H. D., and Jentsch, S. (2000). Activation of a membrane-bound transription factor by regulated ubiquitin/proteasome-dependent processing. Cell *102*, 577-586.

Hoppins, S., Lackner, L., and Nunnari, J. (2007). The machines that divide and fuse mitochondria. Annu Rev Biochem *76*, 751-780.

Hoyt, M. A., Zich, J., Takeuchi, J., Zhang, M., Govaerts, C., and Coffino, P. (2006). Glycine-alanine repeats impair proper substrate unfolding by the proteasome. EMBO J. *25*, 1720-1729.

Hudson, G., Amati-Bonneau, P., Blakely, E. L., Stewart, J. D., He, L., Schaefer, A. M., Griffiths, P. G., Ahlqvist, K., Suomalainen, A., Reynier, P.*, et al.* (2008). Mutation of OPA1 causes dominant optic atrophy with external ophthalmoplegia, ataxia, deafness and multiple mitochondrial DNA deletions: a novel disorder of mtDNA maintenance. Brain *131*, 329-337.

Isaya, G., Kalousek, F., Fenton, W. A., and Rosenberg, L. E. (1991). Cleavage of precursors by the mitochondrial processing peptidase requires a compatible mature protein or an intermediate octapeptide. J. Cell Biol. *113*, 65-76.

Isaya, G., Kalousek, F., and Rosenberg, L. E. (1992). Amino-terminal octapeptides function as recognition signals for the mitochondrial intermediate peptidase. J. Biol. Chem. *267*, 7904-7910.

Ishihara, N., Eura, Y., and Mihara, K. (2004). Mitofusin 1 and 2 play distinct roles in mitochondrial fusion reactions via GTPase activity. J Cell Sci *117*, 6535-6546.

Ishihara, N., Fujita, Y., Oka, T., and Mihara, K. (2006). Regulation of mitochondrial morphology through proteolytic cleavage of OPA1. EMBO J. *25*, 2966-2977.

Jacobs, H. T. (2003). Disorders of mitochondrial protein synthesis. Hum. Mol. Genet. *12*, R293-301.

Jacobs, H. T., and Turnbull, D. M. (2005). Nuclear genes and mitochondrial translation: a new class of genetic disease. Trends Genet. *21*, 312-314.

Jan, P. S., Esser, K., Pratje, E., and Michaelis, G. (2000). Som1, a third component of the yeast mitochondrial inner membrane protease complex that contains Imp1 and Imp2. Mol. Gen. Genet. *263*, 483-491.

Jeon, H. B., Choi, E. S., Yoon, J. H., Hwang, J. H., Chang, J. W., Lee, E. K., Choi, H. W., Park, Z. Y., and Yoo, Y. J. (2007). A proteomics approach to identify the ubiquitinated proteins in mouse heart. Biochem Biophys Res Commun *357*, 731-736.

Jones, J. M., Datta, P., Srinivasula, S. M., Ji, W., Gupta, S., Zhang, Z., Davies, E., Hajnoczky, G., Saunders, T. L., Van Keuren, M. L., *et al.* (2003). Loss of Omi mitochondrial protease activity causes the neuromuscular disorder of *mnd2* mutant mice. Nature *425*, 721-727.

Juhola, M. K., Shah, Z. H., Grivell, L. A., and Jacobs, H. T. (2000). The mitochondrial inner membrane AAA metalloprotease family in metazoans. FEBS Lett. *481*, 91-95.

Kalousek, F., Hendrick, J. P., and Rosenberg, L. E. (1988). Two mitochondrial matrix proteases act sequentially in the processing of mammalian matrix enzymes. Proc. Natl. Acad. Sci. U S A *85*, 7536-7540.

Kalousek, F., Isaya, G., and Rosenberg, L. E. (1992). Rat liver mitochondrial intermediate peptidase (MIP): purification and initial characterization. EMBO J. *11*, 2803-2809.

Kambacheld, M., Augustin, S., Tatsuta, T., Muller, S., and Langer, T. (2005). Role of the novel metallopeptidase Mop112 and saccharolysin for the complete degradation of proteins residing in different subcompartments of mitochondria. J Biol Chem *280*, 20132-20139.

Karbowski, M., Neutzner, A., and Youle, R. J. (2007). The mitochondrial E3 ubiquitin ligase MARCH5 is required for Drp1 dependent mitochondrial division. J Cell Biol *178*, 71-84.

Kenniston, J. A., Baker, T. A., and Sauer, R. T. (2005). Partitioning between unfolding and release of native domains during ClpXP degradation determines substrate selectivity and partial processing. Proc. Natl. Acad. Sci. U S A *102*, 1390-1395.

Kihara, A., Akiyama, Y., and Ito, K. (1996). A protease complex in the *Escherichia coli* plasma membrane: HflKC (HflA) forms a complex with FtsH (HflB), regulating its proteolytic activity against SecY. EMBO J. *15*, 6122-6131.

Kim, I., Rodriguez-Enriquez, S., and Lemasters, J. J. (2007). Selective degradation of mitochondria by mitophagy. Arch Biochem Biophys *462*, 245-253.

Knott, A. B., Perkins, G., Schwarzenbacher, R., and Bossy-Wetzel, E. (2008). Mitochondrial fragmentation in neurodegeneration. Nat Rev Neurosci *9*, 505-518.

Koppen, M. (2007) Reconstitution of mammalian *m*-AAA complexes with variable subunit composition in yeast mitochondria, Dissertation, University of Cologne.

Koppen, M., and Langer, T. (2007). Protein degradation within mitochondria: versatile activities of AAA proteases and other peptidases. Crit. Rev. Biochem. Mol. Biol. *42*, 221-242.

Koppen, M., Metodiev, M. D., Casari, G., Rugarli, E. I., and Langer, T. (2007). Variable and Tissue-Specific Subunit Composition of Mitochondrial *m*-AAA Protease Complexes Linked to Hereditary Spastic Paraplegia. Mol. Cell. Biol. *27*, 758-767.

Korbel, D., Wurth, S., Käser, M., and Langer, T. (2004). Membrane protein turnover by the *m*-AAA protease in mitochondria depends on the transmembrane domains of its subunits. EMBO Rep. *5*, 698-703.

Koshiba, T., Detmer, S. A., Kaiser, J. T., Chen, H., McCaffery, J. M., and Chan, D. C. (2004). Structural basis of mitochondrial tethering by mitofusin complexes. Science *305*, 858-862.

Kremmidiotis, G., Gardner, A. E., Settasatian, C., Savoia, A., Sutherland, G. R., and Callen, D. F. (2001). Molecular and functional analyses of the human and mouse genes encoding AFG3L1, a mitochondrial metalloprotease homologous to the human spastic paraplegia protein. Genomics *76*, 58-65.

Labrousse, A. M., Zappaterra, M. D., Rube, D. A., and van der Bliek, A. M. (1999). C. elegans dynamin-related protein DRP-1 controls severing of the mitochondrial outer membrane. Mol Cell *4*, 815-826.

Laemmli, U. K. (1970). Cleavage of structural proteins during the assembly of the head of bacteriophage T4. Nature *227*, 680-685.

Langer, T. (2000). AAA proteases - cellular machines for degrading membrane proteins. Trends Biochem. Sci. *25*, 207-256.

Langer, T., Käser, M., Klanner, C., and Leonhard, K. (2001). AAA proteases of mitochondria: quality control of membrane proteins and regulatory functions during mitochondrial biogenesis. Biochemical Society Transactions *29*, 431-436.

Lee, Y. J., Jeong, S. Y., Karbowski, M., Smith, C. L., and Youle, R. J. (2004). Roles of the mammalian mitochondrial fission and fusion mediators Fis1, Drp1, and Opa1 in apoptosis. Mol. Biol. Cell *15*, 5001-5011.

Legros, F., Lombes, A., Frachon, P., and Rojo, M. (2002). Mitochondrial fusion in human cells is efficient, requires the inner membrane potential, and is mediated by mitofusins. Mol Biol Cell *13*, 4343-4354.

Legros, F., Malka, F., Frachon, P., Lombes, A., and Rojo, M. (2004). Organization and dynamics of human mitochondrial DNA. J Cell Sci *117*, 2653-2662.

Lemberg, M. K., Menendez, J., Misik, A., Garcia, M., Koth, C. M., and Freeman, M. (2005). Mechanism of intramembrane proteolysis investigated with purified rhomboid proteases. Embo J *24*, 464-472.

Leonhard, K., Herrmann, J. M., Stuart, R. A., Mannhaupt, G., Neupert, W., and Langer, T. (1996). AAA proteases with catalytic sites on opposite membrane surfaces comprise a proteolytic system for the ATP-dependent degradation of inner membrane proteins in mitochondria. EMBO J. *15*, 4218-4229.

Leonhard, K., Stiegler, A., Neupert, W., and Langer, T. (1999). Chaperone-like activity of the AAA domain of the yeast Yme1 AAA protease. Nature *398*, 348-351.

Lin, M. T., and Beal, M. F. (2006). Mitochondrial dysfunction and oxidative stress in neurodegenerative diseases. Nature *443*, 787-795.

Liu, C. W., Corboy, M. J., DeMartino, G. N., and Thomas, P. J. (2003). Endoproteolytic activity of the proteasome. Science *299*, 408-411.

Liu, T., Lu, B., Lee, I., Ondrovicova, G., Kutejova, E., and Suzuki, C. K. (2004). DNA and RNA binding by the mitochondrial lon protease is regulated by nucleotide and protein substrate. J. Biol. Chem. *279*, 13902-13910.

Lopez, M. F., Kristal, B. S., Chernokalskaya, E., Lazarev, A., Shestopalov, A. I., Bogdanova, A., and Robinson, M. (2000). High-throughput profiling of the mitochondrial proteome using affinity fractionation and automation. Electrophoresis *21*, 3427-3440.

Loschen, G., and Azzi, A. (1974). Proceedings: Formation of oxygen radicals and hydrogen peroxide in mitochondrial membranes. Hoppe Seylers Z Physiol Chem *355*, 1226.

Lu, B., Liu, T., Crosby, J. A., Thomas-Wohlever, J., Lee, I., and Suzuki, C. K. (2003). The ATP-dependent Lon protease of *Mus musculus* is a DNA-binding protein that is functionally conserved between yeast and mammals. Gene *306*, 45-55.

Lu, B., Yadav, S., Shah, P. G., Liu, T., Tian, B., Pukszta, S., Villaluna, N., Kutejova, E., Newlon, C. S., Santos, J. H., and Suzuki, C. K. (2007). Roles for the human ATP-dependent Lon protease in mitochondrial DNA maintenance. J Biol Chem *282*, 17363-17374.

Lu, J., Rashid, F., and Byrne, P. C. (2006). The hereditary spastic paraplegia protein spartin localises to mitochondria. J. Neurochem. *98*, 1908-1919.

Luciano, P., Tokatlidis, K., Chambre, I., Germanique, J. C., and Geli, V. (1998). The mitochondrial processing peptidase behaves as a zinc-metallopeptidase. J. Mol. Biol. *280*, 193-199.

Major, T., von Janowsky, B., Ruppert, T., Mogk, A., and Voos, W. (2006). Proteomic analysis of mitochondrial protein turnover: identification of novel substrate proteins of the matrix protease pim1. Mol. Cell. Biol. *26*, 762-776.

Malka, F., Guillery, O., Cifuentes-Diaz, C., Guillou, E., Belenguer, P., Lombes, A., and Rojo, M. (2005). Separate fusion of outer and inner mitochondrial membranes. EMBO Rep *6*, 853-859.

Maltecca, F., Aghaie, A., Schroeder, D. G., Cassina, L., Taylor, B. A., Phillips, S. J., Malaguti, M., Previtali, S., Guenet, J. L., Quattrini, A., *et al.* (2008). The mitochondrial protease AFG3L2 is essential for axonal development. J. Neurosci. *28*, 2827-2836.

Manczak, M., Anekonda, T. S., Henson, E., Park, B. S., Quinn, J., and Reddy, P. H. (2006). Mitochondria are a direct site of A beta accumulation in Alzheimer's disease neurons: implications for free radical generation and oxidative damage in disease progression. Hum Mol Genet *15*, 1437-1449.

Margineantu, D. H., Emerson, C. B., Diaz, D., and Hockenbery, D. M. (2007). Hsp90 inhibition decreases mitochondrial protein turnover. PLoS ONE *2*, e1066.

Martins, L. M., Morrison, A., Klupsch, K., Fedele, V., Moisoi, N., Teismann, P., Abuin, A., Grau, E., Geppert, M., Livi, G. P., *et al.* (2004). Neuroprotective role of the Reaper-related serine protease HtrA2/Omi revealed by targeted deletion in mice. Mol. Cell. Biol. *24*, 9848-9862.

Matsumoto, M., Hatakeyama, S., Oyamada, K., Oda, Y., Nishimura, T., and Nakayama, K. I. (2005). Large-scale analysis of the human ubiquitin-related proteome. Proteomics *5*, 4145-4151.

McBride, H. M., Neuspiel, M., and Wasiak, S. (2006). Mitochondria: more than just a powerhouse. Curr. Biol. *16*, R551-560.

McDermott, C. J., Dayaratne, R. K., Tomkins, J., Lusher, M. E., Lindsey, J. C., Johnson, M. A., Casari, G., Turnbull, D. M., Bushby, K., and Shaw, P. J. (2001). Paraplegin gene analysis in hereditary spastic paraparesis (HSP) pedigrees in northeast England. Neurology *56*, 467-471.

McDermott, C. J., Grierson, A. J., Wood, J. D., Bingley, M., Wharton, S. B., Bushby, K. M., and Shaw, P. J. (2003). Hereditary spastic paraparesis: disrupted intracellular transport associated with spastin mutation. Ann Neurol *54*, 748-759.

McQuibban, G. A., Saurya, S., and Freeman, M. (2003). Mitochondrial membrane remodelling regulated by a conserved rhomboid protease. Nature *423*, 537-541.

Meeusen, S., McCaffery, J. M., and Nunnari, J. (2004). Mitochondrial fusion intermediates revealed in vitro. Science *305*, 1747-1752.

Meeusen, S., DeVay, R., Block, J., Cassidy-Stone, A., Wayson, S., McCaffery, J. M., and Nunnari, J. (2006). Mitochondrial inner-membrane fusion and crista maintenance requires the dynamin-related GTPase Mgm1. Cell *127*, 383-395.

Merkwirth, C., Dargazanli, S., Tatsuta, T., Geimer, S., Lower, B., Wunderlich, F. T., von Kleist-Retzow, J. C., Waisman, A., Westermann, B., and Langer, T. (2008). Prohibitins control cell proliferation and apoptosis by regulating OPA1-dependent cristae morphogenesis in mitochondria. Genes Dev *22*, 476-488.

Metodiev, M. D. (2005) Role of prohibitins for proteolysis in yeast and murine mitochondria, Dissertation, University of Cologne.

Milakovic, T., and Johnson, G. V. (2005). Mitochondrial respiration and ATP production are significantly impaired in striatal cells expressing mutant huntingtin. J Biol Chem *280*, 30773-30782.

Miller, C., Saada, A., Shaul, N., Shabtai, N., Ben-Shalom, E., Shaag, A., Hershkovitz, E., and Elpeleg, O. (2004). Defective mitochondrial translation caused by a ribosomal protein (MRPS16) mutation. Ann. Neurol. *56*, 734-738.

Misaka, T., Miyashita, T., and Kubo, Y. (2002). Primary structure of a dynamin-related mouse mitochondrial GTPase and its distribution in brain, subcellular localization, and effect on mitochondrial morphology. J. Biol. Chem. *277*, 15834-15842.

Nakamura, N., Kimura, Y., Tokuda, M., Honda, S., and Hirose, S. (2006). MARCH-V is a novel mitofusin 2- and Drp1-binding protein able to change mitochondrial morphology. EMBO Rep. *7*, 1019-1022.

Nijtmans, L. G. J., de Jong, L., Sanz, M. A., Coates, P. J., Berden, J. A., Back, J. W., Muijsers, A. O., Van der Speck, H., and Grivell, L. A. (2000). Prohibitins act as a membrane-bound chaperone for the stabilization of mitochondrial proteins. EMBO J. *19*, 2444-2451.

Nolden, M., Ehses, S., Koppen, M., Bernacchia, A., Rugarli, E. I., and Langer, T. (2005). The *m*-AAA protease defective in hereditary spastic paraplegia controls ribosome assembly in mitochondria. Cell *123*, 277-289.

Nunnari, J., Fox, T. D., and Walter, P. (1993). A mitochondrial protease with two catalytic subunits of nonoverlapping specificities. Science *262*, 1997-2004.

Okamoto, K., and Shaw, J. M. (2005). Mitochondrial morphology and dynamics in yeast and multicellular eukaryotes. Annu. Rev. Genet. *39*, 503-536.

Olichon, A., Emorine, L. J., Descoins, E., Pelloquin, L., Brichese, L., Gas, N., Guillou, E., Delettre, C., Valette, A., Hamel, C. P.*, et al.* (2002). The human dynamin-related protein OPA1 is anchored to the mitochondrial inner membrane facing the inter-membrane space. FEBS Lett. *523*, 171-176.

Olichon, A., Baricault, L., Gas, N., Guillou, E., Valette, A., Belenguer, P., and Lenaers, G. (2003). Loss of OPA1 perturbates the mitochondrial inner membrane structure and integrity, leading to cytochrome *c* release and apoptosis. J. Biol. Chem. *278*, 7743-7746.

Olichon, A., Elachouri, G., Baricault, L., Delettre, C., Belenguer, P., and Lenaers, G. (2006). OPA1 alternate splicing uncouples an evolutionary conserved function in mitochondrial fusion from a vertebrate restricted function in apoptosis. Cell. Death. Differ.

Osman, C., Wilmes, C., Tatsuta, T., and Langer, T. (2007). Prohibitins Interact Genetically with Atp23, a Novel Processing Peptidase and Chaperone for the F_1F_O-ATP Synthase. Mol. Biol. Cell *18*, 627-635.

Otsuga, D., Keegan, B. R., Brisch, E., Thatcher, J. W., Hermann, G. J., Bleazard, W., and Shaw, J. M. (1998). The dynamin-related GTPase, Dnm1p, controls mitochondrial morphology in yeast. J. Cell Biol. *143*, 333-349.

Palombella, V. J., Rando, O. J., Goldberg, A. L., and Maniatis, T. (1994). The ubiquitin-proteasome pathway is required for processing the NF-kappa B1 precursor protein and the activation of NF-kappa B. Cell *78*, 773-785.

Park, H. J., Kim, S. S., Seong, Y. M., Kim, K. H., Goo, H. G., Yoon, E. J., Min do, S., Kang, S., and Rhim, H. (2006). Beta-amyloid precursor protein is a direct cleavage target of HtrA2 serine protease. Implications for the physiological function of HtrA2 in the mitochondria. J. Biol. Chem. *281*, 34277-34287.

Pearce, D. A., and Sherman, F. (1995). Degradation of cytochrome oxidase subunits in mutants of yeast lacking cytochrome *c* and suppression of the degradation by mutation of *yme1*. J. Biol. Chem. *270*, 1-4.

Pellegrini, L., Passer, B. J., Canelles, M., Lefterov, I., Ganjei, J. K., Fowlkes, B. J., Koonin, E. V., and D'Adamio, L. (2001). PAMP and PARL, two novel putative metalloproteases interacting with the COOH-terminus of Presenilin-1 and -2. J. Alzheimers Dis. *3*, 181-190.

Peng, J., Schwartz, D., Elias, J. E., Thoreen, C. C., Cheng, D., Marsischky, G., Roelofs, J., Finley, D., and Gygi, S. P. (2003). A proteomics approach to understanding protein ubiquitination. Nat Biotechnol *21*, 921-926.

Piwko, W., and Jentsch, S. (2006). Proteasome-mediated protein processing by bidirectional degradation initiated from an internal site. Nat Struct Mol Biol *13*, 691-697.

Pratje, E., Mannhaupt, G., Michaelis, G., and Beyreuther, K. (1983). A nuclear mutation prevents processing of a mitochondrially encoded membrane protein in *Saccharomyces cerevisiae*. EMBO J. *2*, 1049-1054.

Radke, S., Chander, H., Schafer, P., Meiss, G., Kruger, R., Schulz, J. B., and Germain, D. (2008). Mitochondrial protein quality control by the proteasome involves ubiquitination and the protease Omi. J Biol Chem *283*, 12681-12685.

Rainey, R. N., Glavin, J. D., Chen, H. W., French, S. W., Teitell, M. A., and Koehler, C. M. (2006). A New Function in Translocation for the Mitochondrial *i*-AAA Protease Yme1: Import of Polynucleotide Phosphorylase into the Intermembrane Space. Mol. Cell. Biol. *26*, 8488-8497.

Rape, M., and Jentsch, S. (2004). Productive RUPture: activation of transcription factors by proteasomal processing. Biochim. Biophys. Acta. *1695*, 209-213.

Rawlings, N. D., and Barrett, A. J. (1995). Evolutionary families of metallopeptidases. Methods Enzymol. *248*, 183-228.

Reers, M., Smiley, S. T., Mottola-Hartshorn, C., Chen, A., Lin, M., and Chen, L. B. (1995). Mitochondrial membrane potential monitored by JC-1 dye. Methods Enzymol *260*, 406-417.

Rojo, M., Legros, F., Chateau, D., and Lombes, A. (2002). Membrane topology and mitochondrial targeting of mitofusins, ubiquitous mammalian homologs of the transmembrane GTPase Fzo. J Cell Sci *115*, 1663-1674.

Rossignol, R., Letellier, T., Malgat, M., Rocher, C., and Mazat, J. P. (2000). Tissue variation in the control of oxidative phosphorylation: implication for mitochondrial diseases. Biochem. J. *347 Pt 1*, 45-53.

Rossignol, R., Faustin, B., Rocher, C., Malgat, M., Mazat, J. P., and Letellier, T. (2003). Mitochondrial threshold effects. Biochem. J. *370*, 751-762.

Rugarli, E. I., and Langer, T. (2006). Translating *m*-AAA protease function in mitochondria to hereditary spastic paraplegia. Trends Mol. Med. *12*, 262-269.

Saikawa, N., Akiyama, Y., and Ito, K. (2004). FtsH exists as an exceptionally large complex containing HflKC in the plasma membrane of *Escherichia coli*. J. Struct. Biol. *146*, 123-129.

Sambrook, J., and Russell, D. (2001). Molecular Cloning: A Laboratory Manual (Cold Spring Harbor, NY: Cold Spring Harbor Laboratory Press).

Sanderson, C. M., Connell, J. W., Edwards, T. L., Bright, N. A., Duley, S., Thompson, A., Luzio, J. P., and Reid, E. (2006). Spastin and atlastin, two proteins mutated in autosomal-dominant hereditary spastic paraplegia, are binding partners. Hum. Mol. Genet. *15*, 307-318.

Santel, A., and Fuller, M. T. (2001). Control of mitochondrial morphology by a human mitofusin. J Cell Sci *114*, 867-874.

Sasaki, H., Nishizaki, Y., Hui, C., Nakafuku, M., and Kondoh, H. (1999). Regulation of Gli2 and Gli3 activities by an amino-terminal repression domain: implication of Gli2 and Gli3 as primary mediators of Shh signaling. Development *126*, 3915-3924.

Satoh, M., Hamamoto, T., Seo, N., Kagawa, Y., and Endo, H. (2003). Differential sublocalization of the dynamin-related protein OPA1 isoforms in mitochondria. Biochem. Biophys. Res. Commun. *300*, 482-493.

Sauer, R. T., Bolon, D. N., Burton, B. M., Burton, R. E., Flynn, J. M., Grant, R. A., Hersch, G. L., Joshi, S. A., Kenniston, J. A., Levchenko, I., *et al.* (2004). Sculpting the proteome with AAA(+) proteases and disassembly machines. Cell *119*, 9-18.

Sesaki, H., and Jensen, R. E. (2001). *UGO1* encodes an outer membrane protein required for mitochondrial fusion. J. Cell Biol. *152*, 1123-1134.

Sesaki, H., Southard, S. M., Hobbs, A. E., and Jensen, R. E. (2003). Cells lacking Pcp1p/Ugo2p, a rhomboid-like protease required for Mgm1p processing, lose mtDNA and mitochondrial structure in a Dnm1p-dependent manner, but remain competent for mitochondrial fusion. Biochem. Biophys. Res. Commun. *308*, 276-283.

Sesaki, H., Southard, S. M., Yaffe, M. P., and Jensen, R. E. (2003). Mgm1p, a dynamin-related GTPase, is essential for fusion of the mitochondrial outer membrane. Mol. Biol. Cell *14*, 2342-2356.

Sesaki, H., and Jensen, R. E. (2004). Ugo1p links the Fzo1p and Mgm1p GTPases for mitochondrial fusion. J. Biol. Chem. *279*, 28298-28303.

Shah, Z. H., Migliosi, V., Miller, S. C., Wang, A., Friedman, T. B., and Jacobs, H. T. (1998). Chromosomal locations of three human nuclear genes (RPSM12, TUFM, and AFG3L1) specifying putative components of the mitochondrial gene expression apparatus. Genomics *48*, 384-388.

Shah, Z. H., Hakkaart, G. A. J., Arku, B., DeJong, L., Van der Speck, H., Grivell, L., and Jacobs, H. T. (2000). The human homologue of the yeast mitochondrial AAA metalloprotease Yme1p complements a yeast *yme1* disruptant. FEBS Lett. *478*, 267-270.

Silver, L. M. (1995). Mouse genetics: concepts and practice: Oxford University Press).

Smiley, S. T., Reers, M., Mottola-Hartshorn, C., Lin, M., Chen, A., Smith, T. W., Steele, G. D., Jr., and Chen, L. B. (1991). Intracellular heterogeneity in mitochondrial membrane potentials revealed by a J-aggregate-forming lipophilic cation JC-1. Proc Natl Acad Sci U S A *88*, 3671-3675.

Smirnova, E., Griparic, L., Shurland, D. L., and van der Bliek, A. M. (2001). Dynamin-related protein Drp1 is required for mitochondrial division in mammalian cells. Mol Biol Cell *12*, 2245-2256.

Soderblom, C., and Blackstone, C. (2006). Traffic accidents: Molecular genetic insights into the pathogenesis of the hereditary spastic paraplegias. Pharmacol Ther *109*, 42-56.

Song, Z., Chen, H., Fiket, M., Alexander, C., and Chan, D. C. (2007). OPA1 processing controls mitochondrial fusion and is regulated by mRNA splicing, membrane potential, and Yme1L. J Cell Biol *178*, 749-755.

Spiess, C., Beil, A., and Ehrmann, M. (1999). A temperature-dependent switch from chaperone to protease in a widely conserved heat shock protein. Cell *97*, 339-347.

Stahlberg, H., Kutejova, E., Suda, K., Wolpensinger, B., Lustig, A., Schatz, G., Engel, A., and Suzuki, C. K. (1999). Mitochondrial Lon of *Saccharomyces cerevisiae* is a ring-shaped protease with seven flexible subunits. Proc. Natl. Acad. Sci. USA *96*, 6787-6790.

Steglich, G., Neupert, W., and Langer, T. (1999). Prohibitins regulate membrane protein degradation by the *m*-AAA protease in mitochondria. Mol. Cell. Biol. *19*, 3435-3442.

Strauss, K. M., Martins, L. M., Plun-Favreau, H., Marx, F. P., Kautzmann, S., Berg, D., Gasser, T., Wszolek, Z., Muller, T., Bornemann, A.*, et al.* (2005). Loss of function mutations in the gene encoding Omi/HtrA2 in Parkinson's disease. Hum Mol Genet *14*, 2099-2111.

Suen, D. F., Norris, K. L., and Youle, R. J. (2008). Mitochondrial dynamics and apoptosis. Genes Dev *22*, 1577-1590.

Suno, R., Niwa, H., Tsuchiya, D., Zhang, X., Yoshida, M., and Morikawa, K. (2006). Structure of the Whole Cytosolic Region of ATP-Dependent Protease FtsH. Mol. Cell *22*, 575-585.

Suzuki, C. K., Suda, K., Wang, N., and Schatz, G. (1994). Requirement for the yeast gene LON in intramitochondrial proteolysis and maintenance of respiration. Science *264*, 273-276.

Suzuki, Y., Imai, Y., Nakayama, H., Takahashi, K., Takio, K., and Takahashi, R. (2001). A serine protease, HtrA2, is released from the mitochondria and interacts with XIAP, inducing cell death. Mol. Cell *8*, 613-621.

Sylvester, J. E., Fischel-Ghodsian, N., Mougey, E. B., and O'Brien, T. W. (2004). Mitochondrial ribosomal proteins: candidate genes for mitochondrial disease. Genet. Med. *6*, 73-80.

Tarrade, A., Fassier, C., Courageot, S., Charvin, D., Vitte, J., Peris, L., Thorel, A., Mouisel, E., Fonknechten, N., Roblot, N., *et al.* (2006). A mutation of spastin is responsible for swellings and impairment of transport in a region of axon characterized by changes in microtubule composition. Hum Mol Genet *15*, 3544-3558.

Tatsuta, T., Augustin, S., Nolden, M., Friedrichs, B., and Langer, T. (2007). *m*-AAA protease-driven membrane dislocation allows intramembrane cleavage by rhomboid in mitochondria. EMBO J. *26*, 325-335.

Tatsuta, T., and Langer, T. (2008). Quality control of mitochondria: protection against neurodegeneration and ageing. EMBO J. *27*, 306-314.

Tavernarakis, N., Driscoll, M., and Kyrpides, N. C. (1999). The SPFH domain: implicated in regulating targeted protein turnover in stomatins and other membrane-associated proteins. Trends Biochem. Sci. *24*, 425-427.

Taylor, R. W., and Turnbull, D. M. (2005). Mitochondrial DNA mutations in human disease. Nat. Rev. Genet. *6*, 389-402.

Tian, L., Holmgren, R. A., and Matouschek, A. (2005). A conserved processing mechanism regulates the activity of transcription factors Cubitus interruptus and NF-kappaB. Nat. Struct. Mol. Biol. *12*, 1045-1053.

Todaro, G. J., and Green, H. (1965). Successive Transformations Of An Established Cell Line By Polyoma Virus And Sv40. Science *147*, 513-514.

Towbin, H., Staehelin, T., and Gordon, J. (1979). Electrophoretic transfer of proteins from polyacrylamide gels to nitrocellulose sheets: procedure and some applications. Proc. Natl. Acad. Sci. U S A *76*, 4350-4354.

Urantowka, A., Knorpp, C., Olczak, T., Kolodziejczak, M., and Janska, H. (2005). Plant mitochondria contain at least two *i*-AAA-like complexes. Plant. Mol. Biol. *59*, 239-252.

Van Dyck, L., Pearce, D. A., and Sherman, F. (1994). *PIM1* encodes a mitochondrial ATP-dependent protease that is required for mitochondrial function in the yeast *Saccharomyces cerevisiae*. J. Biol. Chem. *269*, 238-242.

van Loo, G., van Gurp, M., Depuydt, B., Srinivasula, S. M., Rodriguez, I., Alnemri, E. S., Gevaert, K., Vandekerckhove, J., Declercq, W., and Vandenabeele, P. (2002). The serine protease Omi/HtrA2 is released from mitochondria during apoptosis. Omi interacts with caspase-inhibitor XIAP and induces enhanced caspase activity. Cell. Death. Differ. *9*, 20-26.

Ventura, B., Genova, M. L., Bovina, C., Formiggini, G., and Lenaz, G. (2002). Control of oxidative phosphorylation by Complex I in rat liver mitochondria: implications for aging. Biochim Biophys Acta *1553*, 249-260.

Verhagen, A. M., Silke, J., Ekert, P. G., Pakusch, M., Kaufmann, H., Connolly, L. M., Day, C. L., Tikoo, A., Burke, R., Wrobel, C., *et al.* (2002). HtrA2 promotes cell death through its serine protease activity and its ability to antagonize inhibitor of apoptosis proteins. J. Biol. Chem. *277*, 445-454.

Wagner, I., Van Dyck, L., Savel´ev, A., Neupert, W., and Langer, T. (1997). Autocatalytic processing of the ATP-dependent PIM1 protease: Crucial function of a pro-region for sorting to mitochondria. EMBO J. *16*, 7317-7325.

Wallace, D. C. (2005). A mitochondrial paradigm of metabolic and degenerative diseases, aging, and cancer: a dawn for evolutionary medicine. Annu. Rev. Genet. *39*, 359-407.

Wang, J., Song, J. J., Franklin, M. C., Kamtekar, S., Im, Y. J., Rho, S. H., Seong, I. S., Lee, C. S., Chung, C. H., and Eom, S. H. (2001). Crystal structures of the HslVU peptidase-ATPase complex reveal an ATP-dependent proteolysis mechanism. Structure (Camb) *9*, 177-184.

Wang, N., Maurizi, M. R., Emmert, B. L., and Gottesman, S. (1994). Synthesis, processing, and localization of human Lon protease. J. Biol. Chem. *269*, 29308-29313.

Warren, G., and Wickner, W. (1996). Organelle inheritance. Cell *84*, 395-400.

Weber, E. R., Hanekamp, T., and Thorsness, P. E. (1996). Biochemical and functional analysis of the *YME1* gene product, an ATP and zinc-dependent mitochondrial protease from *S. cerevisiae*. Mol. Biol. Cell *7*, 307-317.

Wilkinson, P. A., Crosby, A. H., Turner, C., Bradley, L. J., Ginsberg, L., Wood, N. W., Schapira, A. H., and Warner, T. T. (2004). A clinical, genetic and biochemical study of SPG7 mutations in hereditary spastic paraplegia. Brain *127*, 973-980.

Wong, E. D., Wagner, J. A., Scott, S. V., Okreglak, V., Holewinske, T. J., Cassidy-Stone, A., and Nunnari, J. (2003). The intramitochondrial dynamin-related GTPase, Mgm1p, is a component of a protein complex that mediates mitochondrial fusion. J. Cell. Biol. *160*, 303-311.

Xia, C. H., Roberts, E. A., Her, L. S., Liu, X., Williams, D. S., Cleveland, D. W., and Goldstein, L. S. (2003). Abnormal neurofilament transport caused by targeted disruption of neuronal kinesin heavy chain KIF5A. J Cell Biol *161*, 55-66.

Yang, M., Jensen, R. E., Yaffe, M. P., Oppliger, W., and Schatz, G. (1988). Import of proteins into yeast mitochondria: the purified matrix processing protease contains two subunits which are encoded by the nuclear *MAS1* and *MAS2* genes. EMBO J. *7*, 3857-3862.

Yonashiro, R., Ishido, S., Kyo, S., Fukuda, T., Goto, E., Matsuki, Y., Ohmura-Hoshino, M., Sada, K., Hotta, H., Yamamura, H., *et al.* (2006). A novel mitochondrial ubiquitin ligase plays a critical role in mitochondrial dynamics. EMBO J. *25*, 3618-3626.

Zehnbauer, B. A., Foley, E. C., Henderson, G. W., and Markovitz, A. (1981). Identification and purification of the Lon+ (capR+) gene product, a DNA-binding protein. Proc. Natl. Acad. Sci. USA *78*, 2043-2047.

Zeng, X., Neupert, W., and Tzagoloff, A. (2007). The Metalloprotease Encoded by *ATP23* Has a Dual Function in Processing and Assembly of Subunit 6 of Mitochondrial ATPase. Mol. Biol. Cell. *18*, 617-626.

Zhao, Q., Wang, J., Levichkin, I. V., Stasinopoulos, S., Ryan, M. T., and Hoogenraad, N. J. (2002). A mitochondrial specific stress response in mammalian cells. EMBO J. *21*, 4411-4419.

Züchner, S., Mersiyanova, I. V., Muglia, M., Bissar-Tadmouri, N., Rochelle, J., Dadali, E. L., Zappia, M., Nelis, E., Patitucci, A., Senderek, J., *et al.* (2004). Mutations in the mitochondrial GTPase mitofusin 2 cause Charcot-Marie-Tooth neuropathy type 2A. Nat. Genet. *36*, 449-451.

Züchner, S., and Vance, J. M. (2005). Emerging pathways for hereditary axonopathies. J. Mol. Med. *83*, 935-943.

Züchner, S., Wang, G., Tran-Viet, K. N., Nance, M. A., Gaskell, P. C., Vance, J. M., Ashley-Koch, A. E., and Pericak-Vance, M. A. (2006). Mutations in the novel mitochondrial protein REEP1 cause hereditary spastic paraplegia type 31. Am. J. Hum. Genet. *79*, 365-369.

7   List of Abbreviations

AAA	ATPases associated with a variety of cellular activities
Aβ	amyloid β–peptide
ADOA	autosomal domaint optic atrophy
ADP	adenosine diphosphate
APP	amyloid precursor protein
APS	ammoniumperoxo disulfate
ATP	adenosine triphosphate
bp	base pairs
CCCP	carbonyl cyanide m-chlorophenylhydrazone
cDNA	complementary DNA
CMT2A	Charcot-Marie-Tooth type 2A
C-terminal	carboxyterminal
C-terminus	carboxy terminus
DMSO	dimethyl sulfoxide
DNA	deoxyribonucleic acid
EDTA	ethylene diamine tetraacetic acid
Fig.	Figure
g	standard gravity
GTP	guanosine triphosphate
h	hour(s)
HCl	hydrochloric acid
HEPES	N-2-hydroxyethylpiperazine-N'-2-ethanesulfonic-acid
HSP	hereditary spastic paraplegia
K	potassium
kb	kilobase pairs
KCl	potassium chloride
kDa	kilodalton
KOH	potassium hydroxide
m	meter
M	molar (mole per liter)
MDa	megadalton
MEF	mouse embryonic fibroblast
μg	microgram
μl	microliter
mg	milligram
ml	milliliter
Mg	magnesium
min	minute(s)
MIP	mitochondrial intermediate peptidase
mM	millimolar
mRNA	messenger RNA
Mg	magnesium
MPP	mitochondrial processing peptidase
mRNA	messenger RNA
mt	mitochondrial
mtDNA	mitochondrial DNA
MTS	mitochondrial targeting sequence
NaCl	sodium chloride

NADH	nicotinamide adenine dinucleotide (reduced form)
NaOH	sodium hydroxide
NP-40	Nonidet P-40
N-terminal	aminoterminal
N-terminus	amino terminus
OXPHOS	oxidative phosphorylation
PAGE	polyacrylamide gel electrophoresis
PBS	phosphate buffered saline
PCR	polymerase chain reaction
PMSF	phenylmethylsulphonyl fluoride
RNA	ribonucleic acid
RNAi	RNA interference
ROS	reactive oxygen species
rpm	rounds per minute
RT	room temperature
s	second(s)
SDS	sodium dodecyl sulfate
SPG	spastic paraplegia gene
SRH	second region of homology
Tab.	Table
TBS	Tris buffered saline
TCA	trichloracetic acid
TEMED	N,N,N',N'-Tetramethylethylenediamine
TIM	translocase of the inner membrane
TM	transmembrane domain
TOM	translocase of the outer membrane
Tris	2-amino-2-(hydroxymethyl)-1,3-propandiole
U	unit(s)
UPS	ubiquitin-proteasome system
v/v	volume per volume
V	volt
wt	wild-type
w/v	weight per volume

8   Appendix

Teilpublikationen im Rahmen dieser Arbeit:

Nolden, M., <u>Ehses, S.</u>, Koppen, M., Bernacchia, A., Rugarli, E. I., and Langer, T. (2005)

"The *m*-AAA Protease Defective in Hereditary Spastic Paraplegia Controls Ribosome Assembly in Mitochondria."

Cell 123, 277-289

Abstract:

AAA proteases comprise a conserved family of membrane bound ATP-dependent proteases that ensures the quality control of mitochondrial inner-membrane proteins. Inactivation of AAA proteases causes pleiotropic phenotypes in various organisms, including respiratory deficiencies, mitochondrial morphology defects, and axonal degeneration in hereditary spastic paraplegia (HSP). The molecular basis of these defects, however, remained unclear. Here, we describe a regulatory role of an AAA protease for mitochondrial protein synthesis in yeast. The mitochondrial ribosomal protein MrpL32 is processed by the *m*-AAA protease, allowing its association with preassembled ribosomal particles and completion of ribosome assembly in close proximity to the inner membrane. Maturation of MrpL32 and mitochondrial protein synthesis are also impaired in a HSP mouse model lacking the *m*-AAA protease subunit paraplegin, demonstrating functional conservation. Our findings therefore rationalize mitochondrial defects associated with *m*-AAA protease mutants in yeast and shed new light on the mechanism of axonal degeneration in HSP.

9 Danksagung

Eidesstattliche Erklärung

Ich versichere, dass ich die von mir vorgelegte Dissertation selbständig angefertigt, die benutzten Quellen und Hilfsmittel vollständig angegeben und die Stellen der Arbeit - einschließlich Tabellen, Karten und Abbildungen -, die anderen Werken im Wortlaut oder dem Sinn nach entnommen sind, in jedem Einzelfall als Entlehnung kenntlich gemacht habe; dass diese Dissertation noch keiner anderen Fakultät oder Universität zur Prüfung vorgelegen hat; dass sie - abgesehen von unten angegebenen Teilpublikationen - noch nicht veröffentlicht worden ist sowie, dass ich eine solche Veröffentlichung vor Abschluss des Promotionsverfahrens nicht vornehmen werde. Die Bestimmungen der Promotionsordnung sind mir bekannt. Die von mir vorgelegte Dissertation ist von Herrn Prof. Dr. Thomas Langer betreut worden.

Köln, im August 2008   Sarah Ehses

Teilpublikationen im Rahmen dieser Arbeit:

Nolden, M., **Ehses, S.**, Koppen, M., Bernacchia, A., Rugarli, E. I., and Langer, T. (2005). The m-AAA Protease Defective in Hereditary Spastic Paraplegia Controls Ribosome Assembly in Mitochondria. Cell *123*, 277-289.

Lebenslauf

Vor- und Zuname:	Sarah Marie Ehses
Geburtstag:	22.09.1978
Geburtsort:	Bonn
Staatsangehörigkeit:	deutsch

Schulausbildung

1985 – 1989	Bodelschwingh-Grundschule, Bonn
1989 – 1993	Friedrich-Wilhelm-Gymnasium, Trier
1993 – 1994	Carl-von-Ossietzky-Gymansium, Bonn
1994 – 1998	Ernst-Moritz-Arndt-Gymnasium, Bonn
Juni 1998	Abitur

Hochschulausbildung

Oktober 1998 – Juli 2003	Studium der Biologie an der Universität zu Köln
Juli 2002 – Juli 2003	Diplomarbeit am Institut für Genetik bei Priv.-Doz. Dr. Michael R. Knittler mit dem Thema: „Untersuchungen zur Funktion divergenter Proteinsequenzen in den Untereinheiten des ABC-Transporters TAP"
Juli 2003	Abschluss als Diplom-Biologin
November 2003 – Oktober 2008	Doktorarbeit am Institut für Genetik der Universität zu Köln bei Prof. Dr. Thomas Langer; Dissertation zum Thema: „Functional Analysis of mammalian m-AAA proteases"

Publikationen

Ehses, S., Leonhardt, R. M., Hansen, G., and Knittler, M. R. (2005). Functional role of C-terminal sequence elements in the transporter associated with antigen processing. J Immunol *174*, 328-339.

Nolden, M., **Ehses, S.**, Koppen, M., Bernacchia, A., Rugarli, E. I., and Langer, T. (2005). The m-AAA Protease Defective in Hereditary Spastic Paraplegia Controls Ribosome Assembly in Mitochondria. Cell *123*, 277-289.

Keusekotten, K., Leonhardt, R. M., **Ehses, S.**, and Knittler, M. R. (2006). Biogenesis of functional antigenic peptide transporter TAP requires assembly of pre-existing TAP1 with newly synthesized TAP2. J Biol Chem *281*, 17545-17551.